

**Roadside Features in Crash Prediction Models:
Data Collection and Evaluation**

by

Mohammad Jalayer

A dissertation submitted to the Graduate Faculty of
Auburn University
in partial fulfillment of the
requirements for the Degree of
Doctor of Philosophy

Auburn, Alabama
May 7, 2016

Copyright 2016 by Mohammad Jalayer

Approved by

Huaguo Zhou, Chair, Associate Professor of Civil Engineering
Rod E. Turochy, Associate Professor of Civil Engineering
Jeffrey J. LaMondia, Assistant Professor of Civil Engineering
Wesley C. Zech, Associate Professor of Construction Engineering and Management
Jie Gong, Assistant Professor of Civil Engineering, Rutgers, The State University of New Jersey

Abstract

A roadway departure (RwD) crash, comprising run-off-road (ROR) and cross median/cross centerline head-on collisions, is defined as a crash in which a vehicle crosses an edge line, a centerline, or otherwise leaves the traveled way. These types of crashes tend to be more severe than other crash types (e.g., rear end, head on, sideswipe). According to the U.S. National Highway Traffic Safety Administration (NHTSA), in 2013, 56 percent of all motor vehicle fatalities involved RwD crashes. Moreover, ROR crashes accounted for 62 percent of the total number of fatal motor vehicle crashes in the United States in that year. There are a number of reasons a driver may leave the travel lane, including, but not limited to, an avoidance maneuver, inattention or fatigue, or traveling too fast with respect to weather or geometric road conditions. There are also a number of roadway design factors that can increase the probability that driver error will result in an RwD crash (e.g., travel lanes that are too narrow, substandard curves, and unforgiving roadsides). Moreover, the probability of the severity of RwD crashes depends on the roadside features, including sideslopes, fixed-object density, offset to fixed objects, and shoulder width. The high fatality rates associated with this crash type necessitates further investigation to build a roadside inventory database, identify the factors contributing to crashes, and then to implement effective safety countermeasures. This dissertation is a collection of four papers as separate chapters.

Chapter 1 evaluates the capability of existing methods for collecting roadside features vital to the effective implementation of the Highway Safety Manual (HSM) (published in 2010). Since

the release of the HSM, many states have sought to tailor various safety measures and functions within the report to better reflect road safety in their specific locations. However, the widespread utilization of the HSM faces significant barriers as many state departments of transportation (DOTs) do not have sufficient HSM-required highway inventory data. A significant amount of roadside information is missing in most databases, such as roadside slope, grade, roadside fixed objects and their density, and offset to the edge of the travel way. Many techniques have been used by state DOTs and local agencies to collect highway inventory data for other purposes, but it is unknown which of these methods or combination of methods is capable of efficient data collection while also minimizing cost and safety concerns. By virtue of the fact that many state DOTs are currently redesigning their asset management plans to meet the performance requirements of the national Moving Ahead for Progress in the 21st Century Act (MAP-21), there is a need to better understand the potential applications of existing highway inventory data collection methods for gathering HSM-related roadway inventory data.

Chapter 2 identifies the significant contributing factors to ROR crashes, which have accounted for the majority of Rwd events, using an exploratory data analysis (EDA) technique to determine the dataset structure. To realize the vision of the FHWA's *Toward Zero Deaths*, one of the challenges researchers and state DOTs face is how to identify key contributing factors within large and complex datasets in order to implement effective safety countermeasures accordingly.

Chapter 3 presents an overview of cost-effective improvements for preventing vehicle departures from roadways, and it provides transportation practitioners with a good understanding of the effectiveness of Rwd safety countermeasures. In order to realize the vision of the Federal Highway Administration's (FHWA's) *Toward Zero Deaths*, many safety countermeasures (e.g.,

signs, pavement safety, and roadside design) have recently been implemented by state DOTs and local agencies to mitigate RwD crashes.

Chapter 4 presents a new reliability analysis approach to evaluating roadside safety for rural two-lane roads. Currently, the clear zone width and sideslope are used to determine the roadside hazard rating (RHR) and to quantify roadside safety for rural two-lane roadways on a seven-point pictorial scale. Since these two variables are continuous and can be treated as random variables, probabilistic analysis can be applied as an alternative method to account for uncertainty. Specifically, by emphasizing reliability analysis, it is possible to quantify the roadside safety level by treating the clear zone width and sideslope as two continuous, rather than discrete, variables and to calculate their reliability indices accordingly.

As a national priority, the findings of this dissertation can prevent or mitigate the frequency and severity of RwD crashes, which will result in saving lives and reducing crash costs to society overall. It also provides guidance for all state DOTs, as a national-level resource, to obtain a better knowledge of cost-effective roadside inventory data collection methods, factors contributing to RwD crashes, and associated safety countermeasures, all of which will yield multiple national benefits.

Dedication

To Sara

Acknowledgments

I would like to sincerely express my gratitude to my adviser, Professor Huaguo Zhou, for his guidance, countless support, kindness, and patience during my study. I wish to thank my doctoral committee members, Professor Rod E. Turochy, Professor Jeffrey J. LaMondia, Professor Wesley C. Zech, and Professor Jie Gong, who shared with me their expertise and precious time. A thanks to Professor Ana Franco-Watkins for reading and reviewing my dissertation.

Special thanks to my parents, my sister, and my brothers for their love, care, and support. I acknowledge the Illinois Department of Transportation (IDOT), the Illinois Center for Transportation (ICT), and the American Traffic Safety Services Association (ATSSA) for the support of parts of this research.

Table of Contents

Abstract	ii
Dedication	v
Acknowledgments.....	vi
List of Tables	x
List of Figures	xi
Abbreviations	xii
Symbols.....	xv
CHAPTER 1: A Comprehensive Assessment of Highway Inventory Data Collection Methods...	1
1.1. Introduction.....	2
1.2. Prior Work	3
1.2.1. Highway Inventory Data for Highway Safety Manual	3
1.2.2. Review of Highway Inventory Data Collection Methods	6
1.3. Survey Data Collection and Analysis	8
1.4. Field Trial and Results	11
1.4.1. GPS Data Logger	12
1.4.2. Robotic Total Station	14
1.4.3. GPS Enabled Photo/Video Logging.....	16
1.4.4. Satellite/Aerial Imagery	17
1.4.5. Mobile LiDAR	18
1.5. Comparative Analysis of Selected Data Collection Methods.....	21
1.6. Conclusions and Recommendations	22
CHAPTER 2: Exploratory Analysis of Run-Off-Road Crash Patterns	24
2.1. Introduction.....	25
2.2. Prior Work	26
2.3. Method and Data.....	28
2.3.1. Multiple Correspondence Analysis	28

2.3.1.1. Cloud of Individuals.....	29
2.3.1.2. Cloud of Categories.....	30
2.3.2. Data	31
2.4. Results and Discussions.....	34
2.5. Conclusions.....	38
CHAPTER 3: Overview of Safety Countermeasures for Roadway Departure Crashes.....	40
3.1. Introduction.....	41
3.2. Roadway Departure Safety Countermeasures	43
3.2.1. Signs.....	48
3.2.1.1. Chevrons.....	48
3.2.1.2. Dynamic Curve Warning Systems	48
3.2.1.3. Advanced Curve Warning and Advisory Speed Sign	49
3.2.2. Pavement Safety.....	49
3.2.2.1. High Friction Surface Treatments	49
3.2.2.2. Raised Pavement Markers.....	50
3.2.2.3. Edge Line Pavement Markings	50
3.2.2.4. Safety Edge	51
3.2.2.5. Centerline Rumble Strips	51
3.2.2.6. Shoulder Rumble Strips	52
3.2.3. Roadside Design.....	52
3.2.3.1. Cable Barrier	52
3.2.3.2. Guardrail.....	53
3.2.3.3. Shoulder Widening.....	54
3.2.3.4. Breakaway Supports for Signs and Lighting.....	54
3.2.3.5. Clear Zone Improvements.....	54
3.3. Summary	55
CHAPTER 4: Evaluating the Safety Risks of Roadside Features for Rural Two-Lane Roads using Reliability Analysis.....	56
4.1. Introduction.....	57
4.2. Prior Work	60

4.3. Method and Data.....	63
4.3.1. Reliability Analysis	63
4.3.2. Segment and Crash Data	66
4.4. Results and Discussions.....	67
4.5. Limitations	75
4.6. Conclusions and Recommendations	75
References.....	77
Appendix A.....	96

List of Tables

Table 1.1 Highway Inventory Data Required for Road Segments in the Highway Safety Manual	4
Table 1.2 Highway Inventory Data Required for Intersections in the Highway Safety Manual	5
Table 1.3 Categorization of Highway Inventory Data Collection Methods	6
Table 1.4 Existing Highway Inventory Data Collection Methods and Related Studies	7
Table 1.5 Levels of Satisfaction for Primary Data Collection Method of State DOTs	10
Table 1.6 Level of Satisfaction on Adopted Inventory Data Collection Methods by State DOTs	11
Table 1.7 Proposed Data Reduction Methods.....	12
Table 1.8 Comparison between Different Highway Inventory Data Collection Methods	21
Table 1.9 Evaluation Matrix for Highway Inventory Data Collection Methods	22
Table 2.1 Distributions of Segments Based on Study Categories	32
Table 2.2 Significance of Test Results for Key ROR Contributing Factors in Top Two Dimensions	37
Table 3.1 Results from the 14 Case Studies	46
Table 4.1 Probability of Failure vs. Reliability Index	66
Table 4.2 Distributions of Segments Based on Crash Frequency and Severity.....	67
Table 4.3 Results of Normality Tests for Observed Clear Zone and Sideslope of Segments with No Crash	70
Table 4.4 Statistical Parameters of the Fitted Normal Distribution.....	70
Table 4.5 Statistical Parameters of the Safety Margin Distributions.....	70
Table 4.6 Probability of Non-compliance and Reliability Index vs. Crash Rate.....	71
Table A1. Highway Inventory Data Collection Survey.....	96

List of Figures

Figure 1.1 Technology Adoption Percentage in Respondent States.....	9
Figure 1.2 A GPS Data Logger Device for Data Collection.....	12
Figure 1.3 A Sample of Slope Banding	14
Figure 1.4 A Robotic Total Station Device for Data Collection.....	15
Figure 1.5 A Video Logging System Configurations in Use for Data Collection.....	16
Figure 1.6 A Sample of Object Extraction Using Both Video Logging and High-Resolution Imagery	17
Figure 1.7 Data Extracted Using Satellite/Aerial Imagery Method.....	18
Figure 1.8 A Mobile Lidar System Configuration in Use for Data Collection.....	19
Figure 2.1 A Flowchart of Working Steps.....	34
Figure 2.2 Eigenvalues and Variances of the Top Five Dimensions	35
Figure 2.3 MCA Plot of All Study Variables	36
Figure 2.4 MCA Plot of Top 20 Key Categories	38
Figure 3.1 Percentage of Fatal Motor Crashes in the United States in 2013	41
Figure 3.2 Average Percentage of Rwd Fatalities in Each State (2007-2013)	42
Figure 3.3 Rwd Crash Safety Countermeasures	44
Figure 4.1 Roadside Hazard Rating Scale	58
Figure 4.2 Graphical Relationship between Reliability Index and Statistical Parameters of Pf ..	65
Figure 4.3 Observed Clear Zone of Segments for Five Crash Categories	68
Figure 4.4 Observed Sideslope of Segments for Five Crash Categories	69
Figure 4.5 Safety Margin vs. Crash Rate	73
Figure 4.6 Reliability Index vs. Crash Rate.....	74

Abbreviations

AAA	American Automobile Association
AADT	Annual Average Daily Traffic
AASHTO	American Association Of State Highway And Transportation Officials
ADT	Average Daily Traffic
ALDOT	Alabama Department Of Transportation
ATSSA	American Traffic Safety Services Association
B/C	Benefit-Cost
CAD	Computer Aided Design
CLRS	Centerline Rumble Strips
DCWSs	Dynamic Curve Warning Systems
DOT	Department Of Transportation
DUI	Driving Under Influence
EB	Empirical Bayes
FARS	Fatality Analysis Reporting System
FE	Fixed-Effects
FHWA	Federal Highway Administration
GNSS	Global Navigation Satellite Systems
HFSTs	High Friction Surface Treatments
HIDC	Highway Inventory Data Collection
HMA	Hot-Mix Asphalt
HRRRS	High Risk Rural Roads
HSM	Highway Safety Manual
ICT	Illinois Center For Transportation
IDOT	Illinois Department Of Transportation
Iowa DOT	Iowa Department Of Transportation

KYTC	Kentucky Transportation Cabinet
LEDs	Light-Emitting Diodes
LiDAR	Light Detection And Ranging
LSF	Limit State Function
MAP-21	Moving Ahead For Progress In The 21st Century Act
MCA	Multi-Criteria Analysis
MCA	Multiple Correspondence Analysis
MDOT	Michigan Department Of Transportation
MnDOT	Minnesota Department Of Transportation
MoDOT	Missouri Department Of Transportation
Mph	Mile per Hour
MRI	Midwest Research Institute
MUTCD	Manual On Uniform Traffic Control Devices
NCDOT	North Carolina Department Of Transportation
NCHRP	National Cooperative Highway Research Program
NHTSA	National Highway Traffic Safety Administration
ODOT	Oregon Department Of Transportation
PDF	Probability Density Function
PDO	Property Damage Only
RHR	Roadside Hazard Rating
RMSE	Root-Mean-Square Error
ROR	Run-Off-Road
ROTRR	Run-Off-Road To The Right Side
RPMs	Raised Pavement Markers
RwD	Roadway Departure
SHSP	Strategic Highway Safety Plan
SPF	Safety Performance Function
SRS	Shoulder Rumble Strips
SSD	Stopping Sight Distance

TRP	Technical Review Panel
usRAP	United States Road Assessment Program
WF	Weighing Factor
WSDOT	Washington State Department Of Transportation

Symbols

$(N^j N^{j'})^2$	Squared distance between categories j and j'
$D^2(i, i')$	Overall squared distance between individuals i and i'
D_c	PDF of safe (capacity) clear zone
D_o	PDF of observed clear zone
S_c	PDF of (safe) capacity sideslope
S_o	PDF of observed sideslope
$d_m^2(i, i')$	Squared distance between individuals i and i' for variable m
$d_m^2(i, i')$	Squared distance between individuals i and i' for variable m
$f_{j'}$	Relative frequency of individual records that selected category j'
f_j	Relative frequency of individual records that selected category j
$n_{j'}$	Number of individuals that selected category j'
$n_{jj'}$	Number of individuals that selected both categories j and j'
n_j	Number of individuals that selected category j
μ_g	Mean of the safety margin
I	Set of i individual records
J	Set of categories of all variables
R^2	Coefficient of determination
Φ	Standard normal distribution
M	Set of all variables
g	Limit state function (LSF)
β	Reliability index

**CHAPTER 1: A Comprehensive Assessment of Highway Inventory
Data Collection Methods**

1.1.Introduction

The Highway Safety Manual (HSM) provides decision makers and engineers with the information and tools to improve roadway safety performance [1]. In the first edition of the HSM, predictive methods, which can be employed to quantitatively estimate the safety of a transportation facility in terms of number of crashes, were provided for three types of facilities: rural two-lane roadways, rural multi-lane highways, and urban/suburban arterials. A National Cooperative Highway Research Program (NCHRP) 17-45 project recently developed safety prediction models for freeways and interchanges [2]. Since the release of the HSM in 2010, many states have sought to tailor the various safety measures and functions within the report to better reflect road safety in their specific locations [3, 4]. This manual provides valuable insight that can help practitioners prioritize projects, compare different alternatives, and select the most appropriate countermeasures in the planning, design, construction, and maintenance process. The countermeasures can be any of the three Es: Education (e.g., raising safety awareness), Engineering (e.g., signal timing improvement), and Enforcement (e.g., implementing red light cameras at intersections) [5].

To implement methods presented in the HSM, a major challenge for state and local agencies is the collection of necessary roadway information along thousands of miles of highways [6]. Collecting roadway asset inventory data often incurs significant but unknown cost. To date, state Departments of Transportation (DOTs) and local agencies have employed a variety of methods to collect the roadway inventory data, including field inventory, photo/video log, integrated GPS/GIS mapping systems, aerial photography, satellite imagery, airborne Light Detection and Ranging (LiDAR), static terrestrial laser scanning, and mobile LiDAR [6]. These methods vary based on equipment needed, time required for both collecting data and reducing data, and costs. Each method has its specific advantages and limitations. Particularly, vehicle-mounted LiDAR, a relatively new type of mobile mapping system, is capable of collecting a large amount of detailed 3D highway inventory data, but it requires expensive equipment and significant data reduction efforts to extract the desired highway inventory data. On the other hand, a traditional field survey requires less equipment investment, training, and data reduction efforts. However, this method is not only time-consuming and labor-intensive, but also exposes data collection crews to dangerous roadway environments.

The efforts and costs associated with collecting various data with different techniques vary greatly. Therefore, there is a need to understand the application of existing highway inventory data collection (HIDC) methods for gathering HSM-related roadway inventory data. This chapter sought to present an in-depth review of various roadway asset inventory data collection methods and to compare the quality and desirability of these methods. A national survey was conducted to all the state DOTs to collect the related information towards these various data collection techniques. Additionally, field trials were conducted to identify the most promising methods for collecting and recording highway inventory data to support HSM implementation. By virtue of the fact that many state DOTs are currently redesigning their asset management plans to meet the national Moving Ahead for Progress in the 21st Century Act (MAP-21) requirements, the outcomes of this research effort may provide a resource for saving money and time.

1.2.Prior Work

1.2.1.Highway Inventory Data for Highway Safety Manual

The HSM can be used to predict the safety performance of a roadway segment or an intersection. The safety performance is evaluated by using a system of equations, known as Safety Performance Functions (SPFs), to estimate the average crash frequency based upon roadway characteristics and traffic conditions [1]. The input data for different types of roadway segments and intersections are quite different [7, 8]. Tables 1.1 and 1.2 summarize the required input data for the safety predictive models in the HSM [1]. The check mark indicates the required variables for roadway segments and intersections. Currently, few states have existing highway inventory databases that contain all the required variables for the input of the HSM models. Particularly, a significant amount of roadside information, such as roadside slope, grade, roadside fixed objects and their density, and offset to the edge of travel way are missing in the current Illinois Department of Transportation (IDOT) databases [9]. Therefore, the main objective of this chapter is to evaluate which data collection method is able to collect those roadside features in the most economical and effective way. Due to the fact that these features are also absent in many state DOTs databases, the findings of this chapter will be helpful to provide guidance for other states.

Table 1.1 Highway Inventory Data Required for Road Segments in the Highway Safety Manual [1]

Variables	Rural Two-lane Highways	Rural Multilane Highways	Urban/ Suburban Arterials	Descriptions
Number of through lanes	√	√	√	
Lane width	√	√		
Shoulder width	√	√		
Shoulder type	√	√		
Presence of median		√	√	
Median width		√		
Presence of passing lane	√			
Presence of rumble strips	√			A road safety feature that alert inattentive drivers by causing a tactile vibration
Presence of two-way left-turn lane	√		√	
Driveway density	√			
Number of major/minor commercial driveways			√	
Number of major/minor residential driveways			√	
Number of major/minor industrial/institutional driveways			√	
Number of other driveways			√	
Horizontal curve length	√			A feature that increases road safety and comfort in the design of horizontal curves
Horizontal curve radius	√			A feature that increases road safety and comfort in the design of horizontal curves
Horizontal curve superelevation	√			A feature that allows a driver to negotiate a curve at a higher speed and more convenient
Presence of spiral transition	√			A feature used to gradually change the curvature and superelevation of a roadway
Grade	√			A feature determined by the percent grade for the roadway between each point of change in grade
Roadside hazard rating	√			A feature is used to characterize the potential hazard related to roadside environment

Table 1.1 Highway Inventory Data Required for Road Segments in the Highway Safety Manual, cont. [1]

Variables	Rural Two-lane Highways	Rural Multilane Highways	Urban/ Suburban Arterials	Descriptions
Roadside slope		√		A feature determined by the slope ratio (the vertical rise divided by horizontal run) for the foreslope (the slope extends from the outside of the shoulder to the bottom of the ditch)immediately outside the roadway shoulder
Roadside fixed object density/offset			√	A feature determined by the number of roadside fixed objects on both sides of the roadway segments divided by the length of the segment
Percent of length with on-street parking			√	
Type of on-street parking			√	
Presence of lighting	√	√	√	
Presence of auto speed enforcement	√	√	√	

Table 1.2 Highway Inventory Data Required for Intersections in the Highway Safety Manual [1]

Variables	Rural Two-lane Highways	Rural Multilane Highways	Urban/Suburban Arterials	Descriptions
Number of intersection legs	√	√	√	A feature determined by the number of approaches in each intersection
Number of approaches with left-turn lane(s)	√	√	√	
Number of approaches with right-turn lane(s)	√	√	√	
Intersection skew angle	√	√		A feature determined by angle at which the legs of an intersection meet
Presence of lighting		√	√	
Pedestrian volume/lane			√	
Number of bus stop within 1000 ft			√	
Number of alcohol sales within 1000 ft			√	
Presence of schools within 1000 ft			√	

1.2.2. Review of Highway Inventory Data Collection Methods

Lately, advanced methods have been used to gather data in the fields of traffic safety [10-20], traveler and driver behaviors [21-29], network modeling [30-35], transportation planning [36-41], and asset management [42-46]. HSDC methods can be broadly divided into two different categories: land-based and air- or space-based methods as shown in Table 1.3 [47]. These methods vary in equipment used, data collection time, data reduction time, accuracy, and cost. A brief description of the available data collection methods and related studies is provided in Table 1.4.

Table 1.3 Categorization of Highway Inventory Data Collection Methods

	Land Based	Air or Space Based
GPS	<ul style="list-style-type: none"> • Field Inventory • Integrated GPS/GIS Mapping 	
GPS + Imaging	<ul style="list-style-type: none"> • Photo/Video Log 	<ul style="list-style-type: none"> • Satellite Imagery • Aerial Imagery
GPS + Imaging + LiDAR (using a laser to illuminate a target and measure the reflected light)	<ul style="list-style-type: none"> • Static Terrestrial Laser Scanning (Using direct 3D precision point information acquired from stationary 3D laser scanners to extract highway inventory data) • Mobile LiDAR (driving an instrumented vehicle while collecting direct 3D precision point information using either land-based LiDAR systems or photogrammetry systems while traveling at highway speeds) 	<ul style="list-style-type: none"> • Airborne LiDAR (Using direct 3D precision point information acquired from aircraft-based LiDAR systems to derive highway inventory data)

Table 1.4 Existing Highway Inventory Data Collection Methods and Related Studies

		Methods						
		Field Inventory	Photo/Video Log	Integrated GPS/GIS Mapping Systems	Aerial/Satellite Photography	Terrestrial Laser Scanning	Mobile LiDAR	Airborne LiDAR
Description		Uses GPS survey equipment and conventional optical to collect desired information in the field	Driving a vehicle along the roadway while automatically recording photos/videos which can be examined later to extract information	Using an integrated GPS/GIS field data logger to record and store inventory information	Analyzing high resolution images taken from aircraft or satellite to identify and extract highway information	Using direct 3D precision point information (3D point clouds) acquired from stationary 3D laser scanners to extract highway inventory data	Driving an instrumented vehicle while collecting direct 3D precision point information using either land-based LiDAR systems or photogrammetry systems while traveling at highway speeds	Using direct 3D precision point information acquired from aircraft-based LiDAR systems to derive highway inventory data
Advantages		Low initial cost, low data reduction effort, and capability of collecting rich and highly accurate roadway inventory data	Less exposure to traffic and short field data collection time	Low initial cost, low data reduction effort, and the ability to transfer inventory data back to the home office through a wireless connection	Elimination of field work and data collection time, no traffic exposure, no disruption to traffic, and compatibility of images with GPS	Operating in daylight or darkness, high data accuracy and extremely rich and accurate data collection that is valuable to multiple DOT programs	Collecting huge amounts of data in a very short time, survey crew safety is superior compared with traditional survey methods	No exposure to traffic, short field data collection time, and collection of rich data in a short amount of time
Disadvantages		Crew exposure to traffic and long field data collection time	Inability to measure feature dimensions and need for large data reduction efforts	Crew exposure to traffic, long field collection time, and GPS outage problems due to trees	Difficulty to identify features such as signs or traffic signals from overhead imagery	Long field data collection time, exposure to traffic, high initial cost, long data reduction time, and large data set size	The need for expensive equipment, long data extraction time, and large data set size	High initial cost, large data set size, and long data reduction time
Related Studies		[48]	[49-58]	[59]	[60, 61]	[62-64]	[65-78]	[79-86]

In general, it can be noted that although there are a considerable number of studies on various HIDC methods, none of them have solely focused on supporting HSM implementation. Therefore, the challenge is to match the best methods to HSM-oriented highway inventory applications. Additionally, it is not clear to what extent these methods have been implemented by various state DOTs. Such information might aid other state DOTs and teach valuable lessons regarding which methods are preferred. This chapter was aimed at characterizing the utility of these existing HIDC methods for collecting HSM-required road inventory data through a national survey and field evaluation of selected HIDC methods.

1.3.Survey Data Collection and Analysis

In many states, there is a lack of worthy highway databases that include all the required variables as inputs for the HSM predictive models. On the other hand, many state DOTs do have road inventory databases that provide some data elements that can be used in the HSM predictive models. It was of interest to determine how different state DOTs have collected these inventory data, and whether there is any lesson that can be learned from them. To gain an understanding of the implementation status of various HIDC methods and their perceived strengths and shortcomings, a web-based survey was developed and sent to 50 state DOTs and seven Canadian provinces. More specifically, the respondents were asked to indicate their primary data collection methods and their opinions on the adopted methods regarding cost, time, accuracy, safety, and data storage requirements. The survey (Appendix A) has focused on a few roadside features that are known to be difficult to collect but play an important role in the HSM models.

The survey analysis results, based upon 30 respondent states (60 percent response rate), demonstrated that over 50% of responding states use field inventory, integrated GPS/GIS mapping, video log, and aerial imagery for collecting roadside feature data. In truth, the field inventory method is still required for many roadway features due to equipment limitations since new technologies may not be suitable for all assets. According to the survey results, it is evident that satellite imagery and airborne LiDAR are less popular choices among state DOTs because it is difficult to identify small objects using these methods. Additionally, mobile LiDAR is uncommon but appears to be growing and most popular. Figure 1.1 depicts the percentage of states using each

type of HIDC method. It should be noted that some states use multiple methods that account for the total being more than 100%.

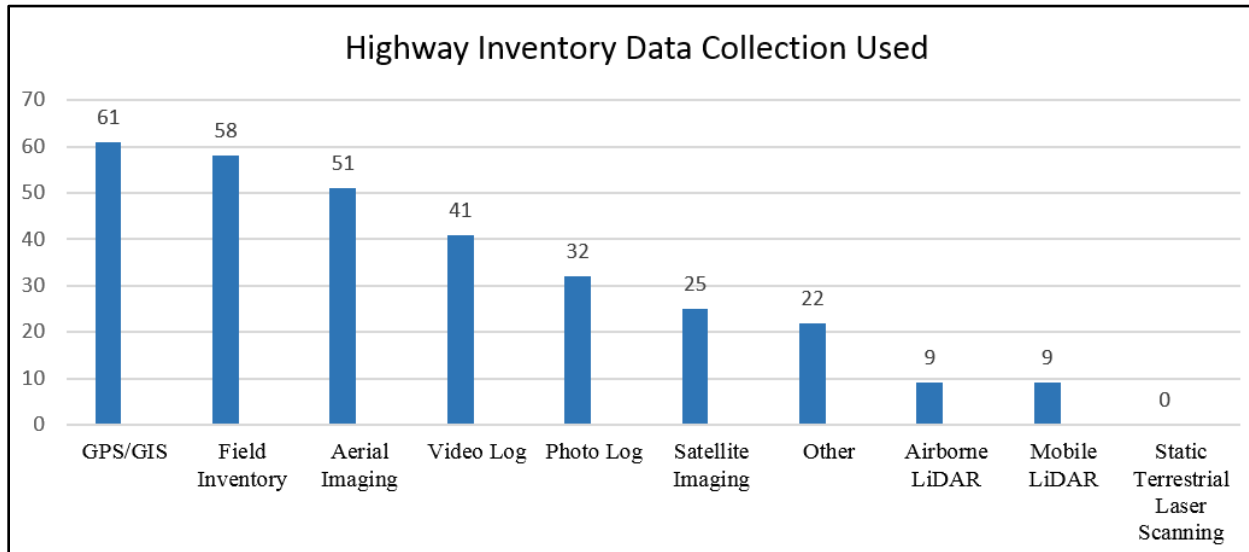


Figure 1.1 Technology Adoption Percentage in Respondent States

It should be noted that most of the respondent states indicated that they use a combination of several data collection methods to meet their roadside inventory data needs. The results revealed that guardrails, shoulders, and mileposts are the most predominant objects being collected but using different methods. Moreover, only 9 % of states collected roadside slope and curvature alignments.

Additionally, the survey respondents were requested to indicate their level of satisfaction with their primary collection method using a scale of 1 to 5 (representing unacceptable, fair, good, very good, and excellent, respectively) where one is worst and five is the best. Table 1.5 illustrates the results for the nine satisfaction indicators considered in the survey, including equipment cost, data accuracy, data completeness, crew hazard exposure, data collection cost, data collection time, data reduction cost, data reduction time, and data storage requirement. Based on these parameters, most states express their level of satisfaction as good for the primary data collection methods, which they have used more frequently to collect the required datasets.

Table 1.5 Levels of Satisfaction for Primary Data Collection Method of State DOTs

Satisfaction Factors	Unacceptable (%)	Fair (%)	Good (%)	Very Good (%)	Excellent (%)	Sum (%)
Equipment Cost Rating	0	21	58	21	0	100
Data Accuracy Rating	0	7	41	45	7	100
Data Completeness Rating	7	17	34	34	7	100
Crew Hazard Exposure Rating	4	29	39	21	7	100
Data Collection Cost Rating	3	24	55	17	0	100
Data Collection Time Rating	3	34	48	14	0	100
Data Reduction Time Rating	11	26	30	26	7	100
Data Reduction Cost Rating	4	39	29	21	7	100
Data Storage Requirement Rating	0	14	52	31	3	100

The data shown in Table 1.5 indicates that most agencies rated their current systems from fair to good for most performance categories. Table 1.6 presents the rating of each satisfaction indicator in Table 1.5 for each data collection method based on the level of satisfaction with the primary data collection method. It showed that satellite imagery, photo logs, and aerial imagery scored highest on all of the evaluation elements. Examination of the scores of different evaluation elements reveals that most methods had lower rankings for data reduction time, data collection time, and data collection cost. This clarifies that the focus of concern of state DOTs is on the time required for data collection and reduction and the associated cost. Moreover, state DOTs who used either airborne LiDAR or mobile LiDAR expressed less satisfaction towards these two methods in equipment cost, data reduction cost, and data reduction time performance categories. Their concerns are clearly related to the data reduction time associated with these two methods. Both methods collect a tremendous volume of data that is difficult to process. Some of the other interesting findings were that the New York State DOT rates its GPS/GIS system as unacceptable to fair in several categories, and the California State DOT appears generally dissatisfied with its photo log system. Overall, no single technology stands out as the obvious choice of methods for roadside feature data collection, and most agencies perceive that their inventory methods could be substantially improved.

Table 1.6 Level of Satisfaction on Adopted Inventory Data Collection Methods by State DOTs

Satisfaction Factors	Highway Inventory Data Collection Methods							
	Satellite Imagery	Photo Log	Aerial Imagery	Field Inventory	Video Log	Integrated GPS/GIS Mapping	Mobile LiDAR	Airborne LiDAR
Equipment Cost Rating	3.1	3.0	3.1	3.1	3.1	2.9	2.0	2.5
Data Accuracy Rating	3.3	3.5	3.6	3.5	3.4	3.8	3.0	3.0
Data Completeness Rating	3.2	3.3	3.3	3.4	3.3	3.3	3.4	2.8
Crew Hazard Exposure Rating	3.2	3.4	2.9	2.9	2.9	3.0	2.5	3.0
Data Collection Cost Rating	3.2	2.9	3.0	2.8	3.0	2.8	2.5	2.5
Data Collection Time Rating	3.2	2.8	2.9	2.8	2.8	2.7	2.6	2.0
Data Reduction Time Rating	2.8	3.1	2.9	3.1	2.8	2.9	2.0	2.0
Data Reduction Cost Rating	3.2	3.1	2.9	2.7	2.8	2.8	2.5	2.0
Data Storage Requirement Rating	3.2	3.5	3.4	3.3	3.1	3.3	3.0	3.4

1.4. Field Trial and Results

Based on the literature review and survey, the research team identified five potential methods to be further evaluated: GPS data logger, robotic total station, GPS enabled photo/video log, satellite/aerial imagery, and mobile LiDAR. Four different types of roadway segments, including rural two-lane highway, rural multi-lane highway, urban and suburban arterial, and freeway segment, were chosen as the test sites for these methods. These segments varied in length but were not shorter than one mile.

The data reduction effort required for each data collection technique has a significant impact on the utility of the technique. Specifically, one previous study revealed that the manual data collection was more cost-effective than automated methods such as mobile mapping systems, as the latter incur high equipment costs and significantly greater data reduction effort [48]. However, recent developments in automated data reduction methods and declining equipment costs (e.g., laser, camera) may have changed this conclusion. Given this fact, the research team recorded the time spent conducting data reduction tasks such as extracting objects, determining clear zone distance, side slope and other parameters from datasets. A list of promising data collection methods and the proposed data reduction methods are provided in Table 1.7. Moreover, researchers also evaluated the feasibility and training needs for DOT personnel to use these programs. In general, the effort of data reduction was directly proportional to the quantity and richness of data collected in the field.

Table 1.7 Proposed Data Reduction Methods

Data Collection Method	Data Reduction Method (if required)	Descriptions
Field Inventory	N/A	
Photo/Video Log	Manual review, photogrammetry	
Integrated GPS/GIS Mapping Systems	N/A	
Aerial Photography	GIS package (ArcGIS)	
Satellite Imagery	GIS package (Google Earth Pro)	
Mobile LiDAR	Point cloud post-processing software	A software which has a capability to decimate files intelligently without losing the important featured-related information such as locations

1.4.1. GPS Data Logger

A GPS data logger is a GPS unit that records time of observation, location, elevation, and crew-entered notes. The data logger is equipped with an internal camera, allowing images of recorded locations to be stored and associated with the location data. Output from the data logger may be viewed on a mapping application such as Google Earth. Figure 1.2 illustrates a sample of this device in use to locate a traffic sign.



Figure 1.2 A GPS Data Logger Device for Data Collection

In general, the GPS data logger device is very user-friendly, reduces the need for extensive training, and can be operated by one surveyor. As for data collection, the GPS data logging technique is accomplished by placing the device next to the object to be recorded. In doing so, at

the beginning of data collection work, the device must be initialized. Initialization refers to the automated startup routine that GPS receivers employ to scan the visible sky, identify observable satellites, and make a location determination. Depending on the number of satellites in view and their geometrical distribution above the target, this process may require from a few minutes to as many as 15 minutes. Once initialization is complete, location data is provided in real time even if the receiver is in motion. Notably, in this method, data collection time is very sensitive to the type of objects, the objects' density, the distance between objects, and the terrain. Therefore, using a four-wheel, all-terrain vehicle can reduce data collection time significantly (Figure 1.2). In this study, by the help of the aforementioned vehicle, the average times for setting up the device and collecting data per object were five minutes and one minute, respectively.

As to the data reduction effort, one of the primary tasks is the organization of all data collected for the purpose. The data reduction steps required by this method, for this research, included importing the collected data files into a Computer Aided Design (CAD) software program (e.g. AutoCAD Civil 3D), establishing a drawing-file template which includes many of the standard file settings and objects for use in a new file, and importing the resulting data files into the drawing format. The latter consisted of a series of discrete points with associated elevation and description attributes. By virtue of the drawing file, a highway alignment drawing was assembled. Moreover, additional processing using the discrete point elevations to define a surface representing the topography, called "slope banding," was simultaneously employed to identify roadside slope based upon percentage of slope (in dark color) (Figure 1.3).

In this study, the analysis of results demonstrated that the GPS data logger not only can gather all the objective highway inventory data to be implemented in the HSM but also can meet the accuracy required by the HSM safety predictive models; i.e., four inches accuracy of feature locations can be achieved. One of the shortcomings is the likelihood of GPS outage in areas with tall buildings and significant tree cover. Crew exposure to traffic is another issue that requires mitigation strategies such as setting up warning signs and traffic cones which consumed a significant percentage of the time required to survey each segment.

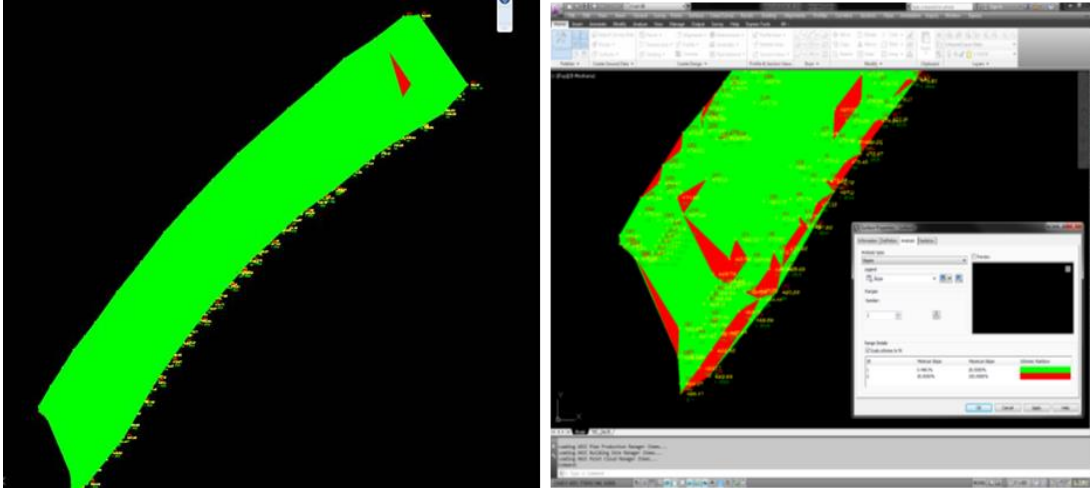


Figure 1.3 A Sample of Slope Banding

1.4.2. Robotic Total Station

During the late 1980s, electronic distance measuring equipment was successfully integrated with electronic theodolites, used for measuring angles in horizontal and vertical planes, to create "total station" surveying instruments. This new generation of surveying instrument directly displays horizontal and vertical angles, slope distance, and derived horizontal distance, vertical distance, and x,y,z coordinates. With the addition of electronic data collection in the early 1990s, survey field work productivity has dramatically improved. A typical survey crew using a total station instrument consists of three people: an instrument person to point the instrument and initiate measurement, a party chief to direct the work and sketch additional data, and a rodman to walk to the object to be recorded and plumb the reflector prism equipped survey rod over the object. Surveying total stations and robotic total stations employ electronic distance measuring systems that measure the time required for light to travel from the instrument to the target and back. A retro-prism mounted on a pole is placed at the target and the instrument's light beam is directed toward it and then sent directly back by the reflective prism. By adding auto tracking of the prism via radio links and robotic servos, total station systems have been developed that automatically continuously track the prism target and transmit data to a data collector and operating controller located on the prism pole. This type of system is referred to as a robotic total station. A robotic total station may be operated by a single person who controls the robotic total station remotely while walking with the prism pole and data collector. During this study, a single surveyor using a

robotic total station required an average of one minute to collect information for each object. Figure 1.4 depicts the robotic total station in use during the data collection activities. Notably, in comparison with the GPS data logging, the initial system setup and data collection time per object were higher.



Figure 1.4 A Robotic Total Station Device for Data Collection

The robotic total station method requires the same data reduction effort. As GPS data logging. A skilled operator, using up-to-date software, has the capability to process survey crew-derived data at rates in excess of 2,000 ft. per hour. The results indicated that this method is able to collect all the required asset roadway inventory data with a precision of 0.01 ft., more than adequate for the accuracy requirements for implementing the HSM. A major deficiency of the robotic total station method is that it has an operating radius of approximately 1,000 ft. from each setup point. Therefore, the robotic total station must be relocated as the survey progresses, a process that requires approximately 15 minutes for each required move. Loss of prism tracking, which is to automatically point the instrument at the prism at all times by a radio link, video imaging system, and light beam recognition system controlled by the instrument's programmable logic system, is an additional issue associated with robotic total stations. Loss of tracking may be caused by line of sight interference do to terrain or highway traffic. Several minutes may be required to reestablish contact with the robotic total station with every loss of tracking event. To operate the system, the surveyor must walk to the object being measured. This exposes the surveyor to traffic especially when collecting edge of pavement, shoulder, and centerline data. Crew safety must be addressed through warning signs, traffic cones, and high-visibility clothing.

1.4.3. GPS Enabled Photo/Video Logging

The collection of geo-tagged digital videos and photos is carried out using a Red Hen video mapping system (www.redhensystems.com) [87, 88]. Equipped with a video camcorder and a GPS antenna, the video mapping system is able to collect geo-tagged digital video with essential locational information, which may be imported into ArcGIS 9.3 software (with a ArcView 9.3 or Arc Editor 9.3 license) using a video for ArcGIS extension (or GeoVideo) (Figure 1.5). In the instance of data collection time, the GPS enabled photo/video logging requires a relatively short time but an extensive feature extraction effort in the office [89, 90]. In this study, the average time for data collection employing this method was nine minutes per mile.



Figure 1.5 A Video Logging System Configurations in Use for Data Collection

In respect to the data reduction effort, with the help of high-resolution imagery (e.g., 1-ft digital orthophotos, an undistorted aerial imagery which can be used to measure the true distances, or satellite imagery) as a background and video files collected in the field in MPG format that produces better quality videos than other formats, features in the form of points, lines, and polygons can be traced through on-screen digitizing and saved as feature classes in ArcGIS. In the present research, extraction of required features took an average of 50 minutes per mile or one minute per object. Figure 1.6 illustrates an example of object extractions using both video logging and high-resolution imagery.

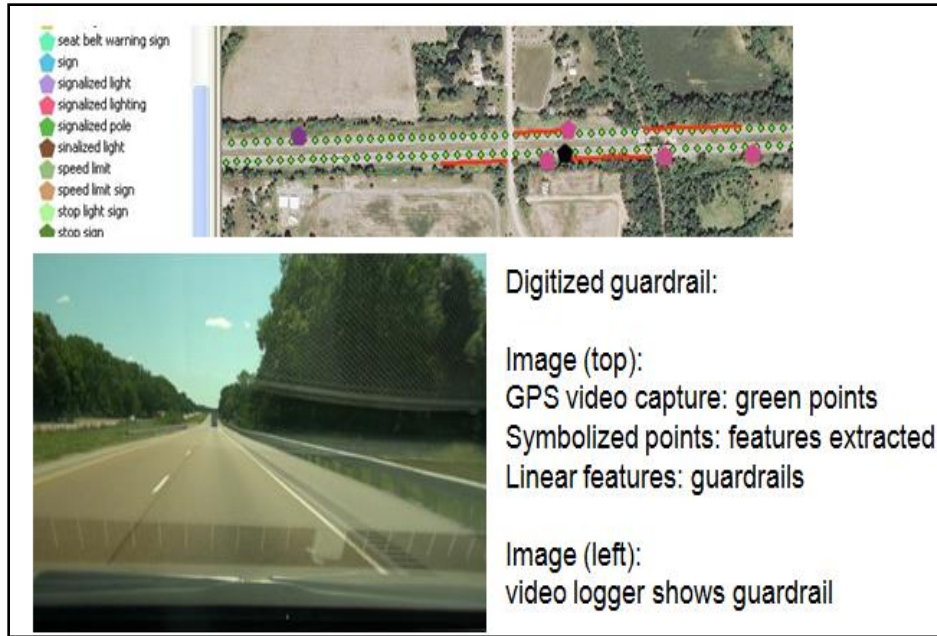


Figure 1.6 A Sample of Object Extraction Using Both Video Logging and High-Resolution Imagery

Due to recording videos on a vehicular platform, this method eliminates the risk of exposing the data collection crew to road traffic. Additionally, working with high-resolution aerial photographs or satellite imagery, the photo/video log method can provide all roadside inventory data to be implemented in the HSM except roadside slope with a reasonable accuracy. A locational accuracy of six inches for all roadside objects is achievable with 1-ft spatial resolution images.

1.4.4. Satellite/Aerial Imagery

Satellite/aerial imagery has been employed over the past several decades to obtain a wide variety of information about the earth’s surface. High-resolution images taken from satellite/aircraft can be utilized to identify and extract highway inventory data input [47, 91]. Therefore, Google maps and Bing maps are two beneficial tools for this purpose. The increasing availability of high-resolution images offers the possibility of leveraging these images to extract some HSM-related roadside features as shown in Figure 1.7. Notably, one of the considerable benefits of the satellite/aerial imagery method is the elimination of data collection efforts since all imagery is already freely accessible. Compared to other methods, therefore, this method is the most economical one due to the absence of the field data collection cost. However, similar to the

photo/video log method, the satellite/aerial imagery is not capable of collecting some HSM-related highway inventory data. For instance, extraction of roadside slope information is very difficult from images and small vertical objects are not quite visible. Based on the analysis of results, in this method, the average extraction time was 1.5 minutes per object.



Figure 1.7 Data Extracted Using Satellite/Aerial Imagery Method (Image: Bing Map)

1.4.5. Mobile LiDAR

Mobile LiDAR is an emerging technology that employs laser scanner technology in combination with Global Navigation Satellite Systems (GNSS) and other sensors to capture accurate and precise geospatial data from a moving vehicle. This system can collect data on approximately 30 miles of highway per day with a high data measurement rate of 50,000 to 500,000 points per second per scanner [47, 75]. Figure 1.8 shows a photo of outside view of a mobile LiDAR van and a picture of computer screen inside the van to show the different mounted cameras and data collection progress.



Figure 1.8 A Mobile Lidar System Configuration in Use for Data Collection (Image: Woolpert Co.)

Regarding data collection, this method is capable of collecting a huge amount of data in a very short time, using an equipped vehicle, in comparison with conventional survey methods. Taking advantage of this technology, in this study, an average of 30 minutes was required to collect information for each mile of segment. However, the data reduction is a major undertaking with mobile LiDAR and the time associated with the data reduction part in this method is significant. Additionally, the processing of and feature extraction from mobile LiDAR data involves a fairly intensive computational effort and requires software and technical expertise. In terms of commercial packages for LiDAR data processing, Terrasolid Suite, Virtual Geomatics, TopoDOT, and QTModeler are found to be applicable for a variety of data extraction purposes. In particular, the Terrasolid Suite is the most commonly used software for airborne and mobile LiDAR data processing. As a result, it was chosen as the program to benchmark the data reduction time. The data processed during the data reduction steps include point clouds which is a set of data points in some coordinate system, geo-referenced imagery, data collection path, and an AutoCAD file. One of concerns with the mobile LiDAR method is the need for large data storage space, here 9.3 Gigabyte (GB) space per mile of roadway. Given this fact, the mobile LiDAR data are typically divided into manageable blocks to reduce any difficulty during the process. For the purpose of this research, a typical block did not exceed 2 GB. As each type of highway segment was broken into

equal sized blocks, data extraction was performed on representative blocks and then the results were utilized to infer the data reduction time for the whole highway segment. In this study, determining roadside slope, roadside fixed objects density, super-elevation rate, and grade took 5, 15, 15 and 15 minutes per block, respectively.

The mobile LiDAR has the capability of collecting all categories of HSM highway inventory data. Although the data collection time in this method is short, the cost of field data collection is higher than other methods. However, these shortcomings cannot overshadow the potential of this method; it collects survey-grade data, which only can be matched by the robotic total station method, but with no traffic exposure or need for road closures. The main strength of this method also lies in its ability to collect data that are valuable for multiple DOT programs. The rapid development of computing hardware and LiDAR data processing methods indicate that the mobile LiDAR method will soon be comparable with other methods in terms of data reduction time.

Overall, GPS data logger and robotic total station can gather all required feature data, but they impose longer field data collection times and expose data collection crews to dangerous road traffic. Photo/video logging and aerial imagery, when used together, can collect nearly all required feature data, except roadside slope. The mobile LiDAR has the capability to collect all required feature data in a short amount of field time, but the data require extensive reduction efforts.

The results of field trials are summarized in Table 1.8. In the table, the capability of each HIDC method is evaluated using the metrics including capability of collecting HSM-related roadside features, total data collection time, total data reduction time, unit data collection and reduction time, and total cost. For cost analysis, two unit labor costs were assumed: \$75 per hour for a person trained at an introductory level and \$130 per hour for an expert level person. Based on the quotes from five LiDAR companies, the average data collection cost per mile for mobile LiDAR was considered to be \$200. In the present research, the photo/video log method required the least total time (man-hr./mi) and the robotic total station method required the most. Specifically, the mobile LiDAR technology ranked at the median level, with 5.5 man-hr./mile.

Furthermore, based on Table 1.8, the total cost per mile to prepare the required highway inventory dataset for photo/video log, satellite/aerial imagery, GPS data logger, mobile LiDAR,

and robotic total station methods were \$72, \$107, \$700, \$915, and \$1,075, respectively. In particular, the photo/video log had the lowest cost and the robotic total station had the highest cost.

Table 1.8 Comparison between Different Highway Inventory Data Collection Methods

Methods	Type of Segment Selected	Capability of Collecting HSM-related Roadside Features	Total Length (mi)	Total Data Collection Time (person-hr)	Total Data Reduction Time (person-hr)	Total Time (person-hr/mi)	Total Cost (\$/mi)
Photo/Video Log	1, 2, 3, 4	Some	28.0	4.0	23.0	0.96	\$72
Satellite/Aerial Imagery	1, 2, 3, 4	Some	7.0	---	10.0	1.43	\$107
Mobile LiDAR	1, 2, 3, 4	All	14.2	8.0	70.0	5.50	\$915
GPS Data Logger	2, 3, 4	All	1.3	6.0	3.5	7.31	\$700
Robotic Total Station	1, 3, 4	All	1.3	13.0	3.5	12.70	\$1,075

(Note: 1= rural multi-lane highways; 2= freeway segment; 3= rural two-lane highway; 4= urban/suburban arterials)

1.5. Comparative Analysis of Selected Data Collection Methods

In addition to unit cost, some other factors are important in selecting data collection method, such as data quality and completeness, safety and disruption of traffic. To consider those factors, based on the field trial results, an evaluation matrix was developed to compare different data collection methods, as shown in Table 1.9. Eleven criteria were utilized to assess the performance of the different technologies. Each criterion was assigned a score of 1 to 5 to rank it (5 being the best and 1 the worst) to indicate the relative performance of one method compared to the others. Specifically, the equipment cost for the satellite/aerial imagery method had a score of "5" because it did not incur any field data collection cost. The total weighted score is the summation of score of each criterion multiple by its corresponding weighing factor. For GPS data logger method, as an example, the total weighted score is 24 which is sum of $(3 \times 0.25) + (2 \times 0.25) + (2 \times 0.25) + (2 \times 1.00) + (3 \times 2.00) + (3 \times 2.00) + (2 \times 1.00) + (5 \times 0.25) + (5 \times 0.25) + (5 \times 0.50) + (5 \times 0.25)$.

Table 1.9 Evaluation Matrix for Highway Inventory Data Collection Methods

	Criteria	GPS Data Logger	Robotic Total Station	GPS Enable Photo/Video Log	Satellite/Aerial Imagery	Mobile LiDAR	Weighting Factor
Field Data Collection	Equipment Cost	3	2	4	5	1	0.25
	Labor Cost	2	1	4	5	3	0.25
	Data Collection Time	2	1	4	5	3	0.25
	Safety	2	1	4	5	3	1.00
	Data Completeness	3	4	2	1	5	2.00
	Data Quality	3	4	2	1	5	2.00
	Disruption to Traffic	2	1	4	5	3	1.00
Field Data Reduction	Software Cost	5	4	3	2	1	0.25
	Labor Cost	5	3	4	2	1	0.25
	Data Reduction Time	5	3	4	2	1	0.50
	Data Storage Size	5	4	2	3	1	0.25
Total Weighted Score		24	23	23	21	29	

Note: Based on 30 responded states

For each evaluation criteria, a weighing factor (WF) was designated. These WFs, that imply the relative importance of each data collection method, were identified through discussions with stakeholders at IDOT. A weight of 2.0 was assigned for data completeness and data quality because the highest data quality and completeness were required to have collected data to serve different offices (planning, design, pavement management, and safety) in the agency. Transportation agencies can assign their own WF for each evaluation criteria for their specific purposes. This method, as used in multi-criteria analysis (MCA) approaches, is widely utilized to assess and recognize the importance of one criterion over another in an intuitive manner when quantitative ratings are not available [92]. All of these criteria were employed to rank various HIDC methods based on the summation of weighted components. The results demonstrated that the mobile LiDAR has the highest overall score when data completeness and data quality are the top priority for the agency. It should be noted that the score results are not transferable but the approach utilized to explore overall preferences among alternative options is.

1.6. Conclusions and Recommendations

The purpose of this chapter was to identify cost-effective methods for collecting highway inventory data for implementing in the HSM. Several promising methods, including the GPS data logger, the robotic total station, the GPS enabled the photo/video log, the satellite/aerial imagery, and the mobile LiDAR, were identified through a comprehensive literature review to compare and

determine their capabilities and limitations. Moreover, field trials for collecting HSM-related highway inventory data on four types of roadway segments (includes rural two-lane two-way roadways, rural multi-lane highways, urban and suburban arterials, and freeway) were performed to evaluate and compare the utility of these methods. The findings of this research indicate that the GPS data logger, the robotic total station, the mobile LiDAR, and the combination of video/photo log method with aerial imagery are all capable of collecting HSM-related information. Based on the perceived advantages and disadvantages of each data collection method, the following recommendations are made for consideration by state and local transportation agencies:

- The GPS data logger method can be employed for short distances, low speeds, and low to medium traffic volume roadways that are not obstructed by buildings or trees.
- The robotic total station technology can be employed for points of specific interest, such as intersections.
- The photo/video log method, together with high-resolution aerial imagery, can be used to collect roadside inventory data for large-scale statewide data collection.
- The mobile LiDAR technology can be used to gather highway inventory data with the highest data quality and completeness for serving multiple offices in state DOTs and local agencies. In order to share the costs of the mobile LiDAR data collection and processing, identifying multiple clients within the DOT is important.

CHAPTER 2: Exploratory Analysis of Run-Off-Road Crash Patterns

2.1.Introduction

Roadway departure (RwD) occurs when a vehicle departs from the traveled way by crossing an edgeline or a centerline [93]. RwD events comprise both run-off-road (ROR) and cross-median/centerline head-on collisions. Most head-on crashes are similar to ROR crashes—in both cases, the vehicle strays from its travel lane [94]. Factors contributing to ROR collisions can be divided into two major categories: infrastructure and environmental factors and driver factors. Examples from the first include the effect of weather on pavement conditions, travel lanes that are too narrow or have substandard curves, and unforgiving roadsides. Driver factors include traveling too fast through a curve or down a grade; a driver attempting to avoid a vehicle, an object, or an animal in the travel lane; and inattentive driving due to distraction, fatigue, sleep, or drugs [95]. Compared to other crash types, RwD is one of the most severe types of crashes [96]. An analysis of statistics from the Fatality Analysis Reporting System (FARS) database for crash data from 2007 to 2013 reveal that an average of 59 percent of annual motor vehicle traffic fatalities in the United States occurred due to RwD [97]. Moreover, according to the FHWA, 80 percent of total ROR fatalities occurred on rural highways, and about 90 percent of those occurred on two-lane roads [98, 99], the roadway type upon which this chapter is focused.

In order to determine the most significant contributing factors, and then develop effective safety countermeasures, these numbers require further analysis. A major challenge for state and local agencies is to find patterns in these huge databases. Exploratory data analysis (EDA) is an approach by which patterns, changes, and anomalies in large datasets may be determined, beyond the hypothesis testing task or formal modeling [100, 101]. Using a variety of mostly graphical techniques (e.g., box plot, scatter plot, multiple correspondence analysis, and principal component analysis), EDA can extract specific information from datasets and transform it into an understandable structure. Since ROR crashes accounted for the majority of RwD events (about 80 percent), this chapter uses multiple correspondence analysis (MCA) to identify the key factors contributing to ROR collisions related to the roadway and roadside geometric design features of rural two-lane roads. The MCA method identifies patterns in complex datasets and measures significant contributing factors and their degree of association. To employ this method, datasets

from the United States Road Assessment Program (usRAP), a program of the American Automobile Association (AAA) Foundation for Traffic Safety, were obtained and five years (2009-2013) of ROR crash data in Illinois were gathered. To achieve the program's Toward Zero Deaths vision, agencies are working to decrease the frequency and severity of ROR crashes. The results of this chapter can help researchers and transportation agencies to get a better knowledge of the major contributing factors to ROR crashes and prioritize the locations where safety countermeasures should be implemented (e.g., signage, pavement safety measures, and roadside design improvements).

2.2.Prior Work

There have been a considerable number of studies identifying various contributing factors to ROR crashes, using a variety of data collection and data analysis methods. In an attempt to identify contributing factors to ROR crashes, McLaughlin et al. [102] obtained the dataset from a 100-car naturalistic driving study. In each car, seven various software and hardware instruments had been installed to collect data. In the study, an ROR event was identified as having occurred when the subject vehicle passed or touched a roadway boundary (e.g., edge line marking and pavement edge). The study results revealed that a single factor contributed to 75 percent of the ROR events, followed by two other factors contributing 22 percent. The analysis results showed that the most common factors contributing to ROR events included: distraction, short following distance, low friction, narrower lane, and roadside geometric configurations. Additionally, 36 percent of the ROR events involved distractions due to non-driving tasks and 30 percent of the ROR events happened on road curves. Liu and Subramanian [103] evaluated various contributing factors associated with single-vehicle ROR crashes. Their results showed that horizontal road alignment, area type, speed limit, roadway geometric characteristics, and lighting conditions significantly affect the frequency and severity of ROR crashes. Lord et al. [98] investigated the factors contributing to ROR crashes on two-way two-lane rural roads in the state of Texas. The authors divided the contributing factors into three groups, comprising highway design characteristics (i.e., lane width, shoulder width and type, roadside design, pavement edge drop-off, horizontal curvature and grades, driveway and pavement surfaces, and traffic volume), human factors (i.e.,

speeding, alcohol and drug use, and age and gender), and other factors (i.e., time of day, vehicle type). The data for the crashes, geometric road characteristics, bridges and curves, and traffic characteristics were gathered from various databases and then combined. The results demonstrated that, compared to tangent sections, wider shoulders yielded greater safety effects on horizontal curves. Additionally, most RWD crashes occurred on weekends, being attributed to people driving under the influence (DUI). Unlike driveway density, which had a little impact on RWD crashes, lighting conditions had a great influence on the probability of an RWD crash occurrence.

In another study conducted by the National Highway Traffic Safety Administration (NHTSA), driver inattention, driver fatigue, roadway surface conditions, driver blood alcohol presence, drivers' level of familiarity with the roadway, and driver gender were identified as the most significant factors contributing to ROR crashes [104]. Jalayer and Zhou [105] presented a new approach to evaluating the safety risk of roadside features for rural two-lane roads based on reliability analysis. The authors confirmed that reliability indices could serve as indicators to gauge safety levels. Eustace et al. [106] identified the most significant factors contributing to severe ROR crashes (i.e., injury and fatal) using generalized ordered logit regression. Their results demonstrated that driver conditions (e.g., impaired drivers), road alignments (e.g., curves), roadway characteristics (e.g., grade), gender (e.g., male), and roadway surface conditions (e.g., wet) increased the likelihood of severe ROR crashes. In an attempt to determine unforgiving roadside contributing factors, Roque et al. [107] collected ROR crash data on freeway road sections in Portugal and developed multinomial and mixed logit regression models, accordingly. The empirical findings of this study indicated that critical slopes and horizontal curves significantly contributed towards the fatal ROR crashes. In 2015, the American Traffic Safety Services Association (ATSSA) published a booklet as an executive summary of various case studies to educate transportation practitioners regarding ROR crashes and associated safety countermeasures [108]. In this booklet, countermeasures are categorized as signs (e.g., chevron), pavement safety (e.g., high friction surface treatments), and roadside design (e.g., clear zone improvements). The results of this study found pavement safety countermeasures, compared to other categories, to be the most effective in reducing total ROR crash frequency and severity.

Regarding the methodology outlined in this study, while there is an extensive body of literature on the application of statistical modeling in transportation science [2-10, 21-39, 109-111], few past studies have applied multiple correspondence analysis (MCA) to highway safety. Das and Sun [112] employed MCA to analyze eight years' worth of vehicle-pedestrian crash data in Louisiana. In another study, Das and Sun [113] applied MCA method to determine the contributing factors in fatal ROR crashes using eight years (2004-2011) of Louisiana crash data. Using MCA, Factor et al. [114] investigated the social morphology of car accidents over a 20-year period. Nallet et al. [115] employed MCA to identify the effect of driving license points recovery courses on attending drivers' road crashes. Kim and Yamashita [116] also used MCA to explore the characteristics of pedestrian-involved collisions in Hawaii. In another study, Fontaine [117] applied MCA method to analyze the topology of vehicle-pedestrian accidents.

It should be noted that although there are a considerable number of studies of the factors contributing to ROR crashes [118-135], very few have used graphical EDA techniques for crash analysis. To our knowledge, no previous analyses of the usRAP database have investigated the effects of roadway and roadside geometric design features on ROR crash frequency and severity, which we address in this chapter.

2.3.Method and Data

2.3.1. Multiple Correspondence Analysis

MCA, as an increasingly popular EDA technique, is a powerful method for analyzing and graphically presenting the relationship patterns among several categorical (nominal-scale) dependent variables in large and complex datasets [112]. MCA is able to interpret the large datasets without the necessity of any preconditions [112, 115, 136]. Moreover, in both of count data models and crash severity models the sample size significantly influences model performance [137]. MCA's graphical overviews simplify the expression of the relationships between variables, thereby making interpretation easier [113, 138-139]. More detailed descriptions of the MCA method and its development history can be found in Das and Sun [112], Greenacre and Blasius [139], Gifi [140] and Le Roux and Rouanet [141].

Denoting I as the set of i individual records and J as the set of j categories of all variables, MCA is performed on an $I \times J$ design or indicator matrix [112, 141]. Therefore, an entry in the cell (i, j) includes the individual record i and category j . For instance, gender is one nominal variable with two values, male vs. female, corresponding “0 1” for the male and “1 0” for the female. Accordingly, the completed matrix includes the binary columns with one and only one column, per nominal variable, which takes the value of “1” [113]. The categories can be either qualitative or represent the outcome of the splitting of quantitative variables into categories. In MCA, associated categories are placed close together in a Euclidean space, leading clouds, or combinations of points that have similar distributions [113, 141]. Notably, MCA produces two point clouds, including an individual records cloud and a categories cloud, which are defined by one-, two-, or three-dimensional graphs [112, 113]. It should be noted that the distances between points within a variable in the N -dimensional graph are summaries of all the information about the similarities between all the individual records [112, 139]. Since a lower-dimensional space that includes all or nearly all of the information is desirable, especially for large and complex databases, the two-dimensional graph is the most convenient, with its illustrative planar surface [112, 139]. The fundamental principles of the two types of point clouds are described in the following sections.

2.3.1.1. *Cloud of Individuals*

As mentioned above, the construction of clouds is based on the set of all distances between individual records for a variable in the database, for which different categories have been selected. In other words, if two individual records i and i' select the same category for variable m , the distance between them will be zero [112]. Otherwise, for each variable, the squared distance between individuals associated with each category is calculated based on Equation 2.1 [112, 113, 141]:

$$d_m^2(i, i') = \frac{1}{f_j} + \frac{1}{f_{j'}} \quad (2.1)$$

where: $d_m^2(i, i')$ = squared distance between individuals i and i' for variable m

f_j = relative frequency of individual records that selected category j

$f_{j'}$ = relative frequency of individual records that selected category j' .

For variable “lane width”, as an example, the individual records i and i' are two different roadway segments and the categories j and j' are two different lane widths (e.g., “less than 9 ft.” and “9 to 10.6 ft.”). The relative selection frequency of each category is defined as the total number of individual records that chose that particular category divided by the total number of individual records (n) in the database [112, 113]. In order to obtain the overall squared distance between two individual records i and i' , all individual squared distances must be added together, as shown in Equation 2.2 [112, 113]:

$$D^2(i, i') = \frac{1}{M} \sum_{m \in M} d_m^2(i, i') \quad (2.2)$$

where: $D^2(i, i')$ = overall squared distance between individuals i and i'

$d_m^2(i, i')$ = squared distance between individuals i and i' for variable m

M = set of all variables.

2.3.1.2. Cloud of Categories

The cloud of categories has the same dimension as the cloud of individuals. Category j is defined by a point, namely N_j , with weight (n_j), which is the number of individuals that selected this category [112]. The squared distance between categories j and j' can be written as in Equation 2.3 [112, 113]:

$$(N^j N^{j'})^2 = \frac{n_j + n_{j'} - 2n_{jj'}}{n_j n_{j'} / n} \quad (2.3)$$

where: $(N^j N^{j'})^2$ = squared distance between categories j and j'

n_j = number of individuals that selected category j

$n_{j'}$ = number of individuals that selected category j'

$n_{jj'}$ = number of individuals that selected both categories j and j' .

2.3.2. Data

In order to evaluate the proposed MCA method, the required data for crashes and roadway/roadside geometric features from two databases were gathered and combined. The historical ROR crash data for a 5-year period from 2009 through 2013 were compiled, from the Illinois Department of Transportation (IDOT) [9]. The roadway/roadside geometric design features of 4,500 300-ft roadway segments were also gathered from the usRAP database in Illinois [142]. The usRAP database is an efficient tool that provides information in accessible formats regarding crash risk from the standpoints of public and highway agencies. In the pilot program, the eight participating states included Florida, Illinois, Iowa, Kentucky, Michigan, New Jersey, New Mexico, and Utah [143]. The usRAP database contains data about roadways, roadsides, and bicycle and pedestrian facilities, all of which contribute to vehicle crashes.

For the purposes of this study, a set of key variables for further investigation from among all the parameters included in the usRAP database was nominated, based on engineering study results gleaned from a comprehensive literature review. These variables comprise roadside severity, paved and unpaved shoulder widths, lane width, shoulder rumble strips, horizontal curvature, delineation condition, vertical alignment variation, road condition, land use, and speed limit. Table 2.1 lists all the contributing variables and categories, along with their frequencies and percentages. According to this table, for some variables, the majority of segments fall into one or two categories. For instance, more than 89 percent of segments have no horizontal curvature, 98 percent of segments are without shoulder rumble strips, and 95 percent have good road conditions. Roadside severity indicates the nature of and/or distance to the nearest roadside object, which could result in a fatal or serious injury to vehicle occupants [144]. Since only segments with the same annual average daily traffic (AADT) range, 6500-7500 vehicles per day were considered, in this study, the effect of AADT on ROR crashes could not be considered. It should be noted that the fixed segmentation rule (i.e., 300ft.) and thresholds for roadway characteristics such as lane width and shoulder width, in this study, are defined by the usRAP database [144]. Moreover, the “crash severity” variable is corresponding to the most severe crash occurring on a segment in cases multiple crashes occurred on a segment. For the sake of readers, a flowchart of working steps is shown in Figure 2.1.

Table 2.1 Distributions of Segments Based on Study Categories

Variable	Category	Frequency	Percentage (%)	Description
Speed limit (mph)	Less than 40	243	5.4	
	40 to 50	1733	38.5	
	Greater than 50	2524	56.1	
Lane width (ft.)	Less than 9	63	1.4	
	9 to 10.6	1422	31.6	
	Greater than 10.6	3015	67.0	
Paved shoulder width (ft.)	Less than 3	2092	46.5	
	3 to 7.9	374	8.3	
	Greater than 7.9	86	1.9	
	None (No Shoulder)	1948	43.3	
Unpaved shoulder width (ft.)	Less than 3	2340	52.0	
	3 to 7.9	1471	32.7	
	Greater than 7.9	36	0.8	
	None (No shoulder)	653	14.5	
Shoulder rumble strips	Present	95	2.1	
	Not present	4405	97.9	
Horizontal curvature	No curvature	4014	89.2	
	Moderate curve	459	10.2	Can be driven at a maximum speed of 45 to 60 mph
	Sharp curve	27	0.6	Can be driven at a maximum speed of 25 to 45 mph
Delineation	Adequate	4428	98.4	Warning signs and pavement marking are generally presented
	Poor	72	1.6	Warning signs and pavement marking are absent or faded
Vertical alignment variation	Level or constant grade	4338	96.4	No roadway gradient or constant grade
	Rolling	162	3.6	Moderate changes in road gradient
Road condition	Good	4279	95.1	Very few to no deficiencies
	Medium	194	4.3	A number of minor deficiencies
	Poor	27	0.6	Substantial deficiencies
Land use-left side	Undeveloped	4018	89.3	
	Residential	315	7.0	
	Commercial	45	1.0	
	Developed other than	122	2.7	

Table 2.1 Distributions of Segments Based on Study Categories, cont.

Variable	Category	Frequency	Percentage (%)	Description
Land use-right side	Undeveloped	3982	88.5	
	Residential	311	6.9	
	Commercial	27	0.6	
	Developed other than residential or commercial	180	4.0	
Roadside severity-left side	Traffic barrier	225	5.0	
	Cut	9	0.2	
	Deep drainage ditches	23	0.5	
	Steep fill embankment slopes	225	5.0	
	Distance to objects 0 to 15 ft.	486	10.8	
	Distance to objects 15 to 30 ft.	2240	49.8	
	Distance to objects greater than 30 ft.	1260	28.0	
	Cliff	32	0.7	
Roadside severity-right side	Traffic barrier	162	3.6	
	Cut	0	0.0	
	Deep drainage ditches	27	0.6	
	Steep fill embankment slopes	189	4.2	
	Distance to objects 0 to 15 ft.	378	8.4	
	Distance to objects 15 to 30 ft.	2250	50.0	
	Distance to objects greater than 30 ft.	1467	32.6	
Crash severity	Fatal	99	2.2	
	Injury	396	8.8	
	Property Damage Only (PDO)	707	15.7	
	None (No Crash)	3298	73.3	
Number of ROR crashes per segment	Zero (No Crash)	3298	73.3	
	One	895	19.9	
	Two	180	4.0	
	Three	68	1.5	
	Four	32	0.7	
	Five	27	0.6	

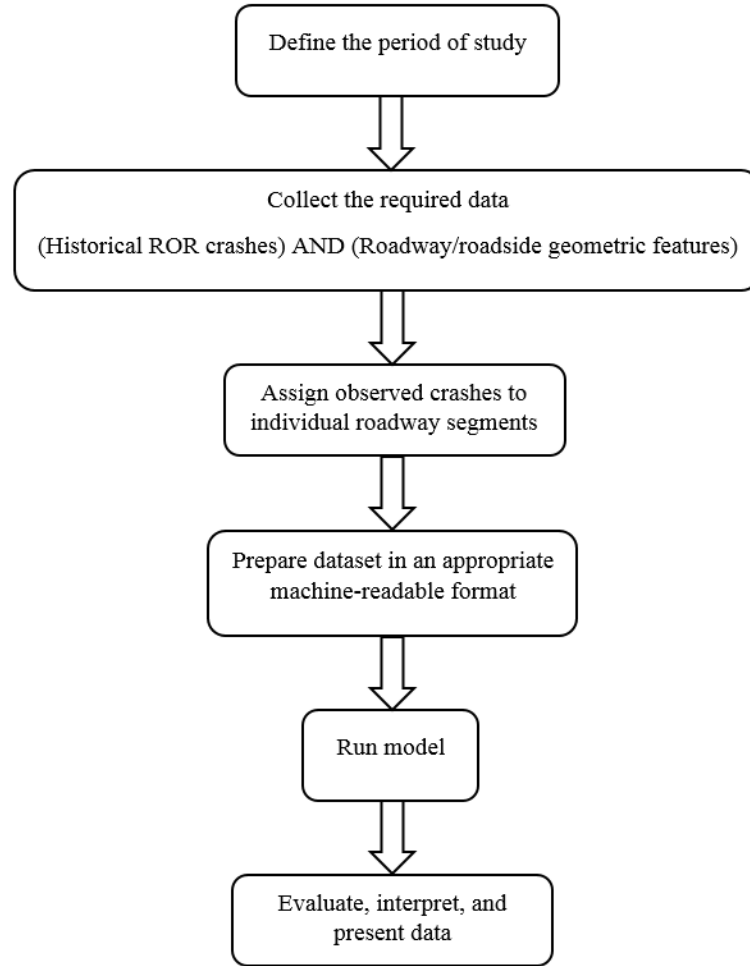


Figure 2.1 A Flowchart of Working Steps

2.4. Results and Discussions

To analyze the dataset and plot the two-dimensional graphs, *R Version 3.02* statistical software and the *FactoMineR* package were employed. In a two-dimensional graphical display with two principle axes, associated categories are close together and form the point clouds [112, 113, 141]. The output is the magnitude of information associated with each dimension, which is given a value between 0 and 1, known as the eigenvalue [112]. The eigenvalue of each dimension can serve as a dependable indicator of the total variance among variables [113]. The eigenvalues of the first, second, and third dimensions are higher than others, so a two-dimensional graph carries most, but not all, the information. Figure 2.2 illustrates the percentages of variance for the top five dimensions.

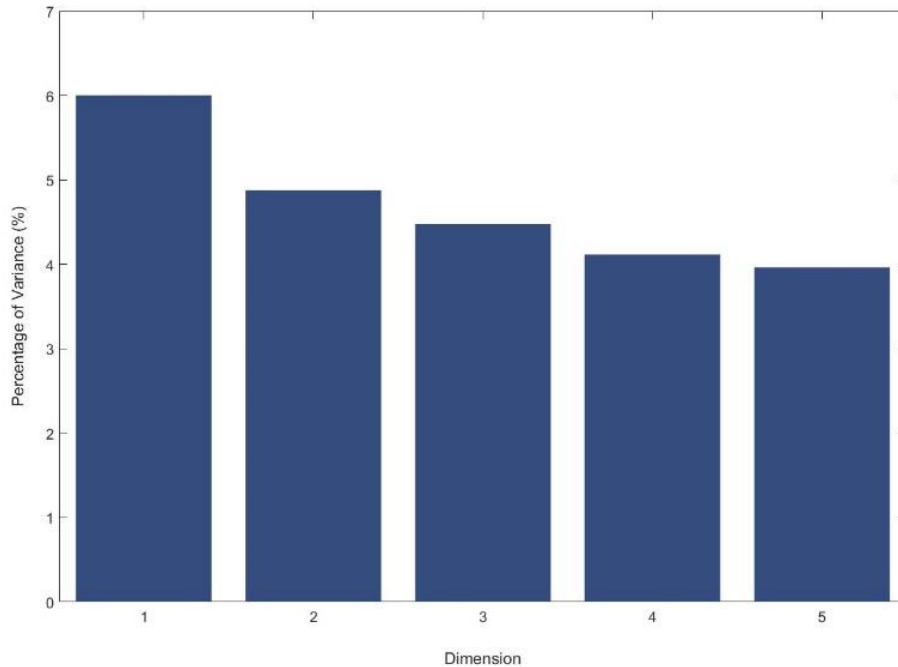


Figure 2.2 Eigenvalues and Variances of the Top Five Dimensions

Based on Figure 2.2, the first and second principle axes on the planar surface, the MCA plot, describes 10.9 percent of the total variances together. The low eigenvalues demonstrate that the variables in the database are heterogeneous due to the random nature of road segments characteristics and occurrence of accidents [112, 113]. Every point on each plot has its own coordination for all dimensions, and, obviously, the scale of the plot depends heavily on the volume of contributions of each dimension. Figure 2.3 depicts all the study variables and their relative proximity on the map.

Regarding the interpretation of the MCA plots, it should be noted that similar objects can be compared based on their relative distances on the graph. In other words, individual records, variables, and categories within a variable may be compared just by looking at the distance between the points on the map [113, 140, 141]. As for non-similar objects, such as categories of different variables, an imaginary line from each point of interest to the centroid of the map must be considered, and then the angle defined between those lines. A very small angle indicates a relatively strong relationship, and a right angle shows that there is no association between those particular objects. An angle of more than 90 degrees denotes a negative association [145]. Figure 2.3 shows that many variables are located closely to each other, thus making the same contribution

to all the variances. The closer a point is located to the centroid in one dimension, the less it contributes to the eigenvalue of that particular dimension, making it as a relatively less important variable [112, 113]. Therefore, for dimension one, the roadside severity of the right side, the roadside severity of the left side, and the horizontal curvature contributed the most. Similarly, for dimension two, the roadside severity of the left side, the roadside severity of the right side, and the paved shoulder width are the most significant variables on ROR crash frequency and severity. Table 2.2 lists in descending order of significance all the ROR contributing factors in this study, considering the coefficient of determination (R^2) and a p-value of the overall test (F-test). R^2 ranges from 0 to 1, with 0 being no relationship and 1 being a very strong relationship between the qualitative variable and the MCA dimension [112, 141]. As it can be seen, compared to roadside severity, the risk of ROR crashes is not strongly associated with delineation, land use, or vertical alignment variation.

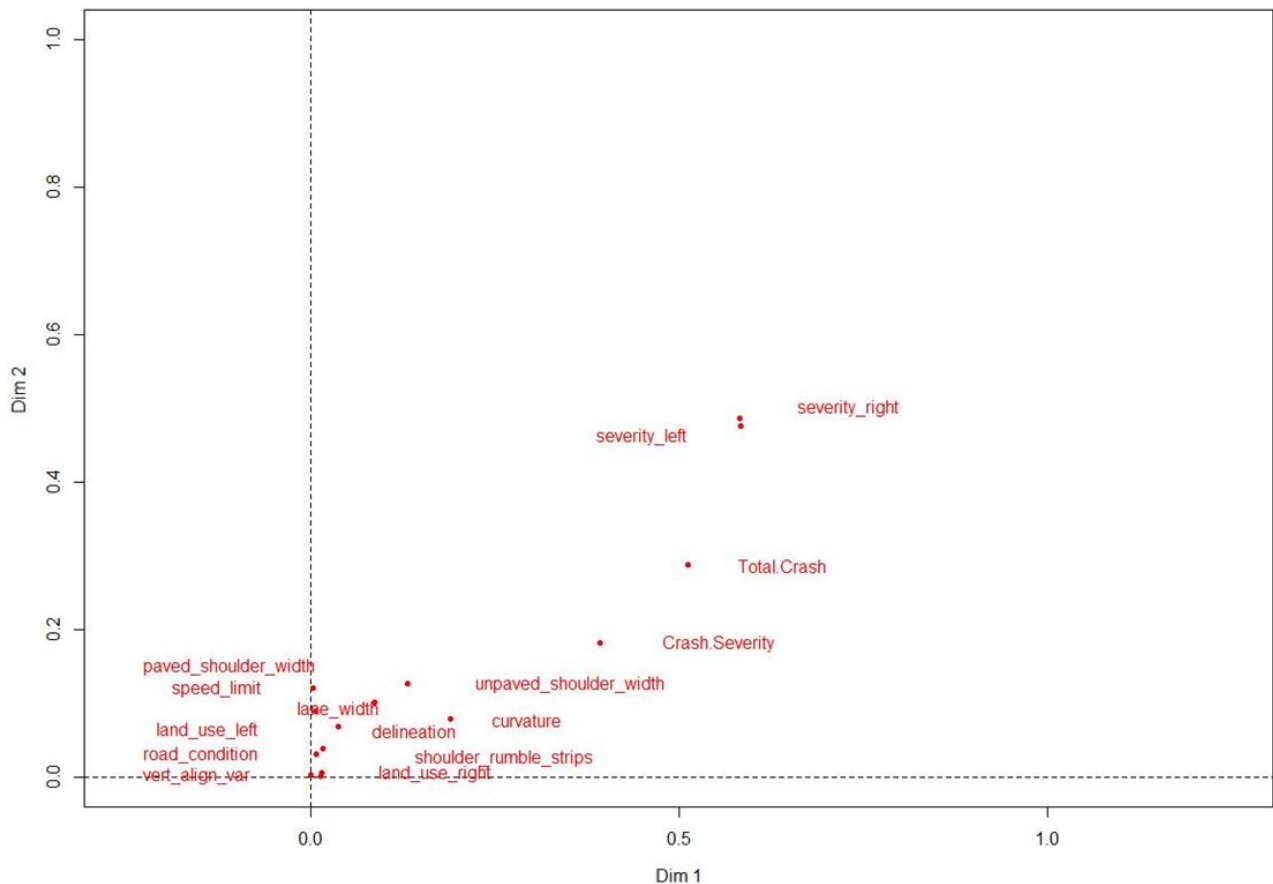


Figure 2.3 MCA Plot of All Study Variables

Table 2.2 Significance of Test Results for Key ROR Contributing Factors in Top Two Dimensions

	Variable	R ²	p-value
Dimension 1	Roadside severity-right side	0.584	<0.001
	Roadside severity-left side	0.582	<0.001
	Total crash	0.512	<0.001
	Crash severity	0.393	<0.001
	Horizontal curvature	0.191	<0.001
	Paved shoulder width	0.131	<0.001
	Unpaved shoulder width	0.088	<0.001
	Lane width	0.037	<0.001
	Delineation	0.017	<0.001
	Road condition	0.015	0.002
	Shoulder rumble strips	0.013	0.003
Dimension 2	Roadside severity-left side	0.487	<0.001
	Roadside severity-right side	0.476	<0.001
	Total crash	0.288	<0.001
	Crash severity	0.182	<0.001
	Paved shoulder width	0.127	<0.001
	Speed limit	0.121	<0.001
	Unpaved shoulder width	0.102	<0.001
	Land use-left side	0.089	<0.001
	Horizontal curvature	0.078	<0.001
	Lane width	0.068	<0.001
	Delineation	0.039	<0.001
	Land use-right side	0.031	<0.001

Figure 2.4 shows the top 20 categories that contributed the most to the two-dimensional plot. Based on the relative proximity of points, several point clouds for categories can be created. According to this figure, one combination cloud correlates five ROR crashes with sharp horizontal curvature and the presence of a cliff as a roadside condition. This means that segments with a severe roadside condition and horizontal curvature are associated with a significant increase in the likelihood of ROR crashes, which is consistent with the findings of the majority of existing literature [105, 107, 121]. Additionally, based on another cloud, most segments with three crashes had no shoulders and moderate horizontal curvature. This indicates that presence of shoulders and curves with larger radii decrease the likelihood of ROR crashes. These results are in good agreement with the findings of Roque et al. [107], Lord et al. [98], and Van Petegem et al. [132]. Another point cloud associates factors such as injury crashes, distance to fixed objects between 0 and 15 ft., two crashes, and the presence of a traffic barrier. Moreover, the cloud links the PDO crashes to the paved shoulder widths of 3 to 7.9 ft. These results are also in line with the finding of another study conducted by Lord et al. [98].

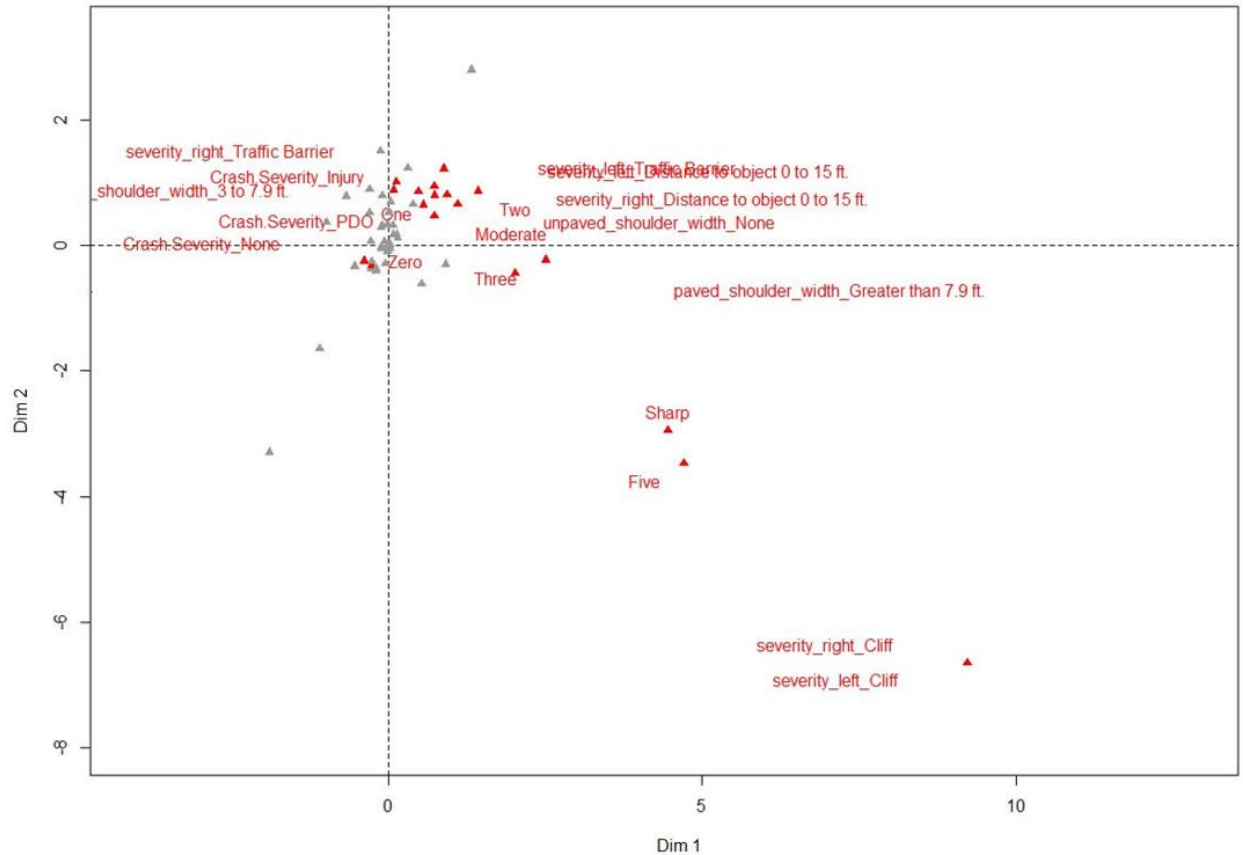


Figure 2.4 MCA Plot of Top 20 Key Categories

2.5. Conclusions

This chapter utilized MCA method to identify the factors contributing to ROR crashes through combining usRAP data and historical crash records. To achieve the FHWA’s Toward Zero Deaths vision, one of the challenges researchers and state DOTs face is how to identify key contributing factors within large and complex datasets, and then how to implement effective safety countermeasures accordingly. In conventional regression models, unlike MCA, it is required to hold the basic assumptions of regression truth and any deviation may result in incorrect outcomes [112]. Moreover, very small and very large sample sizes significantly influence performances of both count data models and crash severity models [137]. Since it is always possible to transform a quantitative variable into a categorical variable, and since a multidimensional approach to a crash will always involve a large set of categorical variables, this method is of particular interest.

To perform the model, five years' worth of ROR crash data from 2009 to 2013 for the state of Illinois were obtained. In this paper, we evaluated the characteristics of the roadways and roadsides that affect ROR crashes for 4,500 300-ft segments, gathered from the usRAP database. More specifically, no previous analyses of the usRAP database have investigated the effects of roadway and roadside geometric design features on ROR crash frequency and severity. These features include roadside severity, paved and unpaved shoulder widths, lane width, shoulder rumble strips, horizontal curvature, delineation condition, vertical alignment variation, road condition, land use, and speed limit. According to the obtained results, the main contributing factors to ROR crashes are roadside severity, horizontal curvature, and shoulder width. Moreover, the likelihood of a collision with a fixed object off the road, such as a concrete barrier, is associated with increased severity of ROR crashes. Additionally, the results indicate that providing paved shoulders, with a minimum width of 3 ft., is associated with reduced ROR crash severity. It was also found that the risk of ROR crashes is not strongly associated with delineation, land use, or vertical alignment variation. One of the reasons we obtained such results is the disproportionate proportion of segments within these variables categories, which can be improved by a wider set of data.

The study results confirm that our proposed approach is suitable for recognizing the patterns of ROR crashes, when combining multiple large datasets at the state level, or even at the regional level. As for the total explained variances by the study variables, eigenvalue correction can be conducted on the Burt matrix to increase the variances [112, 113, 138]. Possible extension of this study can focus on, including person-level data to consider the effect of drivers' characteristics on crash occurrences. It should be noted that although the approach set forth here does not calculate the marginal effects of the variables, the ease of analyzing the big crash data following this approach in identifying the most statistically significant combinations of factors is exceptional. Moreover, taking advantage of the properties of MCA method, it is possible to not only identify contributing factors but also define associations between these factors. As such, MCA certainly has the potential to help state DOTs prioritize effective safety countermeasures with multiple benefits to mitigate ROR crash frequency and severity based on their large databases.

CHAPTER 3: Overview of Safety Countermeasures for Roadway Departure Crashes

3.1.Introduction

As discussed in the previous chapter, Rwd crashes constitute one of the most severe types of crashes. Figure 3.1 depicts the percentage of total Rwd fatal crashes across the United States, categorized by the first event in the crash. According to a query of seven years of crash data (2007–2013) from the Fatality Analysis Reporting System (FARS) database, an average of 57 percent of motor vehicle traffic fatalities occurred each year due to Rwd in the United States [97]. More information about this database can be found at NHTSA [97] and Baratian-Ghorghi et al. [146]. The distribution of this number differs between states (Figure 3.2). In addition, the majority of Rwd crashes occurred during the nighttime and inclement weather conditions (e.g., fog, snow).

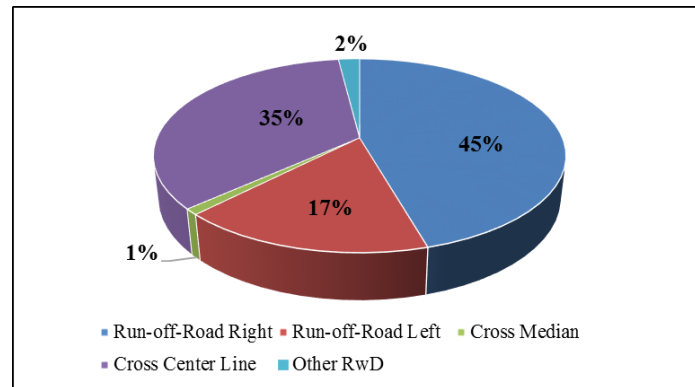
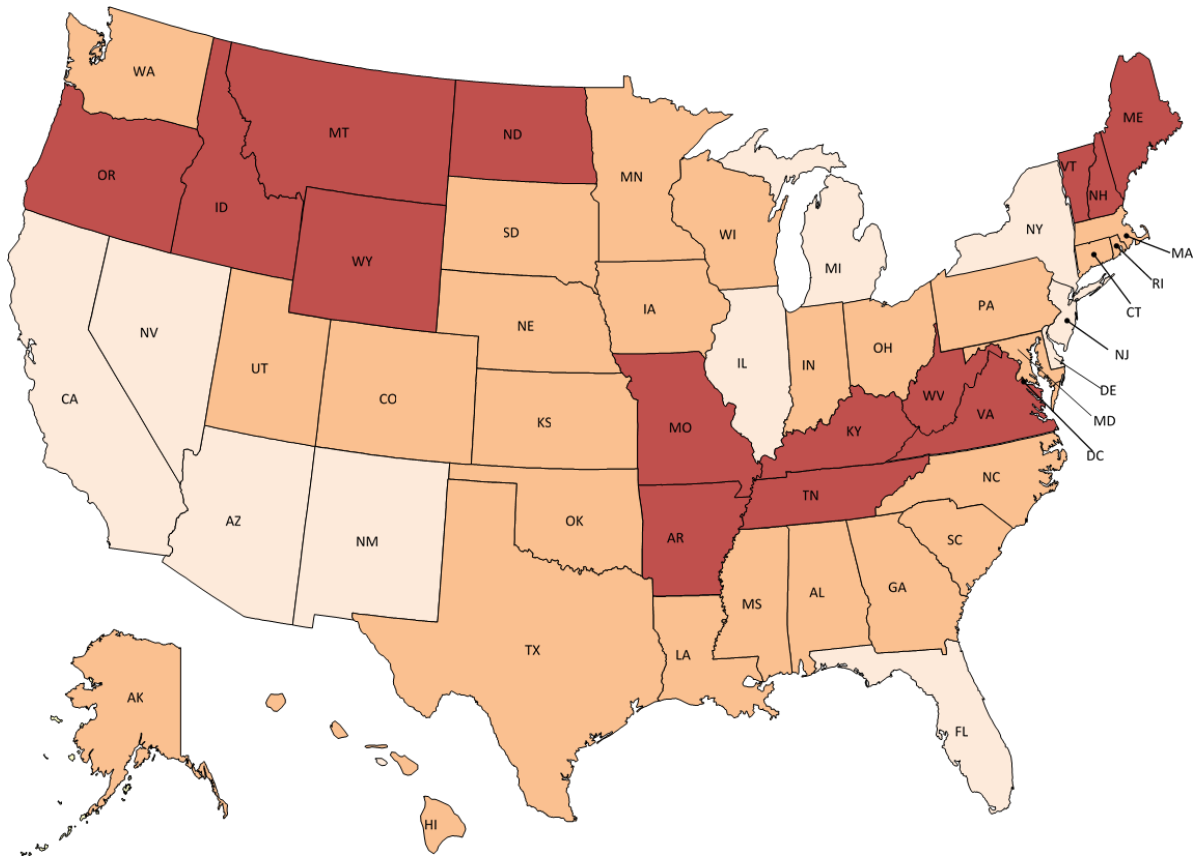


Figure 3.1 Percentage of Fatal Motor Crashes in the United States in 2013 [147]

Several strategies to reduce the number of Rwd crashes have been identified by the American Association of State Highway and Transportation Officials (AASHTO) including [148]:

- Pavement edgeline installation,
- Centerline and shoulder rumble strip installation,
- Pavement marking enhancement,
- Shoulder drop-offs elimination,
- Safer slopes design,
- Object removal/relocation within the clear zone,
- Object delineation using retroreflective tape,
- Barrier design improvement,
- Horizontal curve geometric improvement, and
- Skid-resistant roadway surface provision.



Average Annual Roadway Departure Fatalities (2007-2013)					
Group 1 (65% and Higher)		Group 2 (Between 50-65%)		Group 3 (Below 50%)	
State	RwD	State	RwD	State	RwD
Vermont	79.0%	Alabama	64.0%	California	49.0%
Wyoming	78.0%	Kansas	64.0%	Michigan	49.0%
West Virginia	75.0%	Nebraska	63.0%	Illinois	49.0%
Montana	73.0%	Wisconsin	63.0%	Delaware	48.0%
Arkansas	72.0%	Washington	63.0%	Nevada	48.0%
Maine	71.0%	Alaska	63.0%	Arizona	46.0%
Kentucky	69.0%	Oklahoma	63.0%	New Jersey	46.0%
Tennessee	69.0%	South Dakota	62.0%	New Mexico	44.0%
Idaho	69.0%	Pennsylvania	62.0%	Florida	43.0%
New Hampshire	69.0%	South Dakota	62.0%	Dist. of Columbia	29.0%
Virginia	68.0%	Rhode Island	62.0%		
North Dakota	66.0%	South Carolina	61.0%		
Missouri	65.0%	North Carolina	61.0%		
Oregon	65.0%	Louisiana	61.0%		
		Ohio	61.0%		
		Iowa	60.0%		
		Colorado	60.0%		
		Connecticut	58.0%		
		Indiana	57.0%		
		Massachusetts	57.0%		
		Georgia	56.0%		
		Hawaii	55.0%		
		Texas	54.0%		
		Mississippi	54.0%		
		Utah	52.0%		
		Minnesota	52.0%		
		Maryland	50.0%		

Figure 3.2 Average Percentage of RwD Fatalities in Each State (2007-2013) [147]

Not only are most of these strategies low-cost countermeasures but they can also be implemented systematically. This chapter provides a brief overview of cost-effective improvements for preventing vehicle departures from roadways. It is a summary of a recent publication by the American Traffic Safety Services Association (ATSSA), which can help transportation agencies better understand the effectiveness, and prioritize the implementation of each RwD safety countermeasure [108].

3.2.Roadway Departure Safety Countermeasures

Countermeasure implementation case studies for mitigating RwD crashes were developed based upon a comprehensive literature review and input from state and local agencies. RwD safety countermeasures were divided into three major categories: signs, pavement safety, and roadside design. Figure 3.3 illustrates the 14 RwD safety countermeasures discussed in this chapter. Table 3.1 lists the 14 countermeasures, the evaluation method used, the results obtained, and the relevant contact agencies. As shown in the table, the percentage reduction of the total number of RwD crashes varies between 23 and 91, depending on the safety countermeasure. Similarly, for the total number of ROR crashes, the reduction ranges from 22.1 percent to 61.6 percent. Most agencies used a simple before-and-after evaluation method and a few determined benefit-cost (B/C) ratios. The simple before-and-after method, is based on the assumption that if no improvement has been made, the expected number of the crashes would remain the same as in the before period [149].

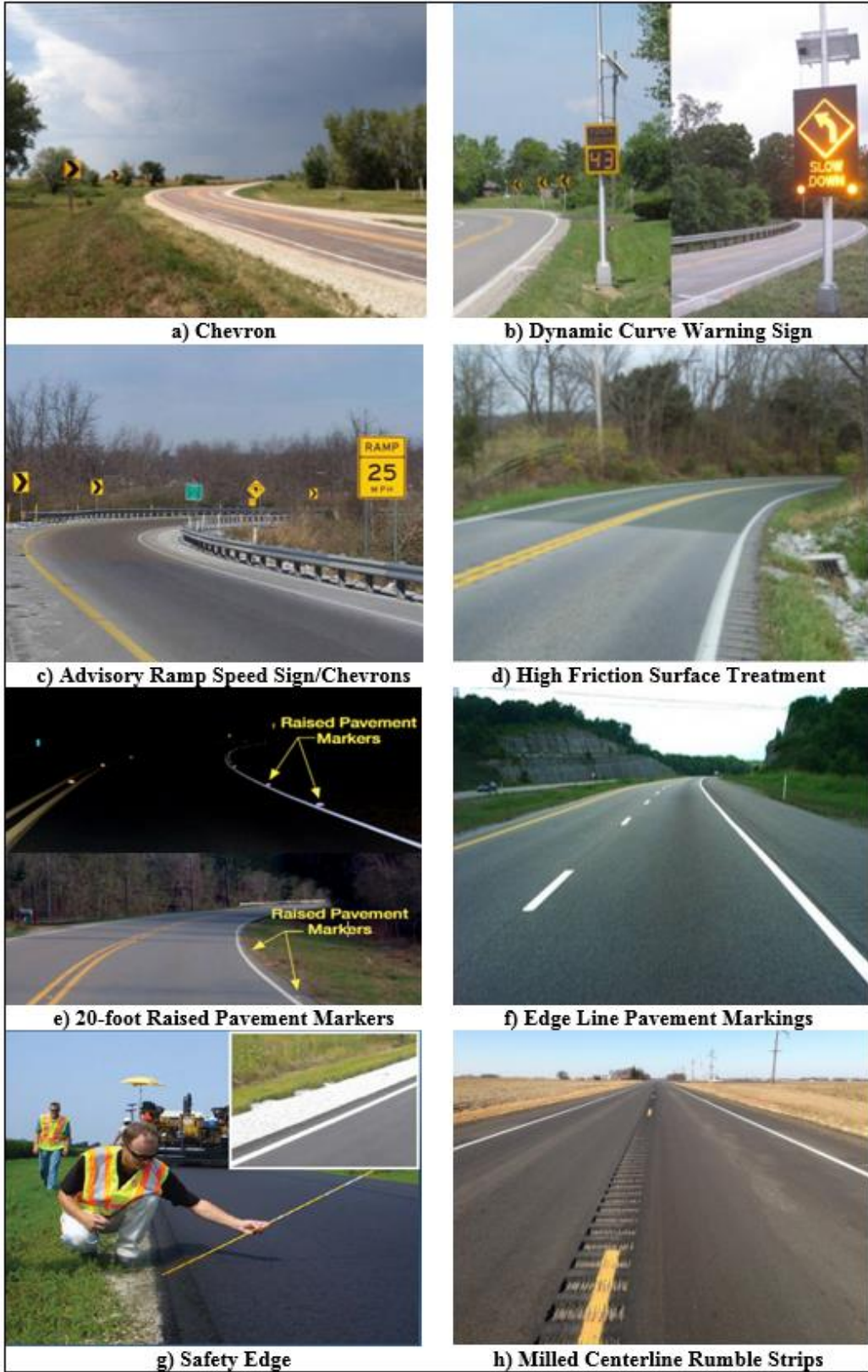


Figure 3.3 Rwd Crash Safety Countermeasures [108]



Figure 3.3 Rwd Crash Safety Countermeasures, cont. [108]

Table 3.1 Results from the 14 Case Studies [108]

	Safety Countermeasure	Safety Evaluation Method	Results	Benefit-cost (B/C) Ratio	State Agency Implementation	Implementation Time
Signs	Chevron	Empirical Bayes (EB)	<ul style="list-style-type: none"> • Total ROR crashes: -22.1 % • Total crashes during dark condition: -24.5 % 	8.0	WSDOT	1994-2006
	Dynamic Curve Warning Systems (DCWSs)	---	<ul style="list-style-type: none"> • 2.6 mile per hour (mph) reduction in mean speed • 76 % of vehicle slowed down 	---	ODOT	2002
	Advanced Curve Warning and Advisory Speed Sign	Simple before-and-after	<ul style="list-style-type: none"> • Before: 1 fatality per year; after: 0 fatality 	---	KYTC	2006
Pavement Safety	High Friction Surface Treatments (HFSTs)	Simple before-and-after	<ul style="list-style-type: none"> • Total RwD crashes in wet weather: -91.0 % • Total RwD crashes in dry weather: -78.0 % 	24	KYTC	2010
	Raised Pavement Markers (RPMs)	Simple before-and-after	<ul style="list-style-type: none"> • Total RwD crashes: -86.0 % • Total injuries: -94.0 % 	---	ALDOT	2009
	Edge Line Pavement Markings	Simple before-and-after	<ul style="list-style-type: none"> • Total RwD crashes: -23.0 % • Total severe RwD crashes: -38.0 % 	---	MoDOT	2009
	Safety Edge	Simple before-and-after	<ul style="list-style-type: none"> • Total crashes: -5.7 % 	<ul style="list-style-type: none"> • Two-lane highways with paved shoulder: 3.8 to 43.6 • Two-lane highways with unpaved shoulder: 2.8 to 62.8 	GDOT and INDOT	2005
	Centerline Rumble Strips (CLRS)	Simple before-and-after	<ul style="list-style-type: none"> • Total crashes: -33.0 % • Total RwD crashes: -31.0 % • Total head-one crashes: -35.0 % • Total opposite-direction sideswipe crashes: -46.0 % 	---	MDOT	2008-2010

	Safety Countermeasure	Safety Evaluation Method	Results	Benefit-cost (B/C) Ratio	State Agency Implementation	Implementation Time
Pavement Safety (cont.)	Shoulder Rumble Strips (SRS)	Simple before-and-after	<ul style="list-style-type: none"> • Total ROTRR crashes: -47.0 to 61.6 % • Total severe ROTRR crashes: -15.3 to 66.6 % 	50	WSDOT	2000
Roadside Design	Cable Barrier	Simple before-and-after	<ul style="list-style-type: none"> • Before: 19 fatal crashes; after: 0 fatal crash 	---	MnDOT	2004-2008
	Guardrail	Simple before-and-after	<ul style="list-style-type: none"> • Total severity and Rwd index: -16.6 to 36.7 % 	---	NCDOT	1997-2010
	Shoulder Widening	Simple before-and-after	<ul style="list-style-type: none"> • Total severity and Rwd index: -43.7 to 69.2 % 	---	NCDOT	2002-2011
	Breakaway Supports for Signs and Lighting	---	---	---	---	---
	Clear Zone Improvements	Simple before-and-after	<ul style="list-style-type: none"> • Total crashes: -38.0 % 	---	Iowa DOT	2006

3.2.1. Signs

According to the FARS database, approximately 83% of horizontal curve fatalities are roadway departures [97]. Enhancing curve delineation with signs is typically considered to be a low-cost safety improvement. These signs alert drivers to changes in road alignment and provide information on the actions to be taken. For example, a sign may encourage drivers to reduce their speeds. When placed and maintained appropriately, curve signage may reduce the frequency and severity of RWD crashes. Based on the previous studies [43, 150], signs are only effective when they clearly convey the intended message in both day and nighttime conditions.

3.2.1.1. Chevrons

According to the Manual on Uniform Traffic Control Devices (MUTCD), chevrons and/or one-direction large (Figure 3.3a) arrows shall be used where the difference between speed limit and the advisory speed is 15 mph or more. It is important to ensure that these signs are placed and aimed properly [151]. The Washington State Department of Transportation (WSDOT) conducted a safety evaluation analysis of chevron signs for 139 treated curves on rural two-lane roads. Empirical Bayes (EB) analysis results demonstrated that chevrons along horizontal curves decreased the total number of lane departures and crashes of all types during dark conditions by up to 22.1 and 24.5 percent, respectively. According to cost analysis results, chevrons are also a very cost-effective countermeasure, with a benefit-cost (B/C) ratio exceeding 8:1 [108].

3.2.1.2. Dynamic Curve Warning Systems

Dynamic curve warning systems (DCWSs) detect the speed of approaching vehicles and are programmed to provide drivers exceeding a certain speed threshold with a message, flashing light-emitting diodes (LEDs), or a display of their speed (Figure 3.3b). Results from a national safety study indicate that, two years after installation, a 2.0 mph mean speed reduction occurred at the beginning of the curve [152]. The Oregon Department of Transportation (ODOT) installed a DCWS system in advance of a curve on Interstate 5 near Myrtle Creek in Douglas County. The

system consists of a dynamic message sign, a 45-mph advisory speed sign, a controller unit, a radar unit, and computer software. The analysis results showed that 76 percent of drivers slowed down following the system's installation, with a 2.6 mph reduction in mean speed for passenger cars [108].

3.2.1.3. Advanced Curve Warning and Advisory Speed Sign

Curve or turn warning signs are placed in advance of curves to alert drivers of what lies ahead on their route (Figure 3.3c). Properly installed curve warning signs have been proven to improve safety for horizontal curves. The cost for most commonly used curve warning signs with advisory speed plates ranges from \$500 to \$700 per sign [153]. The Kentucky Transportation Cabinet (KYTC) installed an LED-enhanced curve warning sign on KY 82 in Estill County. Since its installation in 2006, no fatalities have been recorded, despite a crash history of one fatality per year for three consecutive years prior to the installation of the sign [108].

3.2.2. Pavement Safety

Pavement safety countermeasures can also make significant contributions to reducing the number of Rwd crashes. Insufficient friction between the tire and pavement surface, poor visibility during nighttime hours, and pavement drop-off edge are factors that may contribute to a vehicle leaving the traveled way.

3.2.2.1. High Friction Surface Treatments

High friction surface treatments (HFSTs) consist of a thin layer of durable aggregates (typically calcined bauxite) that are highly resistant to polishing [154] (Figure 3.3d). The aggregate is bonded to asphalt, concrete, or other pavement surfaces using polymer binders. HFST is not meant to change the pavement's structural performance. Rather, HFST provides greater friction, allowing motorists to maintain better control in dry and wet road conditions, resulting in reduced numbers of Rwd crashes. According to the FHWA *Every Day Counts (EDC) 2012 Initiatives*, a B/C ratio

of about 24:1 can be achieved by implementing pavement friction treatments [155]. The KYTC launched a 3-year HFST program to enhance friction on horizontal curves at 75 locations statewide in 2010. The safety analysis results confirm that the total number of Rwd crashes at the treated sites dropped by 91 percent and 78 percent in wet and dry weather conditions, respectively [108].

3.2.2.2. Raised Pavement Markers

Raised pavement markers (RPMs) are often used by transportation agencies as delineation treatments to improve nighttime visibility, particularly in wet pavement conditions (Figure 3.3e). According to the AASHTO's Strategic Highway Safety Plan (SHSP), RPMs are considered to be an effective, low-cost strategy for mitigating Rwd crashes [156]. Assisted by the FHWA and the Alabama Department of Transportation (ALDOT), Mobile County in Alabama systematically applied RPMs along 10 rural roadways with the highest number of Rwd crashes. In this project, RPMs were installed with 80-foot spacing in tangent sections of roadways, 40-foot spacing between the advanced warning curve sign and the beginning of the curve, and 20-foot spacing through the curve. Crash analysis results reveal an average annual decrease of about 86 percent for Rwd crashes and about a 94-percent reduction in injuries [108].

3.2.2.3. Edge Line Pavement Markings

Edge line pavement markings (Figure 3.3f) distinguish travel lanes from the adjacent shoulders to delineate the travel path. According to the MUTCD, the edge line markings on the right edge of the roadway shall be white. In addition, the normal width of edge line markings is 4 to 6 inches and wide edge line markings are to be at least twice the width of a normal line [151]. From 2009 to 2012, the Missouri Department of Transportation (MoDOT) initiated a program to install edge line marking on eligible high risk rural roads (HRRRs). First, MoDOT performed a safety evaluation of implemented countermeasures on 73 high-risk roadway segments. Based on the safety analysis results, the total number of Rwd crashes and severe Rwd crashes decreased by 23 to 38 percent following the installation of edge line markings [108].

3.2.2.4. Safety Edge

As determined by the FHWA in 2012, the Safety Edge is one of nine proven safety countermeasures (Figure 3.3g). This strategy mitigates the vertical elevation difference by sloping the edge of the pavement to 30 degrees during paving or resurfacing projects. A Safety Edge is installed using one of several commercially available devices that can be attached to the hot-mix asphalt (HMA) paver [157], and is also highly cost-effective. The added cost of resurfacing with this treatment was determined to be very small, because the asphalt must simply be reformed to create the Safety Edge. The Midwest Research Institute (MRI) conducted a safety evaluation of the Safety Edge at 261 treated sites (685 miles) in Georgia and 148 sites (514 miles) in Indiana. The evaluation results showed a 5.7 percent reduction in total crashes after the implementation of the Safety Edge. Additionally, the B/C ratio for two-lane highways with paved shoulders ranged from 3.8 to 43.6 for Georgia and from 3.9 to 30.6 for Indiana. For two-lane highways with unpaved shoulders, the B/C ratio ranged from 3.7 to 62.8 for Georgia and from 2.8 to 12.8 for Indiana [108].

3.2.2.5. Centerline Rumble Strips

Centerline rumble strips (CLRS) are a longitudinal safety feature that can be installed at or near the centerline of undivided roadways (Figure 3.3h). CLRSs include a series of milled or raised elements on the pavement [158]. Tires rolling over rumble strips generate noise and vibration which alert a distracted or drowsy driver to make a safe steering correction. The Michigan Department of Transportation (MDOT) initiated a CLRS installation program during the period from 2008 to 2010. Approximately 5,400 miles of non-freeway roadways were included in this program. The study results proved that the implementation of rumble strips resulted in a significant reduction in both center line and edge line encroachments in tangent sections and through curves [108]. More specifically, after CLRS installation, the number of center line encroachments to the left side within the curves dropped by 87 percent, and there was a 33 percent reduction in all crash types. Additionally, the number of opposite-direction sideswipe collisions, multi-vehicle head-on crashes, and single-vehicle RWD crashes decreased by 46, 35, and 31 percent, respectively [108].

3.2.2.6. Shoulder Rumble Strips

Shoulder rumble strips (SRS) are commonly installed in paved shoulders that are adjacent to the travel lane (Figure 3.3i). Like CLRS, SRS provide acoustical and vibrational warnings to drivers who are straying from their travel lane. According to survey results from 50 state DOTs, the B/C ratio for SRSs was estimated to be approximately 50:1 [159]. The WSDOT investigated the possibility of applying SRS on undivided highways. To date, WSDOT has installed over 260 miles of a mix of milled and raised SRS on its rural two-lane undivided highways. In early 2013, the WSDOT undertook a review of historical crash data over the nine years from 2002 to 2010. The study examined a total of 190 roadway miles with SRS in 45 segments, covering all geographic areas of the state [108]. In cases where SRS had been added during or after CLRS installation, the results showed that run-off-road to the right side (ROTRR) crash rates were reduced by 47.0 to 61.6 percent for crashes of all severity types, and by 15.3 to 66.6 percent for fatal and serious injury crashes, respectively.

3.2.3. Roadside Design

The severity of ROR crashes depends on the roadside features, including sideslope, fixed-object density, offset to fixed objects, and shoulder width. Collision with a fixed object has been identified as the primary harmful event in ROR crashes [160]. A recent inquiry of the FARS database revealed that 7,416 people perished in crashes involving roadside fixed objects in 2012, accounting for 22 percent of the total fatalities for that year [97]. Some practical countermeasures to enhance roadside safety include roadway cross-section improvements, hazard removal or modification, and delineation. These countermeasures have been used in all area types (i.e., rural, suburban, and urban) to keep vehicles in travel lanes and to reduce potential collisions with roadside objects, such as trees, signs, and utility poles [94].

3.2.3.1. Cable Barrier

A barrier is a device designed to stop or redirect errant vehicles to prevent a more serious crash. Although barriers cannot reduce the total number of crashes, the benefits of cable barriers are that

they tend to minimize the severity of injuries by absorbing the impact of the crash and have safer consequence compared to vehicles striking the shielded obstacles. Flexible barriers, made from wire rope strung between posts (Figure 3.3j), are the most forgiving type of barriers and the best option for minimizing injuries to vehicle occupants [161]. A number of high-tension cable barrier systems are available, which remain functional after a crash and may not require immediate repairs. In 2004–2008, the Minnesota Department of Transportation (MnDOT) installed cable barriers at 31 segments along approximately 150 freeway miles to reduce the number of fatalities and severe injuries caused by cross-median crashes. The safety evaluation results revealed that the number of fatal cross-median crashes and serious injury cross-median crashes after cable barrier installation dropped from 19 to 0 and 8 to 6, respectively [108].

3.2.3.2. *Guardrail*

Guardrails (Figure 3.3k) are the most common and widely used type of barrier and can be effective in reducing:

- reportable RwD crashes,
- vehicles from hitting fixed objects, and
- vehicles from going over steep embankments.

The most common guardrail system used in the United States is the metal beam guardrail, which consists of W-shaped metal beam rail elements fastened to wood or galvanized steel posts. Guardrails have a low life-cycle cost since they often remain functional without immediate need of repair [156]. The North Carolina Department of Transportation (NCDOT) evaluated the results of spot safety and hazard elimination projects of 14 divisions in the state. Using a before-after analysis at the three treatment sites, the results showed that the percentage reduction in the total Severity Index and RwD Severity Index range from 16.6 percent to 36.7 percent. In this study, crash severity index was defined as being equal to the total number of equivalent property damage only (PDO) crashes (76.8 for “K=Fatal” and “A= Incapacitating injury” crashes, and 8.4 for “B=Non-Incapacitating injury” and “C=Possible injury” crashes) divided by the total number of crashes [108].

3.2.3.3. *Shoulder Widening*

Roadway shoulders, when used as a safety feature, can improve road safety not only by allowing drivers to recover in a stable, clear recovery area, but also by providing drivers with more space to maneuver to avoid crashes. In addition, a wider shoulder improves stopping sight distance (SSD) on horizontal curves and provides better bicycle accommodation (Figure 3.31). Shoulder width can vary between 2 feet for minor rural roads and 12 feet for major roads. It can also be widened both inside and outside curves [162]. For low-volume roads (less than 1,000 vehicles per day) with narrow pavement width (less than 12 feet), it is more effective to consider narrower lanes with a wider shoulder [147]. Based on a before-after analysis of three treatment sites, the NCDOT showed reductions in the total Severity Index and Rwd Severity Index ranging from 43.7 percent to 69.2 percent, respectively [108].

3.2.3.4. *Breakaway Supports for Signs and Lighting*

Breakaway supports (Figure 3.3m) refer to various devices designed and constructed to break or yield when they are hit by a vehicle [163]. It is not always feasible to maintain object-free roadside clear zones (the total roadside border area starting at the edge of the traveled way); however, crash severity can be diminished by using breakaway supports for roadside objects. The 2009 MUTCD mandates that post-mounted roadside sign supports in the clear zone be breakaway, yielding, or shielded [151]. In phone interviews with traffic and safety engineers from several state DOTs regarding the safety effects of breakaway supports, most agencies reported that this countermeasure has been proven to be effective in reducing the severity of Rwd crashes and that no evaluation has been deemed necessary.

3.2.3.5. *Clear Zone Improvements*

A clear zone is defined by the 2011 Roadside Design Guide as “*the unobstructed, traversable area provided beyond the edge of the through traveled way for the recovery of errant vehicles*” [162]. This area includes shoulders, bike lanes, and auxiliary lanes, excepting those auxiliary lanes

that function as through lanes (Figure 3.3n). Recommended clear zone distances are most affected by traffic volume, speed, roadside slope, and curvature [162]. In 2006, the Iowa Department of Transportation (Iowa DOT) initiated a program to mitigate Rwd crashes, mainly focusing on the removal/relocation of hazards (e.g., trees, telephone poles, mailboxes) within the clear zone area and shielding or delineating objects, if achieving the first option was not feasible. The safety evaluation results showed that the number of total crashes dropped by up to 38 percent [108].

3.3.Summary

An investigation of 14 real-world case studies has provided an overview of current safety countermeasures practices for Rwd crashes. These case study examples fall into three major categories: signs (i.e., chevrons, dynamic curve warning systems, and advance curve warning and advisory speed signs), pavement safety (high friction surface treatments, raised pavement markers, edge line pavement markings, safety edge, centerline rumble strips, and shoulder rumble strips), and roadside design (cable barrier, guardrail, breakaway supports for signs and lighting, clear zone improvements, and shoulder widening). The results of this chapter identify pavement safety as the most effective countermeasure for reducing total Rwd-crash frequency and severity. One possible extension of this study is considering papers related to studies in other countries, covering a wider set of data.

CHAPTER 4: Evaluating the Safety Risks of Roadside Features for Rural Two-Lane Roads using Reliability Analysis

4.1.Introduction

As discussed in previous chapters, roadside features (e.g., sideslope, fixed-object density, offset to fixed objects) can significantly impact the frequency and severity of ROR crashes. In order to characterize the potential of accidents with respect to roadside designs, Zegeer et al. [164] developed a roadside hazard rating (RHR) system, which is used in the accident prediction algorithm for rural two-lane highways. The RHR is a visual and subjective measure defined as the average hazard level in a roadside environment and has seven categories from 1 (best) to 7 (worst) (Figure 4.1):

- RHR=1: Clear zone greater than or equal to 30 ft.; sideslope flatter than 1V:4H; recoverable
- RHR=2: Clear zone between 20 and 25 ft.; sideslope about 1V:4H; recoverable
- RHR=3: Clear zone about 10 ft.; sideslope about 1V:3H; marginally recoverable
- RHR=4: Clear zone between 5 and 10 ft.; sideslope about 1V:3H; marginally forgiving
- RHR=5: Clear zone between 5 and 10 ft.; sideslope about 1V:3H; virtually non-recoverable
- RHR=6: Clear zone less than or equal to 5 ft.; sideslope about 1V:2H; non-recoverable
- RHR=7: Clear zone less than 5 ft.; sideslope of 1V:2H or steeper; non-recoverable

A clear zone is defined by the American Association of State Highway and Transportation Officials (AASHTO) as “*An unobstructed, traversable area provided beyond the edge of the through traveled way for the recovery of errant vehicles. The clear zone includes shoulders, bike lanes, and auxiliary lanes, except those auxiliary lanes that function like through lanes*” [148]. The sideslope is defined as the slope of the cut or fill, and is expressed as a ratio of the vertical to the horizontal distance.



RHR=1



RHR=2



RHR=3



RHR=4



RHR=5



RHR=6



RHR=7

Figure 4.1 Roadside Hazard Rating Scale [164]

Consideration of the deterministic design criteria cannot identify the safety margin of the design output, nor does it determine the deviation from the design standards with respect to safety implications (e.g., identification of clear zone and sideslope values that are less than those recommended). A probabilistic approach, on the other hand, allows for the systematic analysis of uncertainties. Reliability analysis is a probabilistic method that specifies the safety margin of a system, based on the system's capability to function under certain specified conditions. This concept has been widely employed in various fields of study, including structural design [165-176], earthquake engineering [177, 178], and mechanical engineering [179]. In transportation engineering applications, reliability analysis has been employed on a smaller scale. Specifically, for transportation safety, in some situations that measuring safety is difficult due to a lack of data or difficulty separating the impact of a single design element on frequency of collision is difficult, this method is of particular of interest [180, 181]. The reliability analysis has the capability to evaluate the safety risk associated with a particular design feature.

In numerous definitions of reliability, establishing the performance function, or limit state function (LSF), is the principal step in reliability analysis. Generally, the LSF is a statement about the expected functional performance of the whole system. Many researchers in a variety of disciplines, and particularly in structural engineering, have put forth definitions of the LSF concept. For example, Nowak and Collins [182] characterized the LSF in terms of the difference between load-carrying capacity and demand or load effect. With respect to the LSF, two essential parameters may contribute to the safety margin: capacity and demand. Using mathematical models to consider the discrepancy between demand and capacity, a reliability index can be defined. This index rates the probabilistic characteristics of the whole system and its safety, in terms of the failure rate or non-compliance events [183].

This chapter uses reliability analysis to evaluate roadside safety levels for rural two-lane roads in order to define their reliability indices. Of particular interest to this study are the clear zone width and sideslope parameters. These two parameters identify a roadway's RHR—the main measure of roadside conditions—and are key factors contributing to ROR crashes. The results of this chapter will help researchers, transportation agencies, and various jurisdictions to obtain greater understanding of the effect of roadside conditions, and specifically, practical clear zone

widths and sideslopes. Based on reliability indices, locations can then be prioritized for implementing safety countermeasures (e.g., removing/relocating roadside hazard objects or flattening slopes) to mitigate ROR crashes.

4.2.Prior Work

In an attempt to reduce the severity of RWD crashes on its roads, in 2006, the Iowa Department of Transportation (Iowa DOT) initiated a program to remove/relocate hazardous objects in the clear zone area (e.g., trees, telephone poles, mailboxes), or to shield or delineate those objects if the first option was not feasible. The safety evaluation results demonstrated that the number of total crashes dropped by up to 38 percent after these changes were implemented [184]. In another study, Zegeer et al. [164] reported that a 27 percent reduction in ROR crashes could be achieved by flattening a sideslope from 1V:2H to 1V:7H or more. Bella [185] investigated driver perceptions of roadside configurations on two-lane roads using simulation models. To evaluate driver behaviors with respect to speed and lateral position, the authors tested two different cross-sections, with and without shoulders, for three roadside configurations, including: (1) only trees, (2) trees and barriers, and (3) trees and barriers having undergone a treatment. They used 36 drivers to drive in a simulator, focusing on six road scenarios. The analysis results demonstrated that only cross-sections influenced driver behaviors and the drivers did not change their behaviors in roads without barriers. In a similar study, Fitzpatrick et al. [186] explored the influence of clear zone width and roadside vegetation on driver behaviors with respect to vehicle speed and lateral position, using four combinations of clear zone widths and densities of roadside vegetation. The results indicated that the wider the clear zone, the greater the observed driver speed. Moreover, as the width of the clear zone increased, drivers tended to drive more closely to the edge of the road.

Using zero-inflated models and nested logit models, Lee and Mannering [120] investigated the impact of roadside features on the frequency and severity of ROR crashes. They analyzed a 96.7-km section of highway in Washington State. The results of this study demonstrated that the frequency of ROR crashes could be decreased by reducing the number of trees along the roads, avoiding cut side slopes, and increasing the distance between the shoulder edge and light poles. Regarding crash severity, the authors concluded that interactions with roadside features (e.g., light

poles, guardrails, trees, and slopes) contributed to crash severity. To analyze the safety level associated with various utility pole locations adjacent to the edge of the travel-way, El Esawey and Sayer [187] developed a safety performance function (SPF) in order to associate utility pole crash frequency with roadway and roadside conditions. The results of the study demonstrated that compared to fixed object density (here utility pole), the offset to the utility poles has a more significant impact on utility pole crash frequency.

Holdridge et al. [188] evaluated the significant contributing factors to the severity of fixed-object crashes using multivariate nested logit models. The authors found that the probability of fatal crashes increased in the presence of leading ends of guardrails and bridge rails, along with large wooden poles. Moreover, speeding and driving under the influence (DUI) increased the likelihood of crashes with severe outcomes. In an attempt to determine unforgiving roadside contributing factors, Roque et al. [107] collected ROR crash data on freeway road sections in Portugal and developed multinomial and mixed logit regression models to analyze the data. The empirical findings of this study indicated that critical slopes and horizontal curves significantly contributed to fatal ROR crashes. In another study, Hallmark et al. [134] evaluated driver behaviors on rural two-lane curves using data from the Strategic Highway Research Program 2 (SHRP 2) naturalistic driving study. Using logistic regression models, they assessed the probability of given types of encroachment, considering the driver, roadway, and environmental characteristics. The results demonstrated that the likelihood of a right-side lane departure was greater on the inside of a curve than on the outside.

Ayati et al. [189] developed a roadside hazard severity indicator based on an evidential reasoning (ER) approach. The approach has the capability to take into account the subjective state of evaluation within a decision maker group. The authors considered bridges, ditches, trees, utility poles, rigid obstacles, dangerous terminal and transitions, and embankment as the main contributing factors to roadside hazard severity. The results demonstrated that the developed indicator can be used as a variable in crash severity prediction models in order to consider roadside conditions and can be employed to prioritize routes for improvements. In another study, Pardillo-Mayora et al. [190] used roadside slope, non-traversable obstacles distance from the roadway edge, safety barrier installation, and alignment that participated significantly on RWD crash severity

levels in order to obtain a roadside hazardousness index (RHI) for Spanish two-lane roads. Based on the obtained results, the newly developed 5-level RHI summarize roadside safety related information and can be treated as a variable that includes roadside conditions in multivariate crash prediction models. Zou et al. [191] studied the risk of injury associated with various hazardous events, including roll over and strike with different roadside objects and barriers such as guardrail, concrete barrier, and cable barrier using a binary logistic regression model with mixed effects. The study found that the risk of injury associated with hitting a barrier was less than other hazardous events such as hitting a pole or rollover. Moreover, when traffic conditions allow, the recommendation to use cable barrier, guardrail, and concrete walls, respectively.

Park and Abdel-Aty [192] evaluated the safety effects of multiple roadside treatments using parametric and nonparametric approaches. The authors developed generalized nonlinear models (GNMs) and multivariate adaptive regression splines (MARS) models to accommodate the nonlinearity in crash predictors. In doing so, four roadside elements, including driveway density, poles density, distance to poles, and distance to trees were selected. Moreover, five years' worth of crash data, from 2008 to 2012, for rural undivided four-lane roadways in Florida were compiled, considering crash types and severity levels. Based on the results of study, the number of crashes was reduced followed by an increase in distance to poles and trees. Roque and Cardoso [135] developed a computer-aided procedure to include cost and benefits in roadside safety intervention decision making using installed equipment on Portuguese roadways. The authors used cost-benefit analysis software, which included a list of roadside safety measures, to compare different alternatives with various average annual daily traffic (AADT), average crash costs, discount rate, etc. and to analyze the effects of roadside characteristics on safety levels.

Hussein et al. [193] presented a reliability analysis method for calibrating geometric design models that would yield consistent risk levels. The authors calibrated middle-ordinate design charts at various probability levels, where middle ordinate is defined as the horizontal distance between the restrictive element and the centerline of the inside lane. The results demonstrated that current design guides are conservative, especially with respect to sharp curves and high speeds. The authors concluded that with reasonable reliability (risk) levels, significant reductions could be made in current design requirements. The Korean Government's Ministry of Land, Transport, and

Maritime Affairs used reliability analysis to evaluate design speed in a 2011 pilot study [194]. Based on the design and observed speeds (and their variations), a reliability index model was developed to measure the crash risk for segments of Korean expressways. The authors treated design speed as capacity in their analysis and observed speeds as demand. Further, they implemented the developed reliability indices into 18 segments and then compared them with the actual number of crashes at these locations. The results revealed that as the safety margin (the differences between capacity and demand) increased, the crash rates tended to decrease.

Although there have been a considerable number of roadside design studies [195-210], none have focused on reliability analysis. This valuable information could provide state departments of transportation (DOTs) and local agencies with a guideline for better understanding the effect of roadside conditions in their jurisdictions and to determine which countermeasures to implement to mitigate ROR crashes.

4.3.Method and Data

4.3.1. Reliability Analysis

In order to define a reliability index, as a factor of safety, a proper LSF must first be established. To do so, a “failure event” or “non-compliance event” for a clear zone was defined as the measured clear distance being less than the practical (capacity) distance, denoted by D_C in the following equations, as identified by the AASHTO *Roadside Design Guide* [148]. The capacity of the segments indicates their resistances against the likelihood of crashes. Although the clear zone width is defined based on a number of factors, including roadway design speed, traffic volume, embankment slope, and horizontal roadway curvature, previous studies have demonstrated that on high-speed roads, about 80 percent of errant vehicles can recover within 30 ft. of the edge of a through-traveled way [148]. Therefore, D_C is assumed to be the minimum practical clear zone distance that provides adequate space for errant vehicles to recover. Regarding sideslope, 1V:3H is the threshold slope for which recovery is less likely on a fill section [148]. Therefore, a practical (capacity) slope (S_C) is defined as a slope beyond which a section is non-recoverable. The LSF (g) of the clear zone can be defined based on the observed clear zone and the practical (capacity) clear zone, as in Equation 4.1:

$$g = D_o - D_c \quad (4.1)$$

where:

g = limit state function (LSF),

D_o = probability density function (PDF) of observed clear zone, and

D_c = PDF of practical (capacity) clear zone.

Since the slope is often calculated as a fraction, the LSF of the sideslope differs only slightly from that of the clear zone, and can be defined based upon the observed sideslope and the practical (capacity) sideslope, as in Equation 4.2:

$$g = S_c - S_o \quad (4.2)$$

where:

g = limit state function (LSF),

S_o = PDF of observed sideslope, and

S_c = PDF of practical (capacity) sideslope.

Consequently, as for the clear zone, the difference between the PDF of the practical (capacity) clear zone and the PDF of the observed clear zone yields the probability distribution of failure, namely (P_f). The state of the failure is the condition in which $g < 0$ (Figure 4.2).

Therefore:

$$P_f = P(D_o - D_c < 0) = P(g < 0) \quad (4.3)$$

Based on the results from our comprehensive analysis, which are described later, the observed clear zone and the observed sideslope follow normal distributions, while the practical (capacity) clear zone and practical (capacity) sideslope are defined based on the manuals' recommendations. Typically, when the distribution of P_f is given and follows the normal distribution, the use of the graphical method is appropriate. In order to calculate the reliability index, a graphical approach was used to determine the probability of non-compliance, based upon data collected from the study segments. The margins of safety for the clear zone and sideslope are defined as the differences between the PDFs of their demand and capacity. The reliability index can be defined in terms of the standard deviation of the P_f , based on the distance between the mean value of the distribution

of the P_f and the safety margin ($g = 0$). Using the graphical method, therefore, it is possible to calculate the reliability index as follows [166, 211]:

$$\beta = \frac{\mu_g}{\sigma_g} \quad (4.4)$$

where:

β = reliability index,

μ_g = mean of the safety margin, and

σ_g = standard deviation of safety margin.

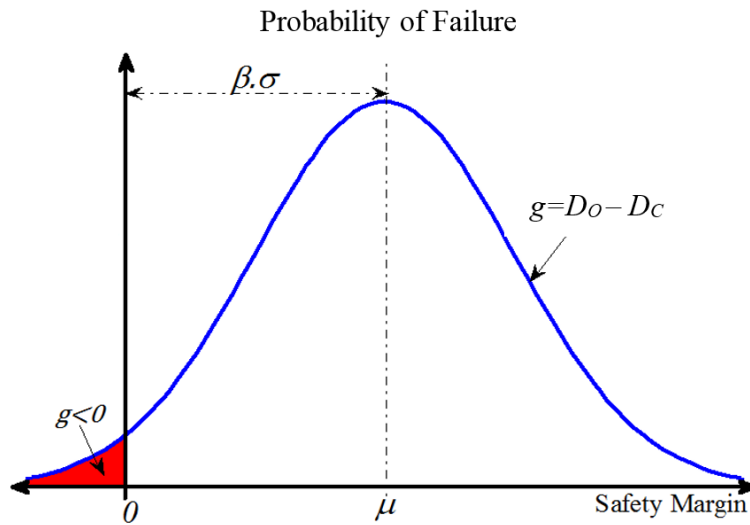


Figure 4.2 Graphical Relationship between Reliability Index and Statistical Parameters of P_f [166]

However, if variables do not follow normal distributions and/or LSF is non-linear and/or LSF has more than two variables, it is inevitable that more complicated mathematical efforts are necessary (e.g., simulations, and approximate method). Using the standard normal distribution function, the probability of non-compliance is defined as in Equation 4.5 [166]:

$$P_f = \Phi(-\beta) \quad (4.5)$$

where:

β = reliability index, and

Φ = standard normal distribution.

If the reliability index is greater than 0, this means that the capacity is greater than demand and the probability of non-compliance is less than 50 percent. On the other hand, if the reliability index

is less than 0, this indicates that demand is greater than capacity and the probability of non-compliance will be greater than 50 percent. Table 1 illustrates the probability of non-compliance against a reliability index for normally distributed data. As can be seen, the probabilities of non-compliance decrease when the reliability indices increase, indicating a more reliable and safe system. In Table 4.1, as an example, it was shown that a reliability index of 1.0 corresponds to a probability of non-compliance of around 16 percent. While for non-normal distributions the change in the probability of non-compliance is different, the same descending trends are present.

Table 4.1 Probability of Failure vs. Reliability Index

Reliability Index	Probability of Failure
0.0	$0.500 \times 10^{+0}$
0.5	$0.309 \times 10^{+0}$
1.0	$0.159 \times 10^{+0}$
1.5	0.668×10^{-1}
2.0	0.228×10^{-1}
2.5	0.621×10^{-2}
3.0	0.135×10^{-2}
3.5	0.233×10^{-3}
4.0	0.317×10^{-4}

4.3.2. Segment and Crash Data

To evaluate the proposed method, data from two databases regarding crashes and roadside geometric design features were gathered and combined. The historical ROR crash data for a 5-year time period, from 2009 through 2013, were compiled from the Illinois Department of Transportation (IDOT) [9]. In this study, ROR crashes were only considered because ROR crashes accounted for the majority of the Rwd events (about 80 percent) and cross centerline head-on collisions are not likely directly related to roadside conditions. The roadside geometric design features (i.e., sideslope and clear zone width) of 4,500 segments, each with a defined segment length of 300 ft, were also obtained from Google Earth Pro. Table 4.2 lists the distributions of the study segments, based on crash frequency and severity. As shown in the table, more than 64 percent of the segments had no crashes, and less than two percent had more than three crashes. Since only those segments with similar roadway characteristics were considered in this study (speed limits between 45 and 55 mile per hour, lane widths greater than 10.6 ft., shoulder widths

less than 3 ft., no horizontal and vertical curvatures present, no shoulder rumble strips present, and good roadway conditions), the effect of those parameters on ROR crashes were not considered.

Table 4.2 Distributions of Segments Based on Crash Frequency and Severity

	Category	Frequency	Percentage (%)
Crash severity	Fatal	194	4.3
	Injury	477	10.6
	Property Damage Only (PDO)	909	20.2
	None (No Crash)	2920	64.9
Crash frequency (number of ROR crashes per segment)	Zero (No Crash)	2920	64.9
	One	1026	22.8
	Two	333	7.4
	Three	162	3.6
	Four	59	1.3

4.4. Results and Discussions

As mentioned previously, both clear zone width and sideslope are not deterministic values; therefore, the application of probabilistic analysis such as reliability analysis appears appropriate. To perform the reliability analysis, first, it is necessary to first identify distributions for the variables. The study segments fall into five categories (i.e., zero, one, two, three, and four) indicating the total number of ROR crashes that occurred in each road segment during the five-year study period. Therefore, the PDFs of the observed clear zone and observed sideslope of segments for each of the five categories of crash frequency were separately specified. Using the *MATLAB® R2014a* application, the best fitted distributions of the clear zone and sideslope, based on their root-mean-square errors (RMSEs) were drawn as shown in Figures 4.3 and 4.4. Theoretically, the procedure to find the fitted normal distribution is deployed by matching the distribution's peak and variance with the mean and the variance of the collected data. According to Figures 4.3 and 4.4, all PDFs behave as normal distributions. Moreover, the obtained normality test results (i.e., Shapiro-Wilk, Kolmogorov-Smirnov, and chi-square) confirmed that the observed clear zone and sideslope follow normal distributions. Table 4.3, as an example, presents the normality test results for both the clear zone and sideslope of segments without crashes with a 95-percent confidence interval. As can be seen in the table, the computed p-values in all the tests are greater than the significance level (α), which means that the null hypothesis cannot be rejected. In this case, the null hypothesis is that all the data were sampled from a population that follow a normal distribution.

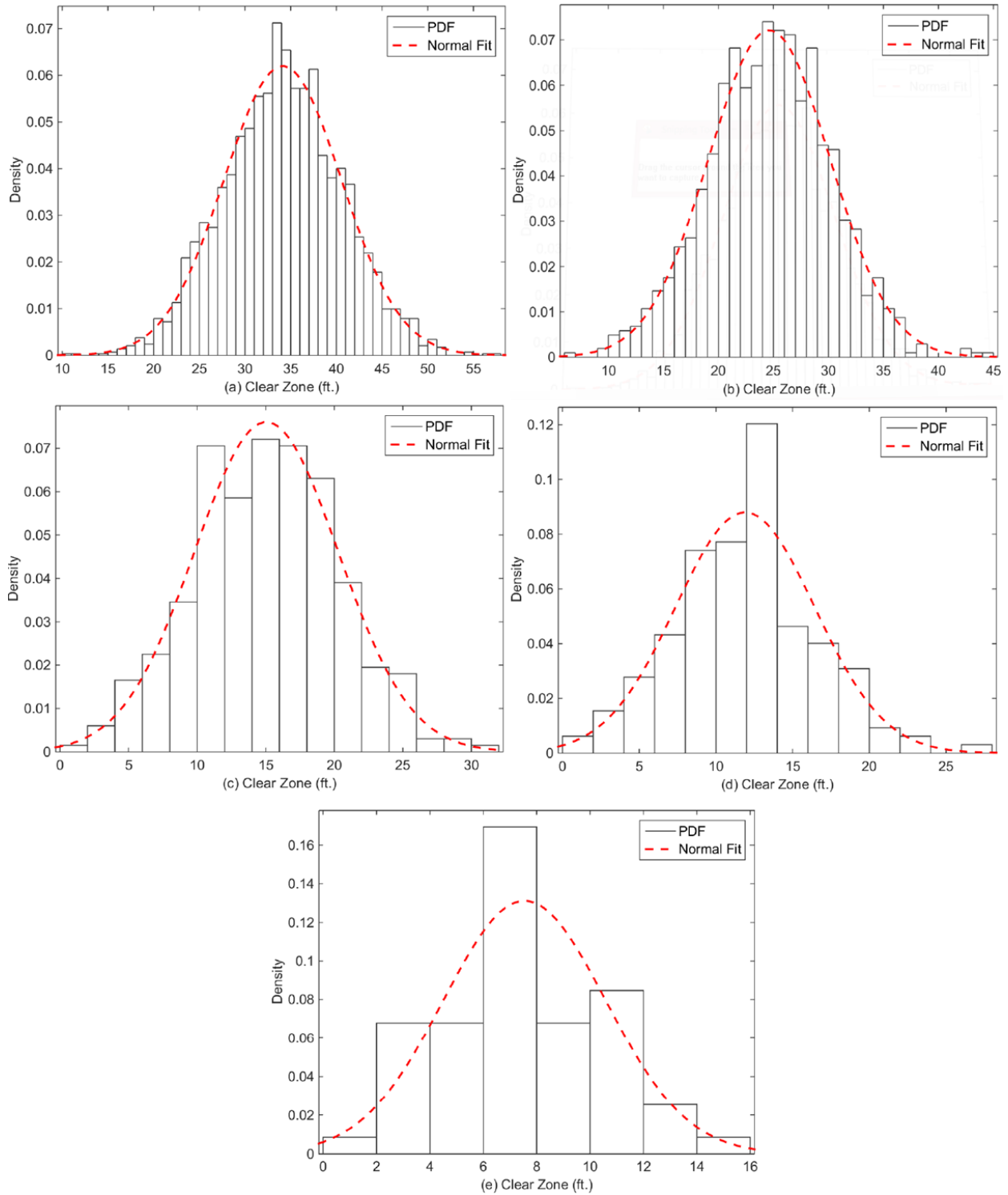


Figure 4.3 Observed Clear Zone of Segments for Five Crash Categories : (a) No Crash; (b) One Crash; (c) Two Crashes; (d) Three Crashes; (e) Four Crashes

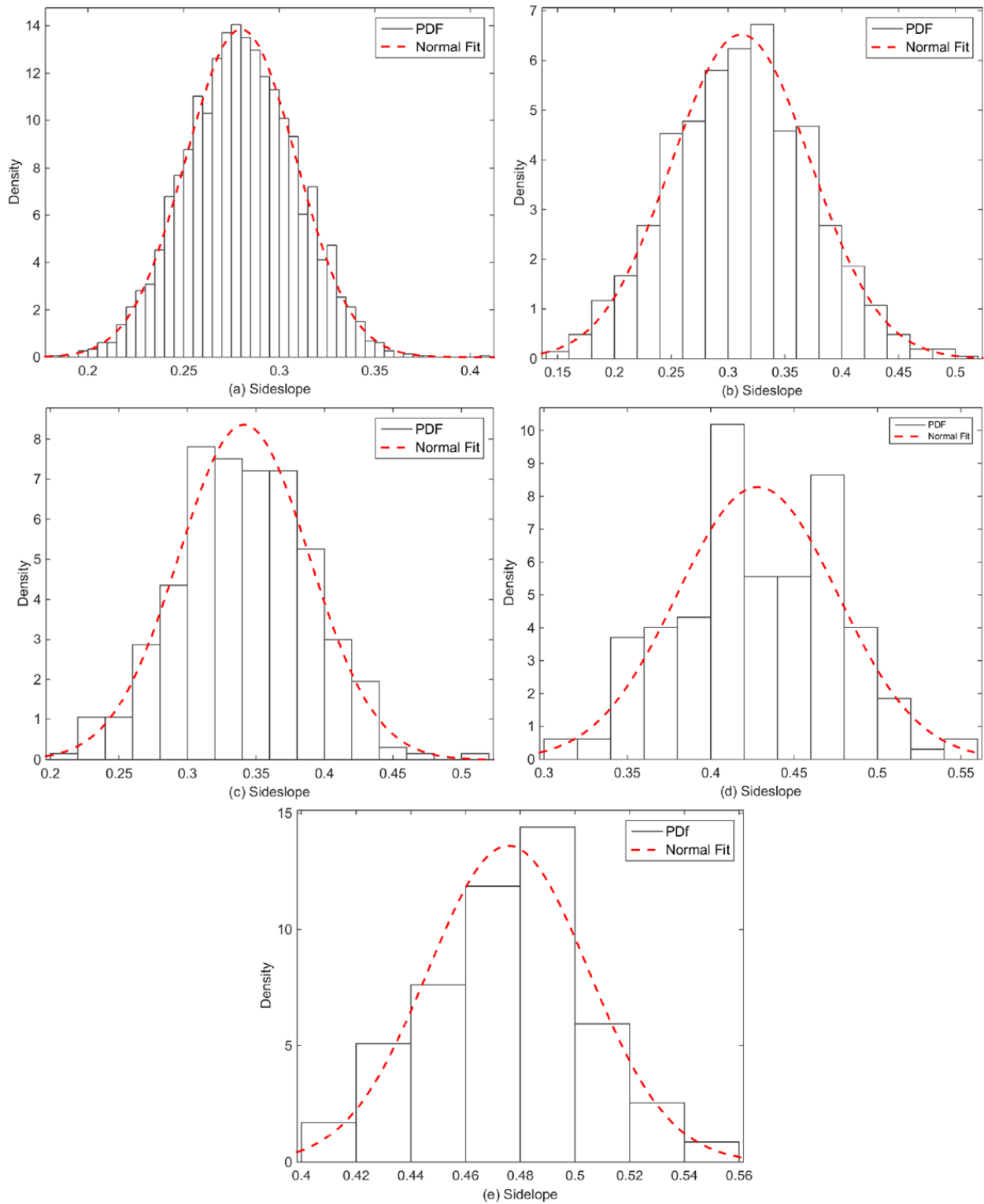


Figure 4.4 Observed Sideslope of Segments for Five Crash Categories :(a) No Crash; (b) One Crash; (c) Two Crashes; (d) Three Crashes; (e) Four Crashes

Table 4.3 Results of Normality Tests for Observed Clear Zone and Sideslope of Segments with No Crash

Normality Test	Observed Clear Zone		Observed Sideslope	
	p-value	α	p-value	α
Shapiro-Wilk	0.51	0.05	0.54	0.05
Kolmogorov-Smirnov	0.43	0.05	0.17	0.05
Chi-Square	0.07	0.05	0.10	0.05

Table 4.4 lists the statistical parameters (i.e., mean (μ) and standard deviation (σ)) of the fitted distributions. When looking at this table, a few points are worth mentioning. For example, the mean values of the observed clear zones of all studied segments vary between 7.5 ft. and 34 ft. and the mean values of the observed sideslopes of all studied segments fall between 0.28 (~1V:3.3H sideslope) and 0.47 (~1V:2H sideslope). The segments with unforgiving roadsides such as steep sideslopes and narrow clear zones experienced more ROR crashes, which is consistent with the findings of the majority of existing literature [102,103, 164, 120,184, 188-190, 207].

Table 4.4 Statistical Parameters of the Fitted Normal Distribution

Crash Frequency	Observed Clear Zone		Observed Sideslope	
	μ	σ	μ	σ
Zero	34.1	6.4	0.28	0.03
One	24.6	5.5	0.31	0.06
Two	15.4	5.2	0.34	0.05
Three	11.9	4.5	0.42	0.04
Four	7.5	3.0	0.47	0.02

Table 4.5 compiles the statistical parameters of the safety margin distributions for both roadside features. Based on these results, the mean value of the safety margins of the clear zone and sideslope of segments with more crashes are negative. This means that these segments have clear zone widths and sideslopes that are less than practical values, as recommended in the manuals.

Table 4.5 Statistical Parameters of the Safety Margin Distributions

Crash Frequency	Observed Clear Zone		Observed Sideslope	
	μ	σ	μ	σ
Zero	+4.1	6.4	+0.05	0.03
One	-5.4	5.5	+0.02	0.06
Two	-14.6	5.2	-0.01	0.05
Three	-18.1	4.5	-0.09	0.04
Four	-22.5	3.0	-0.14	0.02

Using Eqs. (4) and (5), the reliability indices and probabilities of non-compliance for both roadside features for each crash category were calculated, as shown in Table 4.6. This table shows

that the reliability indices for a clear zone ranged between +0.64 and -7.50, which corresponds to the probabilities of non-compliance of 26 percent and 100 percent, respectively.

Table 4.6 Probability of Non-compliance and Reliability Index vs. Crash Rate

Crash Frequency (Number of ROR Crashes per Segment)	Average AADT (veh/day)	Crash Rate (Crashes per Million Vehicle Miles)	Reliability Index		Probability of Non-compliance	
			Clear Zone	Sideslope	Clear Zone	Sideslope
Zero	8,650	0.00	+0.64	+1.67	0.261	0.047
One	8,600	1.12	-0.98	+0.33	0.836	0.370
Two	9,740	1.98	-2.81	-0.20	0.997	0.579
Three	9,010	3.21	-4.02	-2.25	1.000	0.988
Four	8,150	4.73	-7.50	-7.00	1.000	1.000

It should be noted that the probability of non-compliance is not equal to the probability of crash occurrence. A collision may occur if a driver leaves the travel lane due to fatigue or traveling too fast, with respect to weather or geometric road conditions, and an object and/or steep slope exists on the side of the road simultaneously. To correlate the probabilities of non-compliance with the crash occurrences and to verify that reliability indices can be used to indicate the safety levels of roadside segments, five years (2009–2013) of ROR crash data, along with traffic volumes were collected and utilized. Since the reliability indices in this study were calculated based upon non-crash statistical variables (i.e., clear zone and sideslope), it was essential that they be compared with actual crash data to determine whether or not they were reasonable indicators of roadside safety. To determine crash rates for each crash category, the number of crashes that occurred in the segments of the category were divided by the average of AADT volumes of all segments that fall into that particular category, as shown in Table 4.6. Then, the safety margins and the reliability indices for each crash category were separately calculated, using Equations 4.3 and 4.4.

Table 4.6 links the probability of non-compliance to the crash rate of each crash category. As can be seen in the table, the crash rates increase with increases in the probabilities of non-compliance. For example, a crash rate of 1.12 corresponds to probabilities of non-compliance of around 83 percent and 37 percent for the clear zone and sideslope, respectively. It should be noted that the probability of non-compliance describes the unsuccessful performance of whole segments, given only the practical and observed clear zones/sideslopes. Since only segments with similar roadway characteristics, apart from the roadside features studied here (i.e., clear zone and sideslope), were selected, the relationship between the probabilities of non-compliance/reliability

indices and crash occurrences can be confirmed to a great extent, ascertaining the normal distributions of the roadside features for each crash category.

Figures 4.5 and 4.6 illustrate the variations of the safety margins and reliability indices with respect to the crash rates. As shown in Figure 4.5, as the safety margins increase, the crash rates decrease. These results are consistent with the findings of a study by Oh and Mun [194] demonstrating that as the safety margin (the differences between observed speed and design speed) increases, crash rates tend to decrease. This figure also shows that, with respect to the clear zone, the crash rates associated with a safety margin of -20 are much higher than those for a safety margin of 0. The former corresponds to a clear zone width of 10 ft. and the latter corresponds to a clear zone width of 30 ft. These results are in good agreement with the findings of Roque et al. [107], Van Petegem and Wegman [132], Lord et al. [98]; Jurewicz and Pyta [208]; and Ogle et al. [209]. Similarly, regarding sideslopes, the crash rates associated with a safety margin of -1.67, which corresponds to a 1V:2H sideslope, are higher than those with a safety margin of 0, or a 1V:3H sideslope. These results are also in line with the findings of Roque et al. [107], Peng et al. [210], Pardillo-Mayora et al. [190]; and Zegeer et al. [164].

Figure 4.6 demonstrates that the greater the reliability index value, the lower the crash rate. This result is in good agreement with Oh and Mun's findings [194]. More specifically, a crash rate corresponding to a sideslope reliability index value of -2.0 is about two times that with a value of 0. Similarly, as for a clear zone, a crash rate for the reliability index of -4 is roughly three times of that for a reliability index of -1. It should be noted that the coefficients of determination (R^2) in the polynomial regression models for the clear zone and sideslope are 0.99, and 0.98, respectively. Therefore, the relationship between the crash rates and the reliability indices showed a trend with a high coefficient of determination that validates this approach.

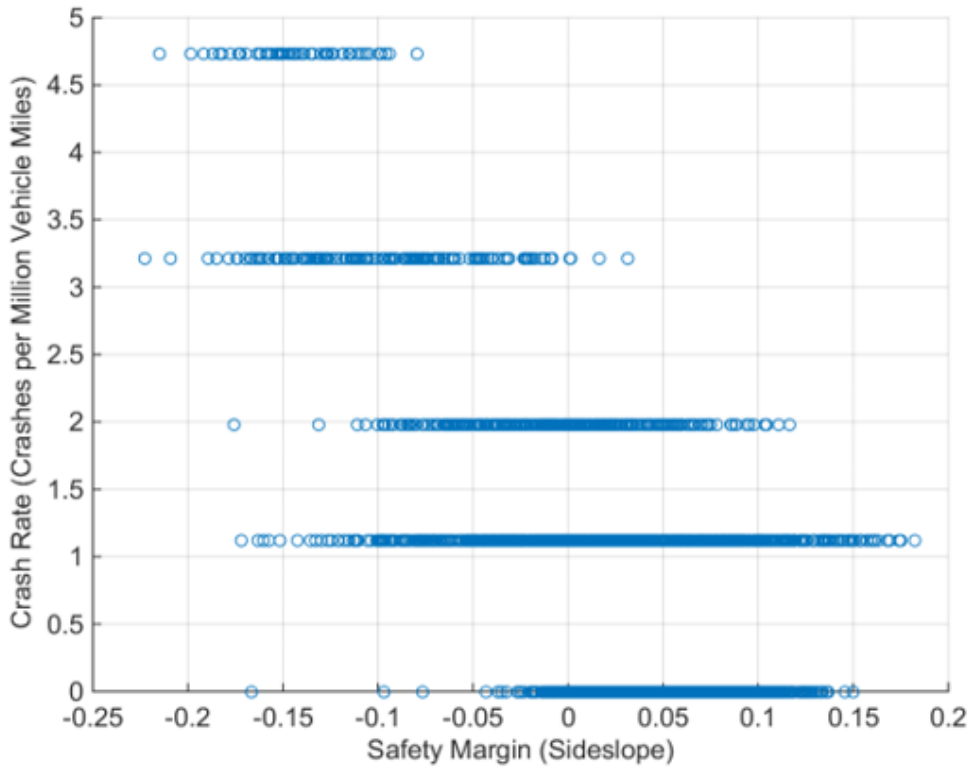
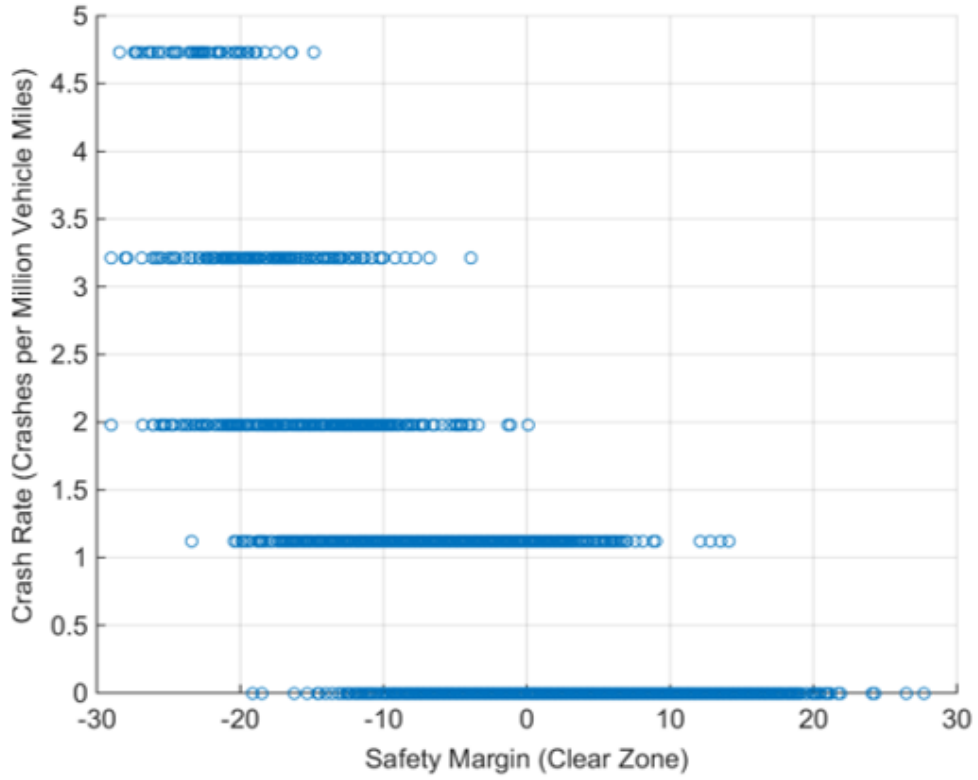


Figure 4.5 Safety Margin vs. Crash Rate

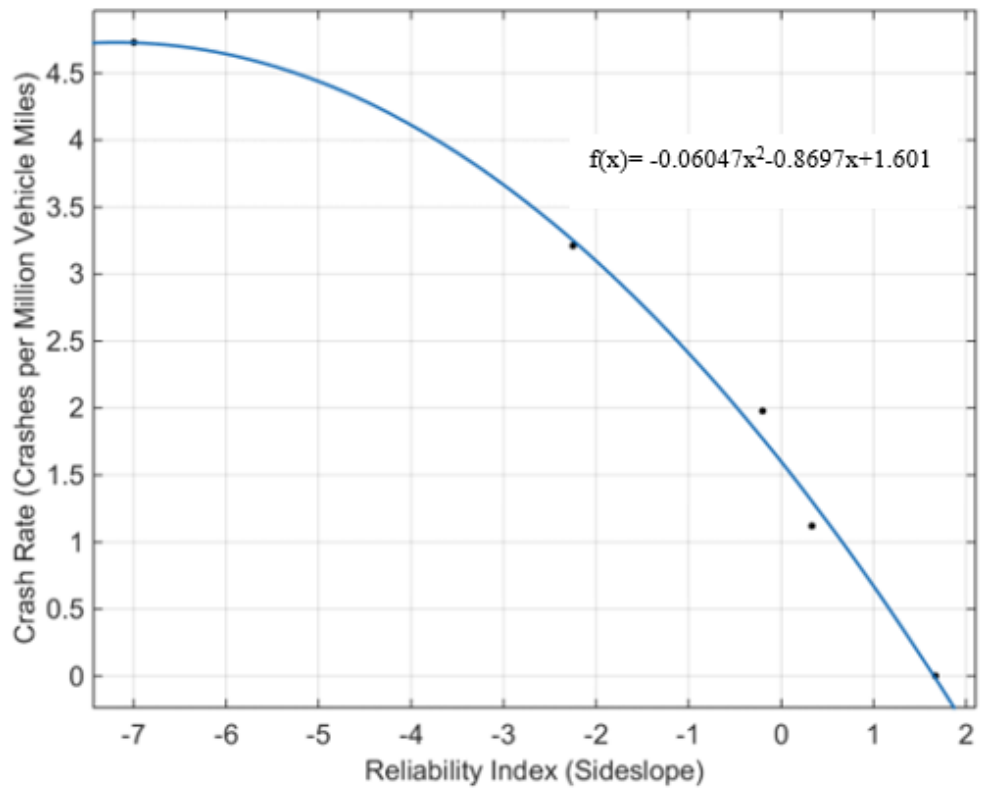
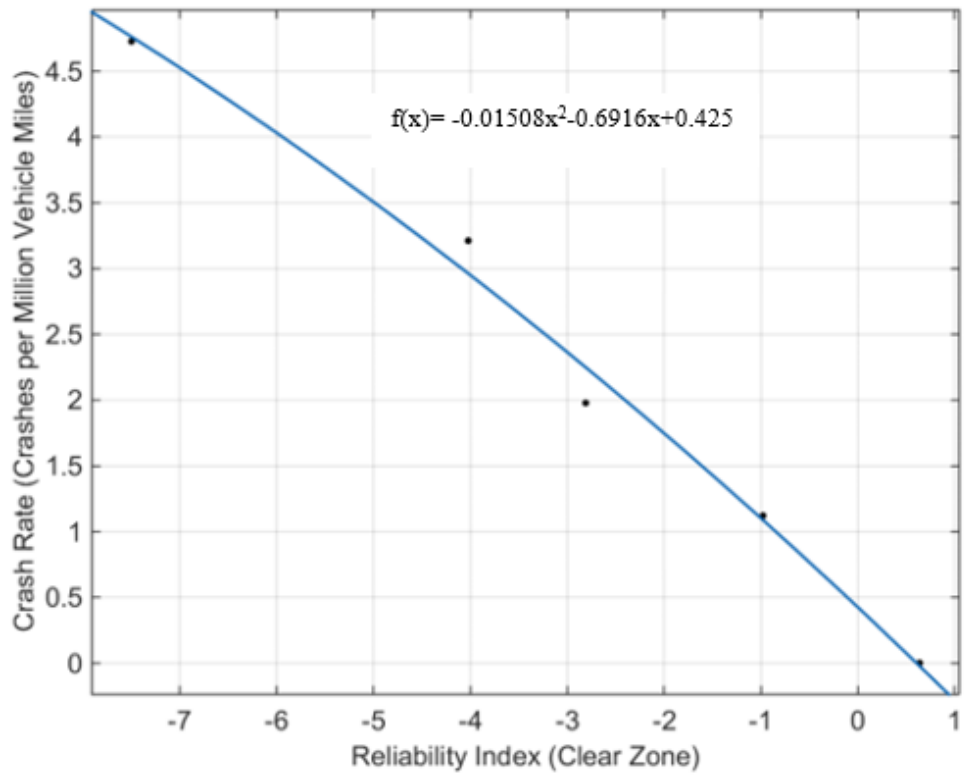


Figure 4.6 Reliability Index vs. Crash Rate

4.5.Limitations

According to previous studies [6, 9], a significant amount of roadside information (e.g., roadside slope, grade, roadside fixed objects and their densities, and offset to the edge of travel way) is missing in many state DOT databases. One of the reasons that there are not many studies on the effects of parameters for RHR is the difficulty of obtaining those parameters for current and past years. Based on a previously conducted study, satellite imagery and aerial imagery are sound methods for extracting planimetric features [129]. With calibrated aerial images, the aerial imagery can also be utilized to derive slope information; however, depending on resolutions, these methods are limited to some extent in extracting information on small vertical roadside objects (e.g., sign posts, and fire hydrants). Therefore, limitations derived from the availability of high-resolution Google Earth Pro images for limited years should be considered.

4.6.Conclusions and Recommendations

This chapter utilized a probabilistic approach to develop reliability indices for roadside features (i.e., clear zone and sideslope) on rural two-lane roads. This represents one of the few early attempts to apply reliability analysis to traffic safety evaluation. The rationale for this effort was the need to quantify roadside safety levels by treating clear zone width and sideslope as two continuous, rather than discrete, variables for use in determining RHR on a scale of 1 to 7. RHR is the main measure of roadside conditions currently used in accident prediction algorithms for rural two-lane highways. This chapter provides researchers and transportation agencies with a better understanding of the effect of roadside conditions, in order to implement effective countermeasures. Relying solely on deterministic design criteria provides no information regarding any deviations from design standards or recommendations. To evaluate our method's performance, five years of ROR crash data from 2009 to 2013 were obtained from a state of Illinois database. Moreover, the required roadside information for 4,500 300-ft segments were also gathered from Google Earth Pro. Based on the obtained results, the reliability indices for clear zones ranged between +0.64 and -7.50 and for sideslopes fell between +1.67 and -7.00. The findings of this study demonstrate that reliability indices can serve as a surrogate measure for the safety levels of roadside conditions. In other words, as the safety level of roadside conditions is

increased, their reliability index values also increase. This means that the higher the reliability index values, the lower the ROR crash rates. Moreover, ROR crash rates increase with an increase in the safety risk or probabilities of non-compliance. By considering only segments with similar roadway characteristics, the relationship between ROR collisions and roadside features (i.e., clear zone and sideslope) can be confirmed to a great extent

To specify appropriate reliability indices, optimum reliability index values must be determined, which involves a determination of the trade-offs between a practical clear zone width and sideslope and failure cost (e.g., crash cost). The approach proposed in this chapter may be suitable for developing reliability indices for different scenarios with respect to various roadway characteristics and the practical values of clear zone widths and sideslopes at the city, county, and state levels. This model is also appropriate for use in road safety assessments (RSAs) and in risk evaluations of road segments in order to prioritize improvements with respect to their reliability indices.

Possible extensions of this study can focus on two different aspects: LSF and roadside data collection. It should be noted that while two separate reliability models were built for clear zone width and sideslope, further research is desirable to combine these reliability indices in order to consider their combined effect on reliability to identify the series systems reliability. Additionally, conducting more research into this particular topic can help identify suitable LSF and target probability of non-compliance. Given the rapid pace of research and development in the field of mobile light detection and ranging (LiDAR) data processing as a highly-accurate emerging technology, it can be expected that this method will be an attractive solution for collecting and managing the nation's roadside inventory data. As such, extraction of roadside features from remotely-sensed images, obtained from mobile LiDAR, can increase the accuracy of collected roadside features.

References

1. American Association of State Highway and Transportation Officials (AASHTO). (2010). Highway Safety Manual. 1st Edition, Washington, D.C.
2. Bonneson, J. A., Geedipally, S., Pratt, M. P., & Lord, D. (2012). Safety prediction methodology and analysis tool for freeways and interchanges. *National Cooperative Highway Research*, 7, 17-45.
3. Jalayer, M., Zhou, H., Williamson, M., & LaMondia, J. J. (2015d). Developing Calibration Factors for Crash Prediction Models with Consideration of Crash Recording Threshold Change. *Transportation Research Record: Journal of the Transportation Research Board*, (2515), 57-62.
4. Jalayer, M., & Zhou, H. (2013). A sensitivity analysis of crash prediction models input in the Highway Safety Manual. In *The 2013 ITE Midwest District Conference*.
5. Baratian-Ghorghi, F., Zhou, H., & Zech, W. C. (2016). Red-light running traffic violations: A novel time-based method for determining a fine structure. *Transportation Research Part A: Policy and Practice*, 93, 55-65.
6. Jalayer, M., Zhou, H., Gong, J., Hu, S., & Grinter, M. (2014). A comprehensive assessment of highway inventory data collection methods. In *Journal of the Transportation Research Forum* (Vol. 53, No. 2, pp. 73-92). Transportation Research Forum.
7. Williamson, M., Jalayer, M., & Zhou, H. (2012). A Study of Crash Modification Factors of Access Management Techniques in Highway Safety Manual. In *The 2012 ITE Midwest District Conference and TRB 4th urban Street Symposium*.
8. Williamson, M., Jalayer, M., Zhou, H., & Rouholamin, M. P. (2015). A Sensitivity Analysis of Crash Modification Factors of Access Management Techniques in Highway Safety Manual. *Access Management Theories and Practices*, 76.
9. Zhou, H., Jalayer, M., Gong, J., Hu, S., & Grinter, M. (2013). Investigation of methods and approaches for collecting and recording highway inventory data. *FHWA-ICT-13-022*. Illinois Center for Transportation, IL.
10. Zhou, H., Chen, H., & Baratian-Ghorghi, F. (2016). Prediction of Intermittent Sight Distance Obstruction at Unsignalized Intersections with Conventional Right-Turn Lanes. *Journal of Transportation Safety & Security*, DOI: 10.1080/19439962.2015.1116478.

11. Pour-Rouholamin, M., & Jalayer, M. (2016). Analyzing the Severity of Motorcycle Crashes in North Carolina USING Highway Safety Information Systems Data. Institute of Transportation Engineers. *ITE Journal*, 86(10), 45.
12. Sharifi, M. S., & Shabaniverki, H. (2016). Modeling crash delays in a route choice behavior model for two way road networks. *Journal of Geotechnical and Transportation Engineering*, 2(1).
13. Jalayer, M., Zhou, H., Gong, J., Hu, S., & Grinter, M. (2015c). Comprehensive Assessment of Highway Inventory Data Collection Methods for Implementing Highway Safety Manual. In *Transportation Research Board 94th Annual Meeting* (No. 15-2288).
14. Jalayer, M., Baratian-Ghorghi, F., & Zhou, H. (2015f). Identifying and characterizing secondary crashes on the Alabama state highway systems. *Advances in Transportation Studies*, (37).
15. Baratian-Ghorghi, F., Zhou, H., & Wasilefsky, I. (2015a). Effect of red-light cameras on capacity of signalized intersections. *Journal of transportation engineering*, 142(1), 04015035.
16. Baratian-Ghorghi, F., Zhou, H., Jalayer, M., & Pour-Rouholamin, M. (2015b). Prediction of potential wrong-way entries at exit ramps of signalized partial cloverleaf interchanges. *Traffic injury prevention*, 16(6), 599-604.
17. Pour-Rouholamin, M., Zhou, H., Jalayer, M., & Williamson, M. (2015). Application of Access Management Techniques to Reduce Wrong-Way Driving Near Interchange Areas. *Access Management Theories and Practices*, 236-246.
18. Zhou, H., Wang, L., Gahrooei, M. R., & Jalayer, M. (2012). Contributing factors to wrong-way driving crashes in Illinois. In *ITE Midwestern District Conference and TRB 4th Urban Street Symposium*.
19. Jalayer, M., Zhou, H., & Zhang, B. (2016). Evaluation of navigation performances of GPS devices near interchange area pertaining to wrong-way driving. *Journal of Traffic and Transportation Engineering (English Edition)*.
20. American Traffic Safety Services Association (ATSSA). (2014). Emerging Safety Countermeasures for Wrong-Way Driving. *Virginia*.
21. Sharifi, M. S. (2016). Analysis and Modeling of Pedestrian Walking Behaviors Involving Individuals with Disabilities.

22. Sharifi, M.S., Stuart, D., Christensen, K.M., Chen, A. (2015a). Traffic flow characteristics of heterogeneous pedestrian stream involving individuals with disabilities. *Transportation Research Record: Journal of the Transportation Research Board*, 2537, 111-125.
23. Sharifi, M.S., Stuart, D., Christensen, K.M., Chen, A., Kim, Y.S., Chen, Y. (2015b). Analysis of walking speeds involving individuals with disabilities in different indoor walking environments. *Journal of Urban Planning and Development* 142 (1) (doi: 10.1061/(ASCE)UP.1943-5444.0000288).
24. Baratian-Ghorghi, F., & Zhou, H. (2016). Effects of Photo Enforcement Cameras on Intersection Delays and Driver Behavior. In *Transportation Research Board 95th Annual Meeting* (No. 16-1502).
25. Asgari, H., Jin, X., & Mohseni, A. (2014). Choice, Frequency, and Engagement: Framework for Telecommuting Behavior Analysis and Modeling. *Transportation Research Record: Journal of the Transportation Research Board*, (2413), 101-109.
26. Christensen, K. M., Sharifi, M. S., & Chen, A. (2013). Considering individuals with disabilities in a building evacuation: An agent-based simulation study. In *92nd Annual Meeting of the Transportation Research Board, Washington, DC*.
27. Amoh-Gyimah, R., Saberi, M., & Sarvi, M. (2016). Macroscopic modeling of pedestrian and bicycle crashes: a cross-comparison of estimation methods. *Accident Analysis & Prevention*, 93, 147-159.
28. Amoh-Gyimah, R., Sarvi, M., & Saberi, M. (2016). Investigating the Effects of Traffic, Socioeconomic, and Land Use Characteristics on Pedestrian and Bicycle Crashes: A Case Study of Melbourne, Australia. In *Transportation Research Board 95th Annual Meeting* (No. 16-1931).
29. Talebpour, A., Mahmassani, H., Mete, F., & Hamdar, S. (2014). Near-crash identification in a connected vehicle environment. *Transportation Research Record: Journal of the Transportation Research Board*, (2424), 20-28.
30. Van de Weg, G. S., Keyvan Ekbatani, M., Hegyi, A., & Hoogendoorn, S. P. (2016). Urban network throughput optimization via model predictive control using the link transmission model. In *95th Annual Meeting Transportation Research Board, Washington, USA, 10-14 January 2016; Authors version*. TRB.

31. Keyvan-Ekbatani, M., Kouvelas, A., Papamichail, I., & Papageorgiou, M. (2012). Exploiting the fundamental diagram of urban networks for feedback-based gating. *Transportation Research Part B: Methodological*, 46(10), 1393-1403.
32. Mahmassani, H. S., Saberi, M., & Zockaie, A. (2013). Urban network gridlock: Theory, characteristics, and dynamics. *Transportation Research Part C: Emerging Technologies*, 36, 480-497.
33. Zockaie, A., Mahmassani, H., Saberi, M., & Verbas, Ö. (2014). Dynamics of Urban Network Traffic Flow During a Large-Scale Evacuation. *Transportation Research Record: Journal of the Transportation Research Board*, (2422), 21-33.
34. Talebpour, A., & Mahmassani, H. S. (2016). Influence of connected and autonomous vehicles on traffic flow stability and throughput. *Transportation Research Part C: Emerging Technologies*, 71, 143-163.
35. Soltani-Sobh, A., Heaslip, K., Stevanovic, A., El Khoury, J., & Song, Z. (2016). Evaluation of transportation network reliability during unexpected events with multiple uncertainties. *International Journal of Disaster Risk Reduction*, 17, 128-136.
36. Heaslip, K., Bosworth, R., Barnes, R., Sobh, A. S., & Thomas, M. (2015). *Do Changing Prices Portend a Shift in Fuel Consumption, Diminished Greenhouse Gas Emissions, and Lower Fuel Tax Revenue?* (No. MPC 15-278).
37. Heaslip, K., Bosworth, R., Barnes, R., Sobh, A. S., Thomas, M., & Song, Z. (2014). *Effects of natural gas vehicles and fuel prices on key transportation economic metrics* (No. WA-RD 829.1).
38. Soltani-Sobh, A., Heaslip, K., & El Khoury, J. (2015a). Estimation of road network reliability on resiliency: An uncertain based model. *International Journal of Disaster Risk Reduction*, 14, 536-544.
39. Soltani-Sobh, A., Heaslip, K., Bosworth, R., & Barnes, R. (2015b). Effect of Improving Vehicle Fuel Efficiency on Fuel Tax Revenue and Greenhouse Gas Emissions. *Transportation Research Record: Journal of the Transportation Research Board*, (2502), 71-79.
40. Asgari, H., & Jin, X. (2015). Toward a Comprehensive Telecommuting Analysis Framework: Setting the Conceptual Outline. *Transportation Research Record: Journal of the Transportation Research Board*, (2496), 1-9.

41. Asgari, H., Jin, X., & Du, Y. (2016). Examining the Impacts of Telecommuting on the Time-Use of Non-Mandatory Activities. In *Transportation Research Board 95th Annual Meeting* (No. 16-1659).
42. Khalilikhah, M., & Heaslip, K. (2016b). GIS-Based Study of the Impacts of Air Pollutants on Traffic Sign Deterioration. In *Transportation Research Board 95th Annual Meeting* (No. 16-3843).
43. Khalilikhah, M., Heaslip, K., & Hancock, K. (2016b). Traffic sign vandalism and demographics of local population: A case study in Utah. *Journal of Traffic and Transportation Engineering (English Edition)*.
44. Balali, V., & Golparvar-Fard, M. (2015c). Evaluation of multiclass traffic sign detection and classification methods for US roadway asset inventory management. *Journal of Computing in Civil Engineering*, 30(2), 04015022.
45. Balali, V., & Golparvar-Fard, M. (2015d). Segmentation and recognition of roadway assets from car-mounted camera video streams using a scalable non-parametric image parsing method. *Automation in construction*, 49, 27-39.
46. Balali, V., Golparvar-Fard, M., & de la Garza, J. M. (2013). Video-based highway asset recognition and 3D localization. *Computing in civil engineering*, 386.
47. Gong, J., Zhou, H., Gordon, C., & Jalayer, M. (2012). Mobile terrestrial laser scanning for highway inventory data collection. *Computing in Civil Engineering*, 545-552.
48. Khattak, A. J., Hummer, J. E., & Karimi, H. A. (2000). New and existing roadway inventory data acquisition methods. *Journal of Transportation and Statistics*, 3(3), 33-46.
49. Maerz, N., & McKenna, S. (1999). Mobile highway inventory and measurement system. *Transportation Research Record: Journal of the Transportation Research Board*, (1690), 135-142.
50. Hu, X., Tao, C. V., & Hu, Y. (2004). Automatic road extraction from dense urban area by integrated processing of high resolution imagery and lidar data. *International Archives of Photogrammetry, Remote Sensing and Spatial Information Sciences. Istanbul, Turkey*, 35, B3.
51. DeGray, J., & Hancock, K. L. (2002). *Ground-based image and data acquisition systems for roadway inventories in New England: A synthesis of highway practice* (No. NETCR 30.). New England Transportation Consortium.

52. Jeyapalan, K., & Jaselskis, E. (2002). *Technology transfer of as-built and preliminary surveys using GPS, soft photogrammetry, and video logging* (No. Iowa DOT Project TR-446).
53. Jeyapalan, K. (2004). Mobile digital cameras for as-built surveys of roadside features. *Photogrammetric Engineering & Remote Sensing*, 70(3), 301-312.
54. Robyak, R., & Orvets, G. (2004). Video based asset data collection at NJDOT. *New Jersey Department of Transportation*.
55. Wu, J., & Tsai, Y. (2006). Enhanced roadway geometry data collection using an effective video log image-processing algorithm. *Transportation Research Record: Journal of the Transportation Research Board*, (1972), 133-140.
56. Tsai, Y. (2009). Using image pattern recognition algorithms for processing video log images to enhance infrastructure data collection. *NCHRP, Final Report for Highway IDEA Project, 121*.
57. Wang, K. C., Hou, Z., & Gong, W. (2010). Automated road sign inventory system based on stereo vision and tracking. *Computer-Aided Civil and Infrastructure Engineering*, 25(6), 468-477.
58. Balali, V., Ashouri Rad, A., and Golparvar-Fard, M. (2015b). "Detection, Classification, and Mapping of U.S. Traffic Signs Using Google Street View Images for Roadway Inventory Management." *Springer Journal of Visualization in Engineering*, 3(15), 1-18.
59. Caddell, R., Hammond, P., & Reinmuth, S. (2009). Roadside features inventory program. *Washington State Department of Transportation*.
60. Hallmark, S. L., Mantravadi, K., Veneziano, D., & Souleyrette, R. R. (2001). Evaluating remotely sensed images for use in inventorying roadway infrastructure features.
61. Veneziano, D. (2001). Roadway intersection inventory and remote sensing. *ISU Center for Transportation Research and Education, ed.*
62. Pagounis, V., Tsakiri, M., Palaskas, S., Biza, B., & Zaloumi, E. (2006, October). 3D laser scanning for road safety and accident reconstruction. In *Proceedings of the XXIIIth international FIG congress* (pp. 8-13).
63. Slattery, D. K., & Slattery, K. T. (2010). Evaluation of 3-D laser scanning for construction application.

64. California State Department of Transportation (Caltrans). (2011). Terrestrial Laser Scanning Specifications. Caltrans Surveys Manual.
65. Tao, C. V. (2000). Mobile mapping technology for road network data acquisition. *Journal of Geospatial Engineering*, 2(2), 1-14.
66. Vosselman, G., Gorte, B. G., Sithole, G., & Rabbani, T. (2004). Recognising structure in laser scanner point clouds. *International archives of photogrammetry, remote sensing and spatial information sciences*, 46(8), 33-38.
67. Laflamme, C., Kingston, T., & McCuaig, R. (2006). Automated mobile mapping for asset managers.
68. Pfeifer, N., & Briese, C. (2007). Geometrical aspects of airborne laser scanning and terrestrial laser scanning. *International Archives of Photogrammetry, Remote Sensing and Spatial Information Sciences*, 36(3/W52), 311-319.
69. Barber, D., Mills, J., & Smith-Voysey, S. (2008). Geometric validation of a ground-based mobile laser scanning system. *ISPRS Journal of Photogrammetry and Remote Sensing*, 63(1), 128-141.
70. Huber, R., Kingston, T., Laflamme, C., & Larouche, C. (2008). Automation and mobile mapping for safe and accurate pavement analysis. In *Seventh International Conference on Managing Pavement Assets*.
71. Lato, M., Hutchinson, J., Diederichs, M., Ball, D., & Harrap, R. (2009). Engineering monitoring of rockfall hazards along transportation corridors: using mobile terrestrial LiDAR. *Nat. Hazards Earth Syst. Sci*, 9(3), 935-946.
72. Garza, J., Figueroa, C. F., Howerton, C. G., Plummer, J., Roca, I., Shogli, O., Sideris, D., & Uslu, B. (2009). Implementation of IP-S2 Mobile Mapping Technology for Highway Asset Visualization in Data Collection to Benefit VT-VDOT TAMS Project. *Center for Highway Asset Management Programs, Virginia Department of Transportation*.
73. Lehtomäki, M., Jaakkola, A., Hyypä, J., Kukko, A., & Kaartinen, H. (2010). Detection of vertical pole-like objects in a road environment using vehicle-based laser scanning data. *Remote Sensing*, 2(3), 641-664.
74. Graham, L. (2010). Mobile mapping systems overview. *Photogrammetric engineering and remote sensing*, 76(3), 222-228.

75. Tang, J., & Zakhor, A. (2011, January). 3D object detection from roadside data using laser scanners. In *IS&T/SPIE Electronic Imaging* (pp. 78640V-78640V). International Society for Optics and Photonics.
76. Yen, K. S., Akin, K., Lofton, A., Ravani, B., & Lasky, T. A. (2010). Using mobile laser scanning to produce digital terrain models of pavement surfaces. *Final Report of the Advanced Highway Maintenance and Construction Technology Research Center Research Project, University of California at Davies: Pittsburgh, PA, USA.*
77. Yen, K. S., Ravani, B., & Lasky, T. A. (2011). *LiDAR for Data efficiency* (No. WA-RD 778.1).
78. Khalilikhah, M. (2016). Traffic Sign Management: Data Integration and Analysis Methods for Mobile LiDAR and Digital Photolog Big Data. Ph.D Dissertation, Utah State University.
79. Jensen, J. R., & Cowen, D. C. (1999). Remote sensing of urban/suburban infrastructure and socio-economic attributes. *Photogrammetric engineering and remote sensing*, 65, 611-622.
80. Hatger, C., & Brenner, C. (2003). Extraction of road geometry parameters from laser scanning and existing databases. *International Archives of Photogrammetry, Remote Sensing and Spatial Information Sciences*, 34(3/W13), 225-230.
81. Souleyrette, R., Hallmark, S., Pattnaik, S., O'Brien, M., & Veneziano, D. (2003). *Grade and cross slope estimation from LiDAR-based surface models* (No. MTC Project 2001-02).
82. Shamayleh, H., & Khattak, A. (2003, August). Utilization of LiDAR technology for highway inventory. In *Proceedings of the 2003 Mid-Continent Transportation Research Symposium, Ames, Iowa.*
83. Zhang, K., & Frey, H. C. (2006). Road grade estimation for on-road vehicle emissions modeling using light detection and ranging data. *Journal of the Air & Waste Management Association*, 56(6), 777-788.
84. McCarthy, T., Fotheringham, S., Charlton, M., Winstanley, A., & O'Malley, V. (2007). Integration of LIDAR and stereoscopic imagery for route corridor surveying. *Mobile Mapping Technology*, 37, 1125-1130.
85. Uddin, W. (2008). Airborne laser terrain mapping for expediting highway projects: Evaluation of accuracy and cost. *Journal of Construction Engineering and Management*, 134(6), 411-420.

86. Chow, T. E., & Hodgson, M. E. (2009). Effects of lidar post-spacing and DEM resolution to mean slope estimation. *International Journal of Geographical Information Science*, 23(10), 1277-1295.
87. Jalayer, M., Hu, S., Zhou, H., & Turochy, R. E. (2015a). An Assessment of the Highway Inventory Data Collection Method Using Photo/Video Logging. In *Transportation Research Board 94th Annual Meeting* (No. 15-2403).
88. Jalayer, M., Hu, S., Zhou, H., & Turochy, R. E. (2015). Evaluation of Geo-Tagged Photo and Video Logging Methods to Collect Geospatial Highway Inventory Data. *Papers in Applied Geography*, 1(1), 50-58.
89. Balali, V., & Golparvar-Fard, M. (2014). Video-based detection and classification of US traffic signs and mile markers using color candidate extraction and feature-based recognition. *Computing in civil and building engineering*, 866.
90. Balali, V., Depwe, E., & Golparvar-Fard, M. (2015a). Multi-class traffic sign detection and classification using google street view images. In *Transportation Research Board 94th Annual Meeting, Transportation Research Board, Washington, DC*.
91. Golparvar-Fard, M., Balali, V., & de la Garza, J. M. (2012). Segmentation and recognition of highway assets using image-based 3D point clouds and semantic Texton forests. *Journal of Computing in Civil Engineering*, 29(1), 04014023.
92. Dodgson, J. S., Spackman, M., Pearman, A., & Phillips, L. D. (2009). *Multi-criteria analysis: a manual*. Department for Communities and Local Government: London.
93. Federal Highway Administration (FHWA). (2014). Roadway Departure Safety. *Washington, D.C.*
94. Neuman, T. R., Pfefer, R., Slack, K., Hardy, K. K., Coucil, F., McGee, H., Prothe, L., & Eccles, K. (2003a). A Guide for Addressing Head-On Collisions. *NCHRP Report 500: Guidance for Implementation of the AASHTO Strategic Highway Safety Plan*.
95. Neuman, T. R., Pfefer, R., Slack, K., Neuman, T., & Pfefer, R. (2003b). A Guide for Addressing Head-On Collisions. *NCHRP Report 500: Guidance for Implementation of the AASHTO Strategic Highway Safety Plan*.
96. Jalayer, M., and H. Zhou. Overview of Safety Countermeasures for Roadway Departure Crashes. *ITE Journal*, Vol. 86, No. 2, 2016, pp. 39-46.

97. National Highway Traffic Safety Administration (NHTSA). (2015). Fatality Analysis Reporting System. *Washington, D.C.*
98. Lord, D., Brewer, M. A., Fitzpatrick, K., Geedipally, S. R., & Peng, Y. (2011). Analysis of roadway departure crashes on two-lane rural roads in Texas. *TxDOT, Austin, TX, Rep. FHWA/TX-11/0-6031-1.*
99. Federal Highway Administration (FHWA). (2016). Safety Compass: Highway Safety Solutions for Saving Lives. *Washington, D.C.*
100. Cook, D., & Swayne, D. F. (2007). Interactive and dynamic graphics for data analysis: with R and GGobi. Springer Science & Business Media.
101. Chatfield C. Problem Solving: a Statistician's Guide. 2nd Edition, Chapman and Hall/CRC, United Kingdom, 1995.
102. McLaughlin, S. B., J. M. Hankey, S. K. Klauer, and T. A. Dingus. (2009). Contributing Factors to Run-off-road Crashes and Near-crashes. Publication DOT HS 811 079. National Highway Traffic Safety Administration (NHTSA), Washington, D. C.
103. Liu, C., & Subramanian, R. (2009). *Factors related to fatal single-vehicle run-off-road crashes* (No. HS-811 232)
104. Liu, C., & Ye, T. J. (2011). *Run-off-road crashes: an on-scene perspective* (No. HS-811 500).
105. Jalayer, M., & Zhou, H. (2016b). Evaluating the safety risk of roadside features for rural two-lane roads using reliability analysis. *Accident Analysis & Prevention*, 93, 101-112.
106. Eustace, D., Almutairi, O., Hovey, P. W., & Shoup, G. (2014). Using Decision Tree Modeling to Analyze Factors Contributing to Injury and Fatality of Run-Off-Road Crashes in Ohio. In *Transportation Research Board 93rd Annual Meeting* (No. 14-5668).
107. Roque, C., Moura, F., & Cardoso, J. L. (2015). Detecting unforgiving roadside contributors through the severity analysis of ran-off-road crashes. *Accident Analysis & Prevention*, 80, 262-273.
108. American Traffic Safety Services Association (ATSSA). (2015). Preventing vehicle departures from roadways. *Virginia.*
109. Khalilikhah, M., & Heaslip, K. (2016). Analysis of factors temporarily impacting traffic sign readability. *International Journal of Transportation Science and Technology*, 5(2), 60-67.
110. Khalilikhah, M., & Heaslip, K. (2016). Important environmental factors contributing to the

- 1 temporary obstruction of the sign messages 2. In *Transportation Research Board 95th Annual Meeting* (No. 16-3785).
111. Khalilikhah, M., Habibian, M., & Heaslip, K. (2016a). Acceptability of increasing petrol price as a TDM pricing policy: A case study in Tehran. *Transport Policy*, *45*, 136-144.
112. Das, S., & Sun, X. (2015). Factor Association with Multiple Correspondence Analysis in Vehicle–Pedestrian Crashes. *Transportation Research Record: Journal of the Transportation Research Board*, (2519), 95-103.
113. Das, S., & Sun, X. (2016). Association knowledge for fatal run-off-road crashes by Multiple Correspondence Analysis. *IATSS Research*, *39*(2), 146-155.
114. Factor, R., Yair, G., & Mahalel, D. (2010). Who by accident? The social morphology of car accidents. *Risk Analysis*, *30*(9), 1411-1423.
115. Nallet, N., Bernard, M., & Chiron, M. (2008). Individuals taking a French driving licence points recovery course: Their attitudes towards violations. *Accident Analysis & Prevention*, *40*(6), 1836-1843.
116. Kim, K., & Yamashita, E. (2008). Corresponding characteristics and circumstances of collision-involved pedestrians in Hawaii. *Transportation Research Record: Journal of the Transportation Research Board*, (2073), 18-24.
117. Fontaine, H. (1995, October). A typological analysis of pedestrian accidents. In *7th workshop of ICTCT*.
118. Lee, J., & Mannering, F. L. (1999). *Analysis of roadside accident frequency and severity and roadside safety management* (No. WA-RD 475.1.). Olympia, WA: Washington State Department of Transportation.
119. McGinnis, R., Davis, M., & Hathaway, E. (2001). Longitudinal analysis of fatal run-off-road crashes, 1975 to 1997. *Transportation Research Record: Journal of the Transportation Research Board*, (1746), 47-58.
120. Lee, J., & Mannering, F. (2002). Impact of roadside features on the frequency and severity of run-off-roadway accidents: an empirical analysis. *Accident Analysis & Prevention*, *34*(2), 149-161.

121. Wu, K. F., Donnell, E. T., & Aguero-Valverde, J. (2014). Relating crash frequency and severity: evaluating the effectiveness of shoulder rumble strips on reducing fatal and major injury crashes. *Accident Analysis & Prevention*, *67*, 86-95.
122. Spainhour, L., & Mishra, A. (2008). Analysis of fatal run-off-the-road crashes involving overcorrection. *Transportation Research Record: Journal of the Transportation Research Board*, (2069), 1-8.
123. Montella, A. (2009). Safety evaluation of curve delineation improvements: empirical Bayes observational before-and-after study. *Transportation Research Record: Journal of the Transportation Research Board*, (2103), 69-79.
124. Albuquerque, F., Sicking, D., & Stolle, C. (2010). Roadway departure and impact conditions. *Transportation Research Record: Journal of the Transportation Research Board*, (2195), 106-114.
125. Savolainen, P. T., Mannering, F. L., Lord, D., & Quddus, M. A. (2011). The statistical analysis of highway crash-injury severities: a review and assessment of methodological alternatives. *Accident Analysis & Prevention*, *43*(5), 1666-1676.
126. Peng, Y., & Boyle, L. (2012). Commercial driver factors in run-off-road crashes. *Transportation Research Record: Journal of the Transportation Research Board*, (2281), 128-132.
127. Fitzpatrick, C. D. (2013). The effect of roadside elements on driver behavior and run-off-the-road crash severity. M.Sc. Dissertation, University of Massachusetts Amherst, Amherst, Massachusetts.
128. Hallmark, S. L., Qiu, Y., Pawlovitch, M., & McDonald, T. J. (2013). Assessing the safety impacts of paved shoulders. *Journal of Transportation Safety & Security*, *5*(2), 131-147.
129. Jalayer, M., Gong, J., Zhou, H., & Grinter, M. (2015). Evaluation of remote sensing technologies for collecting roadside feature data to support highway safety manual implementation. *Journal of Transportation Safety & Security*, *7*(4), 345-357.
130. Dissanayake, S., & Roy, U. (2014). Crash severity analysis of single vehicle run-off-road crashes. *Journal of Transportation Technologies*, *4*(01).
131. Gates, T. J., Savolainen, P. T., Datta, T. K., & Russo, B. (2013). Exterior Roadside Noise Associated with Centerline Rumble Strips as a Function of Depth and Pavement Surface Type.

- Journal of Transportation Engineering*, 140(3), 04013019.
132. Van Petegem, J.W.H., & Wegman, F. (2014). Analyzing road design risk factors for run-off-road crashes in the Netherlands with crash prediction models. *Journal of safety research*, 49, 121-127.
 133. Schrum, K. D., De Albuquerque, F. D. B., Sicking, D. L., Faller, R. K., & Reid, J. D. (2014). Benefits of slope flattening. *Journal of Transportation Safety & Security*, 6(4), 356-368.
 134. Hallmark, S. L., Tyner, S., Oneyear, N., Carney, C., & McGehee, D. (2015). Evaluation of driving behavior on rural 2-lane curves using the SHRP 2 naturalistic driving study data. *Journal of safety research*, 54, 17-27.
 135. Roque, C., & Cardoso, J. L. (2015). SAFESIDE: a computer-aided procedure for integrating benefits and costs in roadside safety intervention decision making. *Safety science*, 74, 195-205.
 136. Panagiotakos, D. B., & Pitsavos, C. (2004). Interpretation of epidemiological data using multiple correspondence analysis and log-linear models. *Journal of Data Science*, 2(1), 75-86.
 137. Ye, F., & Lord, D. (2014). Comparing three commonly used crash severity models on sample size requirements: multinomial logit, ordered probit and mixed logit models. *Analytic methods in accident research*, 1, 72-85.
 138. Abdi, H., & Valentin, D. (2007). Multiple correspondence analysis. *Encyclopedia of measurement and statistics*, 651-657.
 139. Greenacre, M., & Blasius, J. (Eds.). (2006). *Multiple correspondence analysis and related methods*. CRC press.
 140. Gifi, A. (1991). *Nonlinear multivariate analysis*. John Wiley & Sons.
 141. Le Roux, B., & Rouanet, H. (2010). *Multiple correspondence analysis* (Vol. 163). Sage.
 142. usRAP Study of Eight Counties in Illinois. (2013). CH2M Hill, Chicago, Illinois.
 143. Office of the Assistant Secretary for Research and Technology (OST-R). (2016). usRAP: A New Tool for Road Safety Management.
 144. United State Road Assessment Program (usRAP). (2012). usRAP Coding Manual for Star Ratings and Safer Roads Investment Plans. Illinois.
 145. Correspondence Analysis. Numbers International Pty Ltd. (2016). www.wiki.q-

researchsoftware.com/wiki/Correspondence_Analysis.

146. Baratian-Ghorgi, F., Zhou, H., & Shaw, J. (2014). Overview of wrong-way driving fatal crashes in the United States. *Institute of Transportation Engineers. ITE Journal*, 84(8), 41.
147. Federal Highway Administration (FHWA). (2014). Manual for Selecting Safety Improvements on High Risk Rural Roads, *Washington, D.C.*
148. American Association of State Highway and Transportation Officials (AASHTO). (2008). Driving down lane departure crashes: a national priority, *Washington, D.C.*
149. Baratian-Ghorgi, F. B. (2016). Behavioral, Operational and Safety Effects of Red-Light Cameras at Signalized Intersections in Alabama (Doctoral dissertation, Auburn University).
150. Khalilikhah, M., Heaslip, K., & Song, Z. (2015). Can daytime digital imaging be used for traffic sign retroreflectivity compliance?. *Measurement*, 75, 147-160.
151. Federal Highway Administration (FHWA). (2009). Manual on Uniform Traffic Control Devices (MUTCD), *Washington, D.C.*
152. Hallmark, S. L., Qiu, Y., Hawkins, N., & Smadi, O. (2014). Crash Modification Factors for Dynamic Speed Feedback Signs on Rural Curves. Center for Transportation Research and Education, Iowa State University.
153. Oregon Department of Transportation (ODOT). (2015). Systemic Safety Measures-Updated Curve Warning Signs.
154. American Traffic Safety Services Association (ATSSA). (2014). High Friction Surface Treatments, *Virginia*.
155. Federal Highway Administration (FHWA). (2012a). Every Day Counts (EDC)-High Friction Surface Treatment, *Washington, D.C.*
156. American Traffic Safety Services Association (ATSSA). (2011). Cost Effective Local Road Safety Planning and Implementation, *Virginia*.
157. Federal Highway Administration (FHWA). (2012b). The Safety Edge-A Pavement Edge Drop-off Treatment. *Washington, D.C.*
158. Federal Highway Administration (FHWA). (2011). Technical Advisory: Shoulder and Edge Line Rumble Strips. *Washington, D.C.*
159. Oklahoma Department of Transportation (OKLADOT). (2015). Shoulder Treatments-Rumble Strips (Milled SRS, Rolled SRS).

160. Noyce, D. A., Martinez, C., & Chitturi, M. (2008). The Operational and Safety Impacts of Run-Off-Road Crashes in Wisconsin: Tree, Fence, and Pole Impacts. *Traffic Operations and Safety Laboratory, University of Wisconsin–Madison*.
161. International Road Assessment Program (iRAP). iRAP Safety Assessment and Recommended Countermeasures. www.eurorap.org/media/134139/irap_mari_el_report_english_.pdf.
162. American Association of State Highway and Transportation Officials (AASHTO). (2011). Roadside Design Guide. 4th Edition, Washington, D.C.
163. Federal Highway Administration (FHWA) (2012c). Breakaway Features for Sign Supports, Utility Poles and Other Roadside Features, *Washington, D.C.*
164. Zegeer, C. V., Hummer, J., Reinfurt, D., Herf, L., & Hunter, W. (1987). Safety effects of cross section design for two lane roads-volume 1: final report.
165. Ghasemi, S. H., & Nowak, A. S. (2016). Reliability Analysis for Serviceability Limit State of Bridges Concerning Deflection Criteria. *Structural Engineering International*, 26(2), 168-175.
166. Ghasemi, S. H., Jalayer, M., Pour-Rouholamin, M., Nowak, A. S., & Zhou, H. (2016a). State-of-the-Art Model to Evaluate Space Headway Based on Reliability Analysis. *Journal of Transportation Engineering*, 04016023.
167. Ghasemi, S. H., Nowak, A. S., & Parastesh, H. (2016b). Statistical Parameters of In-A-Lane Multiple Truck Presence and a New Procedure to Analyze the Lifetime of Bridges. *Structural Engineering International*, 26(2), 150-159.
168. Ghasemi, S. H., & Nowak, A. S. (2016). Mean maximum values of non-normal distributions for different time periods. *International Journal of Reliability and Safety*, 10(2), 99-109.
169. Ghasemi, S. H. (2014). *Target reliability analysis for structures* (Doctoral dissertation, Auburn University).
170. Yanaka, M., Ghasemi, S. H., & Nowak, A. S. (2016). Reliability-Based and Life-Cycle-Cost Oriented Design Recommendations for Prestressed Concrete Bridge Girders. *Structural Concrete*.
171. Nowak, A. S., & Rakoczy, P. (2013). WIM-based live load for bridges. *KSCE Journal of*

- Civil Engineering*, 17(3), 568-574.
172. Nowak, A., Eom, J., & Sanli, A. (2000). Control of live load on bridges. *Transportation Research Record: Journal of the Transportation Research Board*, (1696), 136-143.
173. Gokce, H., Catbas, F., & Frangopol, D. (2011). Evaluation of load rating and system reliability of movable bridge. *Transportation Research Record: Journal of the Transportation Research Board*, (2251), 114-122.
174. Saraf, V., Sokolik, A., & Nowak, A. (1996). Proof load testing of highway bridges. *Transportation Research Record: Journal of the Transportation Research Board*, (1541), 51-57.
175. Szerszen, M., & Nowak, A. (2000). Fatigue evaluation of steel and concrete bridges. *Transportation Research Record: Journal of the Transportation Research Board*, (1696), 73-80.
176. Kim, S., Sokolik, A., & Nowak, A. (1996). Measurement of truck load on bridges in Detroit, Michigan, area. *Transportation Research Record: Journal of the Transportation Research Board*, (1541), 58-63.
177. Ghasemi, S. H., Nowak, A. S., & Ashtari, P. (2013). Estimation of the Resonance-Response Factor Regarding to the Critical Excitation Methods. In *11th International Conference on Structural Safety and Reliability*, New York.
178. Ashtari, P., & Ghasemi, S. H. (2013). Seismic design of structures using a modified non-stationary critical excitation. *Earthquakes and Structures*, 4(4), 383.
179. Cruse, T. A. (1997). *Reliability-based mechanical design* (Vol. 108). CRC Press.
180. Wood, J., & Donnell, E. (2014). Stopping Sight Distance and Horizontal Sight Line Offsets at Horizontal Curves. *Transportation Research Record: Journal of the Transportation Research Board*, (2436), 43-50.
181. Richl, L., & Sayed, T. (2006). Evaluating the safety risk of narrow medians using reliability analysis. *Journal of transportation engineering*, 132(5), 366-375.
182. Nowak, A. S., & Collins, K. R. (2012). *Reliability of structures*. CRC Press.
183. O'Connor, P., & Kleyner, A. (2011). *Practical reliability engineering*. John Wiley & Sons.
184. Sperry, R., Latterell, J., & McDonald, T. (2008). Best Practices for Low-Cost Safety Improvements on Iowa's Local Roads.

185. Bella, F. (2013). Driver perception of roadside configurations on two-lane rural roads: Effects on speed and lateral placement. *Accident Analysis & Prevention*, 50, 251-262.
186. Fitzpatrick, C. D., Harrington, C. P., Knodler, M. A., & Romoser, M. R. (2014). The influence of clear zone size and roadside vegetation on driver behavior. *Journal of safety research*, 49, 97-e1.
187. El Esawey, M., & Sayed, T. (2012). Evaluating safety risk of locating above ground utility structures in the highway right-of-way. *Accident Analysis & Prevention*, 49, 419-428.
188. Holdridge, J. M., Shankar, V. N., & Ulfarsson, G. F. (2005). The crash severity impacts of fixed roadside objects. *Journal of Safety Research*, 36(2), 139-147.
189. Ayati, E., asghar Sadeghi, A., & Moghaddam, A. M. (2012). Introducing roadside hazard severity indicator based on evidential reasoning approach. *Safety science*, 50(7), 1618-1626.
190. Pardillo-Mayora, J. M., Domínguez-Lira, C. A., & Jurado-Piña, R. (2010). Empirical calibration of a roadside hazardousness index for Spanish two-lane rural roads. *Accident Analysis & Prevention*, 42(6), 2018-2023.
191. Zou, Y., Tarko, A. P., Chen, E., & Romero, M. A. (2014). Effectiveness of cable barriers, guardrails, and concrete barrier walls in reducing the risk of injury. *Accident Analysis & Prevention*, 72, 55-65.
192. Park, J., & Abdel-Aty, M. (2015). Assessing the safety effects of multiple roadside treatments using parametric and nonparametric approaches. *Accident Analysis & Prevention*, 83, 203-213.
193. Hussein, M., Sayed, T., Ismail, K., & Van Espen, A. (2014). Calibrating Road Design Guides Using Risk-Based Reliability Analysis. *Journal of Transportation Engineering*, 140(9), 04014041.
194. Oh, H. U., & Mun, S. (2012). Design speed based reliability index model for roadway safety evaluation. *KSCE Journal of Civil Engineering*, 16(5), 845-854.
195. Nambisan, S. S., Dangeti, M. R., Vanapalli, V. K., & Singh, A. K. (2007). Effectiveness of Continuous Shoulder Rumble Strips in Reducing Single-Vehicle Ran-Off-Roadway Crashes in Nevada. In *Proceedings of the 2007 Mid-Continent Transportation Research Symposium*.
196. Ozelim, L. C. D. S. M. (2015). *A Study of the Effects of Pavement Widening, Rumble Strips, and Rumble Stripes on Rural Highways in Alabama* (Doctoral dissertation, Auburn

University).

197. Meuleners, L. B., Hendrie, D., & Lee, A. H. (2011). Effectiveness of sealed shoulders and audible edge lines in Western Australia. *Traffic injury prevention, 12*(2), 201-205.
198. Federal Highway Administration (FHWA) (2015). Crash Modification Factors Clearinghouse. *Washington, D.C.*
199. Zhu, H., Dixon, K., Washington, S., & Jared, D. (2010). Predicting single-vehicle fatal crashes for two-lane rural highways in Southeastern United States. *Transportation Research Record: Journal of the Transportation Research Board, (2147)*, 88-96.
200. Freeman, P., Neyens, D. M., Wagner, J., Switzer, F., Alexander, K., & Pidgeon, P. (2015). A video based run-off-road training program with practice and evaluation in a simulator. *Accident Analysis & Prevention, 82*, 1-9.
201. Roque, C., & Cardoso, J. L. (2014). Investigating the relationship between run-off-the-road crash frequency and traffic flow through different functional forms. *Accident Analysis & Prevention, 63*, 121-132.
202. Schrum, K. D., De Albuquerque, F. D. B., Sicking, D. L., Falle, R. K., & Reid, J. D. (2014b). Correlation between crash severity and embankment geometry. *Journal of Transportation Safety & Security, 6*(4), 321-334.
203. Gross, F., & Donnell, E. T. (2011). Case-control and cross-sectional methods for estimating crash modification factors: Comparisons from roadway lighting and lane and shoulder width safety effect studies. *Journal of safety research, 42*(2), 117-129.
204. Hummer, J. E., Rasdorf, W., Findley, D. J., Zegeer, C. V., & Sundstrom, C. A. (2010). Curve collisions: road and collision characteristics and countermeasures. *Journal of Transportation Safety & Security, 2*(3), 203-220.
205. Polus, A., Pollatschek, M. A., & Farah, H. (2005). Impact of infrastructure characteristics on road crashes on two-lane highways. *Traffic injury prevention, 6*(3), 240-247.
206. Persaud, B. N., Retting, R. A., & Lyon, C. A. (2004). Crash reduction following installation of centerline rumble strips on rural two-lane roads. *Accident Analysis & Prevention, 36*(6), 1073-1079.
207. Hunter, A. G. M. (1993). A review of research into machine stability on slopes. *Safety science, 16*(3), 325-339.

208. Jurewicz, C., & Pyta, V. (2010). Effect of clear zone widths on run-off-road crash outcomes.
209. Ogle, J., Sarasua, W., Dillon, J., Bendigieri, V., Anekar, S., & Alluri, P. (2009). *Support for the Elimination of Roadside Hazards: Evaluating Roadside Collision Data and Clear Zone Requirements* (No. FHWA-SC-09-01).
210. Peng, Y., Geedipally, S., & Lord, D. (2012). Effect of roadside features on single-vehicle roadway departure crashes on rural two-lane roads. *Transportation Research Record: Journal of the Transportation Research Board*, (2309), 21-29.
211. Cornell, C.A. (1969). A probability-based structural code. *ACI Structural Journal*, 66(12), 974-985.

Appendix A

Table A1. Highway Inventory Data Collection Survey

Highway Safety Inventory Survey Illinois Department of Transportation		
Highway Asset Inventory Platform 0=Not Used 1=Used	Oracle Spatial Network Data Model (Oracle database)	0
	ArcGIS Shapefiles (dBase database)	0
	ArcGIS Geodatabase (Access database)	0
	SQL database	0
	Excel Spreadsheet	0
	Other (please specify)	0
Asset Inventory Method Technology Used 0=Not Used 1=Used	Field Inventory (Conventional Surveying)	0
	GPS/GIS Data Logger Technology	0
	Video Log Technology	0
	Photo Log Technology	0
	Static Terrestrial Laser Scanner Technology	0
	Mobile Terrestrial Laser Scanner Technology	0
	Airborne LiDAR Technology	0
	Aerial Imagery Technology	0
	Satellite Imagery Technology	0
	Other (please specify)	0

Primary Method	Conventional Survey Technology	0
	GPS/GIS Data Logger Technology	0
	Video Log Technology	0
	Photo Log Technology	0
	Static Terrestrial Laser Scanner Technology	0
	Mobile Terrestrial Laser Scanner Technology	0
	Airborne LiDAR Technology	0
	Satellite Imagery Technology	0
1=Primary Method	Aerial Imagery Technology	0

Equipment Cost Rating for Primary Method	Unacceptable	0
	Fair	0
	Good	0
	Very Good	0
	Excellent	0

Data Accuracy Rating for Primary Method	Unacceptable	0
	Fair	0
	Good	0
	Very Good	0
	Excellent	0

Data Completeness Rating for Primary Method	Unacceptable	0
	Fair	0
	Good	0
	Very Good	0
	Excellent	0

Crew Hazard Exposure Rating for Primary Method	Unacceptable	0
	Fair	0
	Good	0
	Very Good	0
	Excellent	0

Data Collection Cost Rating for Primary Method	Unacceptable	0
	Fair	0
	Good	0
	Very Good	0
	Excellent	0

Data Collection Time Rating for Primary Method	Unacceptable	0
	Fair	0
	Good	0
	Very Good	0
	Excellent	0

Data Reduction Time Rating for Primary Method	Unacceptable	0
	Fair	0
	Good	0
	Very Good	0
	Excellent	0

Data Reduction Cost Rating for Primary Method	Unacceptable	0
	Fair	0
	Good	0
	Very Good	0
	Excellent	0

Data Storage Requirement Rating for Primary Method	Unacceptable	0
	Fair	0
	Good	0
	Very Good	0
	Excellent	0